UNIVERSIDAD COMPLUTENSE DE MADRID
FACULTAD DE MEDICINA

TESIS DOCTORAL

Inmunoterapia "STAb" para el tratamiento de neoplasias hematológicas

MEMORIA PARA OPTAR AL GRADO DE DOCTOR

PRESENTADA POR

Ángel Ramírez Fernández

Directores

Luis Álvarez-Vallina
Belén Blanco Durango

Madrid

UNIVERSIDAD COMPLUTENSE DE MADRID

FACULTAD DE MEDICINA

TESIS DOCTORAL

INMUNOTERAPIA "STAb" PARA EL TRATAMIENTO DE NEOPLASIAS HEMATOLÓGICAS

MEMORIA PARA OPTAR AL GRADO DE DOCTOR

PRESENTADA POR

ÁNGEL RAMÍREZ FERNÁNDEZ

DIRECTORES

DR. LUIS ÁLVAREZ-VALLINA

DRA. BELÉN BLANCO DURANGO

MADRID, 2022

UNIVERSIDAD COMPLUTENSE DE MADRID

FACULTAD DE MEDICINA

DOCTORADO EN INVESTIGACIÓN BIOMÉDICA

TESIS DOCTORAL

INMUNOTERAPIA “STAb” PARA EL TRATAMIENTO DE NEOPLASIAS HEMATOLÓGICAS

AUTOR

ÁNGEL RAMÍREZ FERNÁNDEZ

DIRECTORES

DR. LUIS ÁLVAREZ-VALLINA

DRA. BELÉN BLANCO DURANGO

HOSPITAL UNIVERSITARIO 12 DE OCTUBRE

MADRID, 2022

Esta Tesis Doctoral, realizada en la Unidad de Inmunoterapia del Cáncer (UNICA), del Servicio de Inmunología del Hospital Universitario 12 de Octubre de Madrid, ha sido financiada por la Fundación CRIS contra el Cáncer (FCRIS-2018-0042, FCRIS-2021-0090), el Ministerio de Ciencia e Innovación (SAF2017-89437-P, PID2020-117323RB-100, PDC2021-121711-100), y el Instituto de Salud Carlos III (DTS/00089 y PI/2001030) con el apoyo del Consejo Regional Europeo Fondos FEDER para el desarrollo

A mis padres

Es difícil resumir en un trabajo lo que realmente implica hacer una tesis doctoral… Lo mismo sucede con los agradecimientos. Estas líneas intentarán expresar mi gratitud.

De manera especial me gustaría empezar con Luis y Belén, mis directores de tesis. Gran parte de la inmunología que he aprendido ha sido gracias a ellos pero si de algo estoy agradecido no es de lo sabido, sino de la ilusión que han transmitido por la investigación, por hacer las cosas bien y sobre todo por descubrir cosas nuevas. Gracias por todas las oportunidades, por los éxitos, los fracasos, por las innumerables charlas y por animarme a dar lo mejor de mí. Sin duda, dos personas a las que admiro y considero verdaderos mentores y compañeros. Este trabajo es vuestro. Los Dres. Grijander, Gromenauer, MS, SG, MM y CJ estarían orgullosos.

A mi tutor Pedro Roda por haber formado parte de todo este trabajo, por toda su ayuda y por todos los conocimientos transmitidos sobre inmunología. Por supuesto a Óscar, un amigo que me ha dado esta tesis y mejor compañero de investigación.

A Marta Compte, la cual ocupa un lugar especial en esta tesis. Sin su ayuda al principio, no habría podido llegar tan lejos. Seguramente, una experta en misiones imposibles, capaz de enseñarte a clonar en un día y en vez de preguntarte el resultado, interesarse en saber cómo estás.

Gracias a Estela Paz por su apoyo durante la residencia de inmunología y tras haberla terminado, por permitirme desarrollar mi formación como especialista y por todas las oportunidades que me ha brindado. Gracias a Pablo Morales, Mª José Castro y Esther Mancebo por su gran acogida, por su seguimiento y por enseñarme a desenvolverme bien en las diferentes áreas de la inmunología. A Dani Pleguezuelo y Óscar Cabrera, siempre dispuestos a enseñarme como conseguir financiación para los diferentes congresos, estancias, cursos o incluso masters. A las mejores compañeras de despacho, Paloma y Rocío, con las que he compartido un último año casi como en casa. A Luis Allende y Cecilia Muñoz por toda la citometría enseñada y no es poca… Gracias a Ángeles por preocuparse no solo de que aprendiera a hacer todas las técnicas de laboratorio, sino también a organizar bien los viajes y contar las mejores historias del servicio.

Gracias a Pablo Menéndez y Manel Juan por haberme acogido en sus respectivos equipos, su disposición y toda la colaboración en los trabajos incluidos en esta tesis. Las estancias en Barcelona han sido un descanso gracias a su gente y la excusa perfecta para ver a Kela o a Néstor, que han hecho todo más fácil siempre.

Mil gracias a todos los resis, tanto mayores como pequeños. No habrá un día en el que no eche de menos que Javi.G señale a alguien, que María ponga orden en la puesta de guardias, que Dani.A derrame la coca cola, que Alex lo sepa todo sobre todo o incluso vivir con Laura.N en Barcelona. Gracias a Javi.A por su complicidad, a Sara por no aburrirse de mis sustos y a Marta por aguantarme siempre. Gracias en especial a Laura.D, la primera persona que me acogió y seguramente la última que me despida. Gracias a los CucaNecas, la mejor vía de escape y los mejores secretos. Simplemente, los mejores. Me llevo infinidad de momentos con todos vosotros. Creo que somos un equipo maravilloso y el mejor regalo de la residencia. Gracias de corazón.

No podría olvidarme de mis compañeros de la UNICA que ya no son únicos sino múltiples. Gracias a Anaïs por compartir TOC conmigo, a Rodri por enseñarme a escalar o a Ivana por enseñarme a correr. A Marina, Oana, Ainhoa, Laura.R y Carmen por todos los momentos divertidos vividos en el laboratorio. Parte de este trabajo también es vuestro. Estoy seguro de que a todos os espera un futuro prometedor.

A Laura por este maravilloso último año y a Irene por haber estado desde el principio. A mi Granada, por recogerme siempre que lo necesito, darme paz, tranquilidad y poesía.

Para terminar y más importante, a mi familia y amigos. Estoy seguro de que a día de hoy siguen sin saber que es un linfocito y aun así, siguen preguntándome con el mismo entusiasmo. Ellos me han enseñado lo más importante: el amor, la amistad y el valor del esfuerzo, y por ello les dedico esta tesis.

Y por último, a ti mismo. Has tardado cinco años en entender que este proyecto no era el más importante ni tampoco único… Pero si el día de mañana logra ayudar a un paciente con cáncer, habrá sido extraordinario. Tu afán siempre ha sido entender por qué suceden las cosas. Pues bien, la ciencia es eso. Y por ello seguirá siendo

emocionante ver cómo las ideas se hacen realidad. A tus treinta años has conseguido todo lo que te has propuesto. Ahora ya sabes que el secreto del éxito es el fracaso.

Gracias

ÍNDICE

Página

ABREVIATURAS

AAT:	Antígeno asociado a tumor
Ac:	Anticuerpo
AcBis:	Anticuerpo biespecífico
AcMo:	Anticuerpo monoclonal
Ag:	Antígeno
ATTACK:	AcBis tipo TCE asimétrico (del inglés, *Asymmetric Tandem Trimerbody for T cell Activation and Cancer Killing*)
BCMA:	Antígeno de maduración de la célula B (del inglés, *B Cell Maturation Antigen*)
BiTE:	AcBis tipo TCE (del inglés, *Bispecific T cell Engager*)
BiTE-19:	TCE anti-CD19 x anti-CD3 en formato BiTE
CAR:	Receptor de antígeno quimérico (del inglés, *Chimeric Antigen Receptor*)
CAR-19:	CAR anti-CD19 de segunda generación
CAR-T:	Célula T que expresa un CAR
CAR-T19:	Célula T que expresa un CAR anti-CD19
CRISPR-Cas9:	Repeticiones palindrómicas cortas agrupadas y regularmente interespaciadas (del inglés, *Clustered Regularly Interspaced Short Palindromic Repeats-CRISPR-associated protein 9*)
cSMAC:	Complejo de activación supramolecular central (del inglés, *central SupraMolecular Activation Cluster*)
dSMAC:	Complejo de activación supramolecular distal (del inglés, *distal SupraMolecular Activation Cluster*)
ERK:	Quinasa regulada por señales extracelulares (del inglés, *Extracellular-signal Regulated Kinase*)
Fab:	Fragmento de unión al antígeno (del inglés, *Fragment antigen-binding*)
Fc:	Fragmento cristalizable de la inmunoglobulina (del inglés, *Fragment crystallizable*)
FcR:	Receptor Fc (del inglés, *Fc receptor*)
GFP:	Proteína verde fluorescente (del inglés, *Green Fluorescent Protein)*
IFN-γ:	Interferón gamma
KDEL:	Receptor 1 de retención de proteína del retículo endoplasmático (del inglés, *K-Lysine, D-Aspartic acid, E-Glutamic acid, L-Leucine*)
LAMP1:	Proteína asociada al lisosoma 1 (del inglés, *Lysosome-Associated Membrane glycoProtein 1)*
LiTE:	AcBis tipo TCE (del inglés, *Light T cell Engager*).
MHC:	Complejo principal de histocompatibilidad (del inglés, *Major Histocompatibility Complex)*
MOI:	Multiplicidad de infección (del inglés, *Multiplicity Of Infection*)

mRNA:	RNA mensajero (del inglés, *messenger RNA*)
NSG:	Ratones inmunodeficientes (del inglés, *NOD scid gamma*)
PB:	Sangre periférica (del inglés, *Peripheral Blood*)
PBMCs:	Células mononucleares de sangre periférica (del inglés, *Peripheral Blood Mononuclear Cells)*
PD-1:	Proteína de muerte celular programada 1 (del inglés, *Programmed cell Death protein 1*)
PD-L1:	Ligando 1 de muerte programada (del inglés, *Programmed Death-ligand 1)*
PDX:	Xenoinjerto derivado del paciente (del inglés, *Patient-Derived Xenograft*)
PLC-γ1:	Fosfolipasa C gamma 1
pSMAC:	Complejo de activación supramolecular periférico (del inglés, *peripheral SupraMolecular Activation Cluster*)
scFv:	Fragmento variable monocadena (del inglés, *single-chain fragment variable*)
sdAb:	Anticuerpo monodominio (del inglés *single-domain Antibody*)
SEE:	Enterotoxina E del estafilococo (del inglés *Staphylococcal Enterotoxin E*)
SI:	Sinapsis inmunológica
SMAC:	Complejo de activación supramolecular (del inglés, *SupraMolecular Activation Cluster*)
STAb:	Secreción de anticuerpos tipo TCE (del inglés, *Secreting T-cell redirecting Antibodies*)
STAb-T:	Célula T secretora de AcBis tipo TCE
STAb-T-CD19:	Célula T secretora de AcBis tipo TCE anti-CD19
TCE:	AcBis activador de células T (del inglés, *T Cell Engager*)
TCM:	Célula T de memoria central (del inglés *T Central Memory*)
TCR:	Receptor específico de la célula T (del inglés*, T Cell Receptor*)
tdTo:	Proteína fluorescente dTomato
TE:	Célula T efectora
TEM:	Célula T de memoria efectora (del inglés, *T Effector Memory)*
Tn:	Célula T naive
TNF-α:	Factor de necrosis tumoral alfa (del inglés, *Tumor Necrosis Factor-alpha*)
Treg:	Célula T reguladora
VCN:	Número de copias virales (del inglés, *Virus Copy Number*)
ZAP70:	Proteína quinasa 70 asociada a la cadena zeta (del inglés, *Zeta-chain-associated protein kinase 70)*

RESUMEN

La inmunoterapia del cáncer ha progresado considerablemente gracias al desarrollo de tratamientos potencialmente curativos para la leucemia linfoblástica aguda de células B (LLA-B). Las estrategias más efectivas se basan en el uso de anticuerpos biespecíficos (AcBis) anti-CD19 x anti-CD3 y terapias celulares adoptivas con linfocitos T modificados que expresan en su membrana un receptor de antígeno quimérico (CAR, del inglés, *Chimeric Antigen Receptor*) capaz de reconocer la molécula CD19 (CAR-T19). La administración de células CAR-T19 y la infusión sistémica de AcBis anti-CD19 x anti-CD3 en formato BiTE (del inglés, *Bispecific T cell Engager*), han demostrado una tasa de respuesta considerable en pacientes con LLA-B refractaria o en recaída (LLA-B R/R). Sin embargo, a pesar de los resultados obtenidos, un 30-60% de los pacientes recaen o progresan al año del tratamiento. En nuestro laboratorio se ha desarrollado la inmunoterapia STAb (del inglés, *Secretion of T cell redirecting Antibodies*)-T que consiste en la modificación de células T para que secreten AcBis activadores (TCEs, del inglés: *T Cell Engagers*).

En este trabajo hemos realizado un estudio comparativo para determinar la eficacia de las terapias CAR-T y STAb-T anti-CD19 en modelos de LLA-B. Además, hemos estudiado la topología de la sinapsis inmunológica (SI) inducida por ambas estrategias, con especial énfasis en la expresión y dinámica de las moléculas involucradas en la señalización y activación celular. Para el desarrollo de este estudio se generaron vectores lentivirales que codifican un CAR anti-CD19 (CAR-19) de segunda generación (4-1BB-CD3ζ) y un TCE anti-CD19 x anti-CD3 en formato BiTE (BiTE-19). Ambas construcciones están basadas en el anticuerpo (Ac) anti-CD19 A3B1, clínicamente validado. A partir de células T primarias y de una línea celular T se generaron, mediante transducción lentiviral, células STAb-T19 que secretaban BiTE-19 funcionalmente activo y activaban específicamente linfocitos T frente a células $CD19^+$. El BiTE-19 promovió la generación de SIs fisiológicas, con la formación de complejos de activación supramolecular central (cSMAC) y un aclaramiento de F-actina similar al observado en linfocitos T activados a través del receptor específico (TCR, del inglés, *T Cell Receptor*). Por el contrario, las células CAR-T19 formaron SIs con cúmulos de CD3ε dispersos y un aclaramiento de F-actina difuso.

Los ensayos de función linfocitaria demostraron la capacidad de las células STAb-T19 para inducir el reclutamiento policlonal de los linfocitos T no modificados, originando respuesta citotóxicas más rápidas y potentes que las inducidas por células CAR-T19. Además, las células STAb-T19 evitaron el escape leucémico *in vitro,* incluso a ratios de células T efectoras:células diana muy bajas. Por el contrario, las células CAR-T no controlaron el escape tumoral a ratios bajas, probablemente debido a la disminución de la expresión de CD19 en las células diana y de CAR-19 en las células efectoras. En modelos *in vivo*, utilizando xenoinjertos LLA-B derivados de líneas celulares y de muestras de pacientes (PDX), tanto las células STAb-T como las células CAR-T19 controlaron la leucemia a corto plazo. Sin embargo, en modelos PDX con tiempos observacionales más largos, en el grupo CAR-T19 se detectó recidiva leucémica a partir de la semana 4, mientras que el grupo tratado con las células STAb-T19 se mantuvo en remisión completa durante 13 semanas.

Estos resultados demuestran el potencial de la terapia STAb-T19 como alternativa a las estrategias de redirección de células T actualmente utilizadas en clínica y avalan la realización de ensayos clínicos para evaluar su eficacia y seguridad.

SUMMARY

Cancer immunotherapy has progressed significantly with the emergence of potentially curative strategies for B-cell acute lymphoblastic leukemia (B-ALL). The most effective approaches are based on the use of anti-CD19 x anti-CD3 bispecific antibodies, and adoptive cell therapies with engineered T lymphocytes expressing a chimeric antigen receptor (CAR) that recognizes the CD19 molecule (CAR-T19). The administration of CAR-T19 cells and the systemic infusion of anti-CD19 x anti-CD3 bispecific T cell engagers (BiTEs) have demonstrated a remarkable response rate in patients with refractory or relapsed B-ALL (R/R B-ALL). However, despite the excellent results reported, 30-60% of treated patients relapse or progress within one year of treatment. In our laboratory, we have developed the immunotherapy STAb (Secretion of T cell redirecting bispecific Antibodies)-T, which consists of the modification of T cells to secrete T cell engagers (TCEs).

We have performed a comparative study to determine the efficacy of anti-CD19 CAR-T and STAb-T therapies in B-ALL models. In addition, we have studied the topology of the immunological synapse (IS) induced by both strategies, with special emphasis on the expression and dynamics of molecules involved in cell signaling and activation. To conduct this study, lentiviral vectors encoding a second generation (4-1BB- CD3ζ) anti-CD19 CAR (CAR-19) and an anti-CD19 x anti-CD3 BiTE (BiTE-19) were generated. Both constructs are based on the clinically validated anti-CD19 A3B1 antibody. STAb-T19 cells, generated from primary T cells and from a T cell line by lentiviral transduction, secreted functionally active BiTE-19 and specifically activated T cells against $CD19^+$ cells. The BiTE-19 promoted the generation of physiological ISs, with the formation of central supramolecular activation complexes (cSMAC) and F-actin clearance similar to that observed in T cell receptor (TCR)-activated T cells. In contrast, CAR-T19 cells formed ISs with dispersed CD3 clusters and diffuse F-actin clearance.

Lymphocyte function assays demonstrated the ability of STAb-T19 cells to induce polyclonal recruitment of unmodified T cells, eliciting rapid and more potent cytotoxic responses than those induced by CAR-T19 cells. Moreover, STAb-T19 cells prevented leukemic escape *in vitro,* even at very low effector:target (E:T) cell ratios. On the contrary, CAR-T cells were not able to control tumor escape at low E:T ratios, probably due to the downmodulation of CD19 expression on target cells, and of CAR-19 on T cells. In *in vivo* studies performed with a leukemic B cell line- and with patient-derived

xenografts (PDX), STAb-T19 cells were as effective as CAR-T19 cells, eliciting complete remissions in short-term models. However, in PDX models with longer observational periods, the CAR-T19 group relapsed by week 4 post-treatment while the group treated with STAb-T19 cells remained in complete remission for 13 weeks.

These results demonstrate the potential of STAb-T19 therapy as an alternative to the T cell redirection strategies currently used in the clinic and support clinical trials to evaluate its efficacy and safety.

INTRODUCCIÓN

1. INMUNOLOGÍA E INMUNOTERAPIA DEL CÁNCER

La relación entre sistema inmune y cáncer ha suscitado gran interés y controversia desde los inicios de la inmunología como disciplina científica. En 1957 Lewis Thomas y Frank Macfarlane Burnet introdujeron el concepto de "vigilancia inmunológica del cáncer" (1), y esta hipótesis ha generado un prolongado debate sobre si la protección contra el cáncer es una función primaria del sistema inmune. Sin embargo, datos recientes apoyan claramente los principios básicos de la inmunovigilancia del cáncer y la capacidad del sistema inmune para reconocer y eliminar las células tumorales (2).

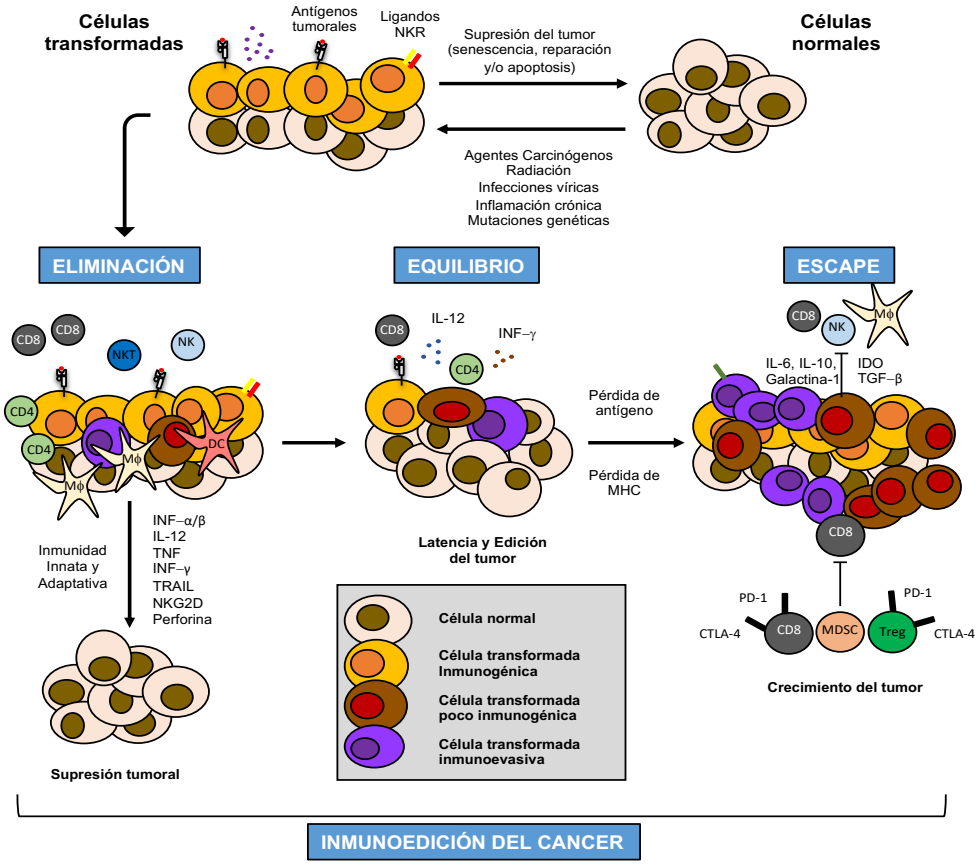

Figura 1. Teoría de la inmunoedición del cáncer. El proceso de inmunoedición del cáncer pasa por tres fases: eliminación, equilibrio y escape. Durante la fase de eliminación, la respuesta inmune innata y adaptativa cooperan para reconocer las células transformadas, que han escapado a los mecanismos de supresión intrínseca del tumor. Los tumores que superan la fase de eliminación pueden pasar a la fase de equilibrio, en la que el crecimiento es limitado y la inmunogenicidad es modulada por el sistema inmune adaptativo. Los tumores entrarían en la fase de escape, en la que podrían crecer, debido a mecanismos inmunosupresores y/o inmunoevasivos (3). Abreviaturas del inglés: IDO, *Indoleamine 2,3-Dioxygenase*; MDSC, *Myeloid Derived Suppressor Cells*; NKR, *NK receptor*; NKG2D, *Natural-Killer Group 2 member D*; TRAIL, *TNF-Related Apoptosis-Inducing Ligand*; Abreviaturas: CD4, célula T CD4; CD8, célula T CD8; Mϕ, macrófago; NK, célula asesina natural; NKT, célula T asesina natural; Treg, célula T reguladora.

Igualmente, se ha demostrado que el sistema inmune modula o esculpe la inmunogenicidad del tumor. Por ello, se ha propuesto el uso del término "inmunoedición del cáncer" para describir de forma más adecuada la interacción entre sistema inmune y el tumor (**Figura 1**) (2). La inmunoedición del cáncer es un proceso que evoluciona a lo largo de tres etapas sucesivas: eliminación, equilibrio y escape. Durante la fase de eliminación, el sistema inmune detecta y destruye las células tumorales. Sin embargo, si las células tumorales no son completamente eliminadas, entran en la fase de equilibrio en la que el sistema inmune controla el crecimiento tumoral. Durante este periodo pueden aparecer variantes tumorales que finalmente escapan al control del sistema inmune, dando lugar a la aparición de tumores clínicamente detectables (2). El impacto del proceso de inmunoedición es diverso, induciendo la eliminación completa de algunos tumores, generando respuestas inmunitarias no protectoras frente a otros o permitiendo el desarrollo de tumores menos inmunogénicos o que han adquirido mecanismos para evadir la acción del sistema inmune (4).

La inmunoterapia del cáncer se basa en la manipulación o utilización de diferentes componentes del sistema inmune para potenciar su respuesta, con el fin de vencer los mecanismos de escape y establecer respuestas antitumorales efectivas (5, 6) (**Figura 2**). El desarrollo de la inmunoterapia del cáncer durante las últimas décadas ha propiciado éxitos clínicos notables como el de los anticuerpos monoclonales (AcMos) que inhiben los puntos de control inmunológico (7), los anticuerpos biespecíficos (AcBis) o la terapia celular adoptiva con células CAR-T, células T modificadas genéticamente para que expresen en membrana un receptor de antígeno quimérico (CAR) (8). Estas estrategias han supuesto un punto de inflexión en el tratamiento de algunos tipos de cáncer (9, 10). Sin embargo, pese a los avances realizados, solo una proporción de pacientes oncológicos se beneficia de estas terapias, por lo que es necesario el desarrollo de nuevas estrategias de inmunoterapia antitumoral.

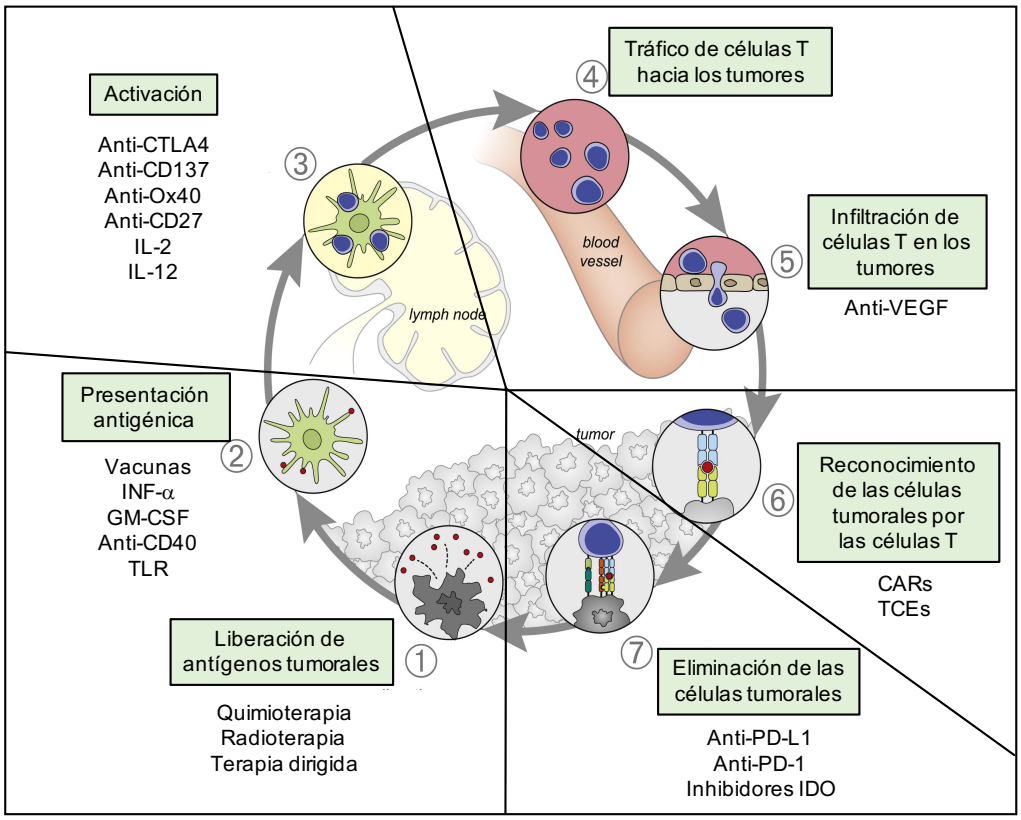

Figura 2. Estrategias terapéuticas para modular el ciclo de inmunidad del cáncer. En esta figura se ilustran algunas de las aproximaciones en desarrollo, a nivel preclínico o clínico, para modular los diferentes estadios del ciclo de inmunidad del cáncer. Abreviaturas del inglés: CAR, *Chimeric Antigen Receptor*; CTLA-4, *Cytotoxic T Lymphocyte Antigen 4*; GM-CSF, *Granulocyte Macrophage-Colony Stimulating Factor;* IDO, *Indoleamine 2,3-Dioxygenase*; PD-1, *Programmed Death 1*; PD-L1, *Programmed Death-Ligand 1*; TCE, *T cell Engager*; TLR, *Toll-Like Receptor;* VEGF, *Vascular Endothelial Growth Factor.* Figura modificada de (11).

2. ESTRATEGIAS ACTUALES DE INMUNOTERAPIA DEL CÁNCER BASADAS EN LA REDIRECCIÓN DE CÉLULAS T

En los últimos años han surgido diferentes abordajes de inmunoterapia basados en la redirección de las células T hacia antígenos asociados a tumor (AATs) expresados en la superficie de las células tumorales (12). La redirección está mediada por moléculas diseñadas para establecer uniones o "puentes artificiales" entre la célula T y el AAT de interés (9, 10). Dos de estas estrategias, la terapia celular adoptiva con células CAR-T y la administración de AcBis, están revolucionado el tratamiento de las neoplasias hematológicas (13).

2.1. Células CAR-T

Un CAR es un receptor sintético que permite al linfocito T reconocer específicamente un AAT, evitando la necesidad de interacción del TCR con el complejo bimolecular formado por el péptido procesado asociado con moléculas del complejo principal de histocompatibilidad (MHC, del inglés *Major Histocompatibility Complex*) (13). Así, las células CAR-T combinan la maquinaria de señalización dependiente del TCR con un reconocimiento antigénico TCR-independiente, lo que les permite reconocer un AAT que no es presentado en un contexto MHC. Por esta razón, la modificación de células T con un CAR específico para un AAT es aplicable a cualquier paciente, independientemente de su haplotipo MHC, y además elude algunos de los principales mecanismos de evasión de las células tumorales, como defectos en la presentación antigénica y la pérdida de expresión de MHC (14).

La estructura de un CAR de primera generación consta de: i) un dominio de reconocimiento extracelular, normalmente un fragmento variable monocadena (scFv, del inglés, *single-chain fragment variable*) formado por los dominios variables (V) de la cadena pesada (V_H) y ligera (V_L) de un AcMo, unidos mediante un conector peptídico flexible en una sola cadena polipeptídica; ii) una región transmembrana y iii) un dominio de señalización intracelular, en la mayoría de los casos derivado del CD3ζ, que actúa como secuencia activadora de la célula T (10, 15). La fusión en tándem con un dominio de co-estimulación derivado de CD28 o 4-1BB (CD137) es la base de los CARs de segunda generación. Los CARs de segunda generación han sido esenciales para el desarrollo clínico de las terapias CAR-T, ya que la co-estimulación es fundamental para una correcta activación de la célula T y, por tanto, para la proliferación, supervivencia, inducción de actividad citotóxica y secreción de citoquinas (16). Modificaciones posteriores han originado los denominados CARs de tercera, cuarta y quinta generación (**Figura 3**).

Los resultados obtenidos con células CAR-T en diferentes ensayos clínicos han derivado en la aprobación por la Administración de Alimentos y Medicamentos de los Estados Unidos (FDA, del inglés, *U.S. Food and Drug Administration*) y la Agencia Europea del Medicamento (EMA, del inglés, *European Medicines Agency*) de cinco productos CAR-T comerciales en neoplasias hematológicas (**Tabla 1**).

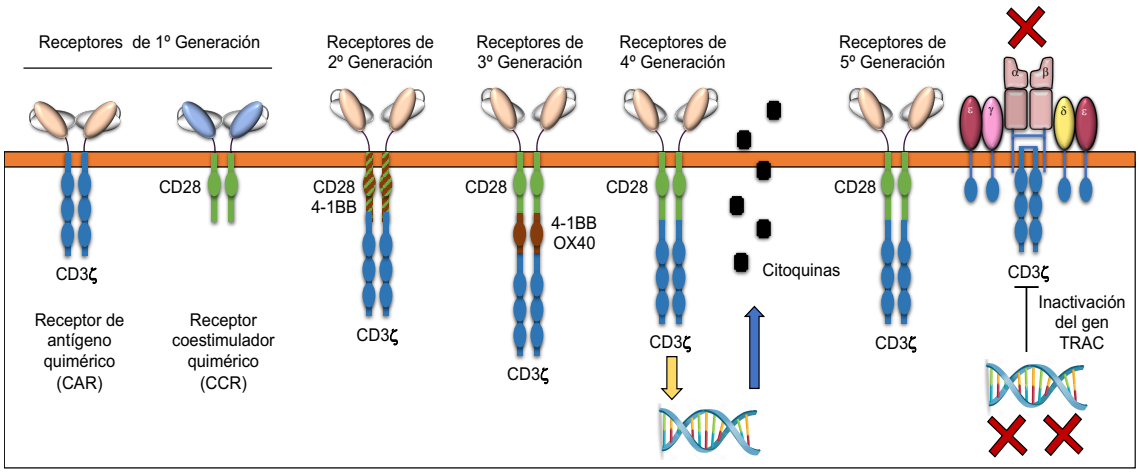

Figura 3. Diagrama esquemático que ilustra el desarrollo y evolución de los receptores quiméricos. Los receptores de primera generación presentaban un dominio de señalización único: CD3ζ en los CARs y CD28 en los CCRs. La fusión en tándem de un dominio de co-estimulación, derivado de CD28 o 4-1BB, y del CD3ζ es la base de los CARs de segunda generación. Los receptores de tercera generación incluyen dominios de co-estímulo adicionales (4-1BB u OX40). La cuarta generación de células CAR-T (también denominados TRUCKS, del inglés, *T cells Redirected for antigen-Unrestricted Cytokine-initiated Killing)* inducen la secreción de citoquinas tras la interacción del CAR con el antígeno diana. La quinta generación de CARs, utiliza la edición génica para inactivar el gen de la región constante de la cadena alfa del receptor específico de la célula T (TRAC del inglés, *T cell Receptor Alpha Chain*), lo que determina la pérdida de expresión del TCR$\alpha\beta$ (17).

Cuatro de estos productos están indicados en el tratamiento de leucemias (18) y linfomas CD19$^+$ (19): *tisagenlecleucel* (2017) (20), *axicabtagene ciloleucel* (2018) (20), *brexucabtagene autoleucel* (2020) (20) y *lisocabtagene maraleucel* (2021). En el año 2021 se aprobó un CAR-T específico para el antígeno de maduración de la célula B (BCMA, del inglés, *B Cell Maturation Antigen*), *idecabtagene vicleucel* (20), para el tratamiento de pacientes con mieloma múltiple. Todos los productos aprobados son CAR de segunda generación, formados por un scFv anti-CD19 (21, 22) o anti-BCMA (20), un dominio de co-estímulo [4-1BB (21) o CD28 (22)] y el dominio de señalización CD3ζ. Cabe destacar que, recientemente la EMA ha aprobado el CAR académico ARI-0001 para el tratamiento de neoplasias hematológicas, consiguiendo la designación PRIME (del inglés, *Priority Medicines*) (**Tabla 1**).

El uso clínico de las células CAR-T se ha visto limitado por diferentes tipos de reacciones adversas (23). El síndrome de liberación de citoquinas y la neurotoxicidad constituyen efectos secundarios graves que pueden originar la muerte del paciente (24). En neoplasias sólidas, la estrategia CAR-T se enfrenta a desafíos adicionales, como las toxicidades asociadas a la expresión de AAT en tejidos sanos (toxicidad *on-target/off-tumor*) (23, 25) o la existencia de microambientes muy inmunosupresores.

Estudios clínicos realizados con terapias CAR-T anti-CD19 han demostrado que un 30-60% de los pacientes que alcanzan remisión completa recidiva en el plazo de un año (26), debido a múltiples factores, como la persistencia limitada de las células CAR-T o la pérdida de expresión del Ag diana (26, 27), entre otros. Por otra parte, diversos estudios han cuestionado la idoneidad de la estructura de la sinapsis inmunológica (SI) durante la interacción CAR-AAT, demostrando la formación de sinapsis "no canónicas", multifocales y desorganizadas, muy diferente de la SIs fisiológicas promovidas por la interacción TCR-péptido-MHC (28-30). Los estudios para analizar la estructura de la SI se deberán incluir en la hoja de ruta para el desarrollo de CARs de nueva generación más seguros y eficaces (31).

Tabla 1: CAR-T aprobados en neoplasias hematológicas.

		Comerciales					Académicos
Nombre Comercial Promotor		**Yescarta™ Kite/Gilead**	**Kymriah™ Novartis**	**Tecartus™ Kite/Gilead**	**Breyanzi™ Bristol-Myers Squibb**	**Abecma™ Bristol-Myers Squibb**	**ARI-0001 Hospital Clinic**
Nombre genérico Abreviatura		Axicabtagén Ciloleucel (Axi-cel)	Tisagenlecleucel (Tisa-cel)	Brexucabtagene Autoleucel (Brexu-cel)	Lisocabtagene Maraleucel (Liso-cel)	Idecabtagene Vicleucel (Ide-cel)	Varnimcabtagene autoleucel
Especificidad clon	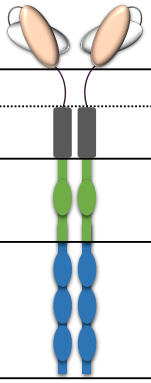	anti-CD19 FMC63	anti-CD19 FMC63	anti-CD19 FMC63	anti-CD19 FMC63	anti-BCMA -	anti-CD19 A3B1
Region bisagra		IgG_1	CD8A	CD8A	IgG_4	CD8A	CD8A
Dominio transmembrana		IgG_1	CD8A	CD8A	IgG_4	CD8A	CD8A
Dominio de Co-estimulación		CD28	4-1BB	CD28	4-1BB	4-1BB	4-1BB
Dominio de Señalización		CD3ζ	CD3ζ	CD3ζ	CD3ζ	CD3ζ	CD3ζ
Indicaciones		LBDCG LBPM	LBDCG LLA-B	LCM	LBDCG LBPM LF3B	MM	LLA-B

Abreviaturas: LBDCG, Linfoma B Difuso de Células Grandes; LBPM, Linfoma B Primario Mediastínico de Células Grandes; LCM, Linfoma de Células del Manto; LLA-B, Leucemia Linfoblástica Aguda de Células B; LF3B, Linfoma Folicular de grado 3B; MM, Mieloma Múltiple.

2.2. Anticuerpos biespecíficos

En condiciones fisiológicas las inmunoglobulinas G (IgG) son moléculas monoespecíficas bivalentes. La excepción son las moléculas IgG_4 que, debido a un único cambio de aminoácido en la región bisagra, pueden intercambiar una unidad de cadena-pesada cadena-ligera (lo que se denomina "intercambio de medio anticuerpo") para formar moléculas biespecíficas (32-34). El diseño seminal de los AcBis artificiales se

propuso hace 60 años cuando se re-asociaron dos fragmentos de unión al antígeno (Fabs) derivados de dos anticuerpos policlonales en moléculas $F(ab')_2$ biespecíficas (35).

Como se ilustra en la **Figura 4**, los tres componentes básicos para la generación de un AcBis son: (i) los dominios de unión al antígeno (Ag); (ii) el núcleo de multimerización que determina la formación de homo o hetero-multímeros; y (iii) los péptidos flexibles que conectan los diferentes bloques. Los dominios de unión al Ag pueden ser fragmentos derivados de anticuerpos, como Fabs, scFvs, anticuerpos monodominio (sdAbs, del inglés *single-domain antibodies*), o alternativamente "miméticos de anticuerpos", proteínas artificiales con un tamaño variable (3 a 20 kDa) y capacidad de unión al Ag. Recientemente, los AcBis han incorporado como dominios de unión al Ag las regiones extracelulares de determinados receptores de membrana o ligandos naturales. Se han utilizado diferentes estrategias para inducir la multimerización, como las fusiones genéticas, los sistemas de intercambio de dominios o diferentes péptidos y dominios proteicos con capacidad de formar homo o hetero-multímeros (**Figura 4**).

Actualmente existen múltiples plataformas tecnológicas que han permitido generar más de 100 formatos de AcBis diferentes con un control preciso sobre la valencia, la estequiometría, el tamaño, la flexibilidad y las propiedades farmacocinéticas (36, 37). El concepto de *multitargeting* que permiten los AcBis es especialmente atractivo desde el punto de vista terapéutico, ya que numerosas patologías son multifactoriales, con la intervención de múltiples receptores, ligandos y cascadas de señalización. En consecuencia, el bloqueo o la modulación de varios factores y vías patológicas pueden ser determinantes para obtener una eficacia terapéutica superior. Una característica interesante de los AcBis es su potencial para promover la interacción entre dos tipos celulares diferentes (*trans co-engagement*) o entre dos moléculas diferentes expresadas en la misma membrana celular (*cis co-engagement*).

Una de las áreas de mayor actividad en el campo de los AcBis es la que persigue reclutar, redirigir, y/o potenciar efectores inmunes. Las moléculas más utilizadas para el reclutamiento y activación de las células del sistema inmune son los receptores FcR para el fragmento cristalizable (Fc) y las cadenas del complejo TCR/CD3. La evolución de las técnicas de ingeniería de anticuerpos ha permitido generar numerosos AcBis con

capacidad de redirigir a las células T hacia las células tumorales, estableciendo un "puente" entre un AAT y la cadena CD3ε del complejo TCR/CD3. Estos AcBis activadores de células T (TCE, del inglés *T Cell Engagers*) originan la activación, proliferación, y secreción de citoquinas y desencadenan funciones citolíticas, como la liberación de perforina, granzimas y granulisina.

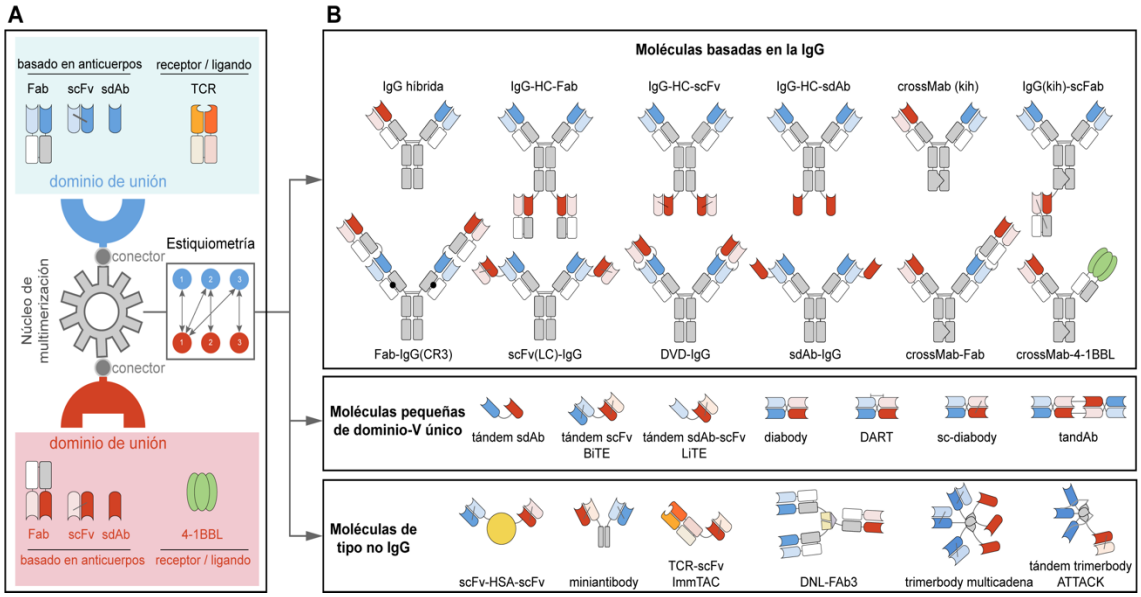

Figura 4. Representación esquemática de los componentes básicos de un AcBis y de algunas de las principales estrategias utilizadas para su generación. (A) Para la generación de un AcBis se requieren tres componentes fundamentales: los dominios de unión, el "núcleo de multimerización" que permite la formación de homo o hetero-multímeros, y los conectores flexibles. Los dominios de unión pueden derivar de anticuerpos, como Fabs, scFvs o sdAbs; o de receptores y/o ligandos naturales. Existen múltiples plataformas tecnológicas que permiten ajustar la valencia, el tamaño y la estequiometría (A y B). En la configuración más sencilla, un AcBis contiene un sitio de unión para cada antígeno (1 + 1), pero se han generado formatos con estequiometrías de 1 + 2, 1 + 3, 2 + 2 o 3 +3 (A y B). (B) Los AcBis simétricos basados en IgG contienen regiones constantes de la cadena pesada (HC, del inglés, *Heavy Chain*); los AcBis basados en IgG asimétricos contienen HC modificadas para forzar la heterodimerización, como la estrategia "*knobs-into-holes*" (kih). Los dominios de unión se pueden fusionar directamente, lo que origina moléculas de pequeño tamaño formados por dominios variables (V). Como alternativa, se pueden fusionar los dominios de unión con otras proteínas, como la albúmina sérica humana (HSA, del inglés, *Human Serum Albumin*), los dominios de homotrimerización del colágeno humano, etc. Abreviaturas del inglés: ATTACK, *Asymmetric Tandem Trimerbody for T-cell Activation and Cancer Killing*; DART, *Dual Affinity Retargeting*; DNL, *Dock-aNd-Lock*; DVD-Ig, *Dual Variable Domain Immunoglobulin*; LiTE, *bispecific Light T cell Engager*; tandAb, *tandem diabody.* Figura modificada de (38).

Uno de los principales problemas de los TCEs de primera generación era consecuencia de la inclusión de regiones Fc con capacidad de interaccionar con células FcR^+, originando fenómenos de activación *"off-target"* que pueden dar lugar al desarrollo de síndromes de liberación de citoquinas muy intensas (37, 39). Para evitar este problema se diseñó una nueva generación de TCEs que, o bien incluyen regiones Fc modificadas o "silenciadas", para evitar la interacción con los FcRs, o bien no incluyen regiones Fc (36). Entre estos últimos, también denominados TCE "*Fc-free o Fc-less*"

destacan aquellos formatos basados en scFvs y sdAbs (**Figura 4**). Los *diabodies* (dAbs) se generan mediante el apareamiento de dos scFvs en los que los dominios V_H y V_L están unidos por conectores cortos que impide su apareamiento intramolecular (40) (**Figura 4**). Los tándem scFvs (ta-scFvs), más comúnmente conocidos como BiTEs, están formados por dos scFvs conectados mediante un péptido flexible (41) (**Figura 4**). Los TCEs no proporcionan señal de co-estimulación, por lo que podría esperarse que indujeran respuestas linfocitarias menos eficientes. Sin embargo, diversos estudios con BiTEs que reconocen diferentes AATs han demostrado que este tipo de TCEs son capaces de desencadenar potentes respuestas anti-tumorales sin necesidad de señal de co-estímulo (42, 43). Aunque se desconoce la razón por la que la señal co-estimuladora es dispensable, se han propuesto distintas hipótesis, entre ellas, que las células T de memoria, que son menos dependientes de las señales co-estimuladoras, sean los efectores predominantes en las respuestas citotóxicas mediada por BiTEs. Por otra parte, la activación mediada por BiTEs podría promover la agrupación de complejos TCR, lo que favorecería la señalización (44). Además, se ha demostrado que la interacción del BiTE con el AAT induce la formación de SIs canónicas, con una morfología prácticamente idéntica a la inducida por el TCR (45).

Las estrategias terapéuticas basadas en AcBis están en expansión y actualmente hay más de cien prototipos en fase de ensayo clínico (46), aunque solo tres de ellos (*blinatumomab, emicizumab y amivantamab*) están actualmente aprobados para su uso clínico (**Tabla 2** (**Anexos**)). El *blinatumomab,* un TCE anti-CD19 x anti-CD3 en formato BiTE, fue aprobado por la FDA en 2008 para el tratamiento de la LLA-B refractaria (47) y la enfermedad mínima residual positiva en LLA-B (48). A pesar de las respuestas clínicas obtenidas con el *blinatumomab* (49-51), el desarrollo de los TCEs se enfrenta a retos importantes. Así, la eliminación de la región Fc no elimina completamente la toxicidad, como el desarrollo de cuadros de "tormenta" de citoquinas o neurotoxicidad. Por otra parte, debido al pequeño tamaño de este tipo de moléculas, su vida media plasmática corta obliga a una administración intravenosa continua mediante bombas de infusión para alcanzar niveles séricos terapéuticos (52), lo que dificulta y encarece este tipo de tratamientos.

3. NUEVAS ESTRATEGIAS DE INMUNOTERAPIA DEL CÁNCER BASADAS EN LA REDIRECCIÓN DE CÉLULAS T

Como se ilustra en la **Figura 5**, tanto la terapia celular adoptiva con células CAR-T como la administración sistémica de TCEs presentan algunas limitaciones. Por este motivo, nuestro grupo ha desarrollado una nueva estrategia de inmunoterapia denominada STAb (del inglés, *endogenous **S**ecretion of **T** cell-redirecting **A**nti**b**odies),* basada en la secreción de TCEs por células modificadas. Esta estrategia combina algunas ventajas de las terapias con TCEs y con células CAR-T y solventa algunas de sus limitaciones (**Figura 5**).

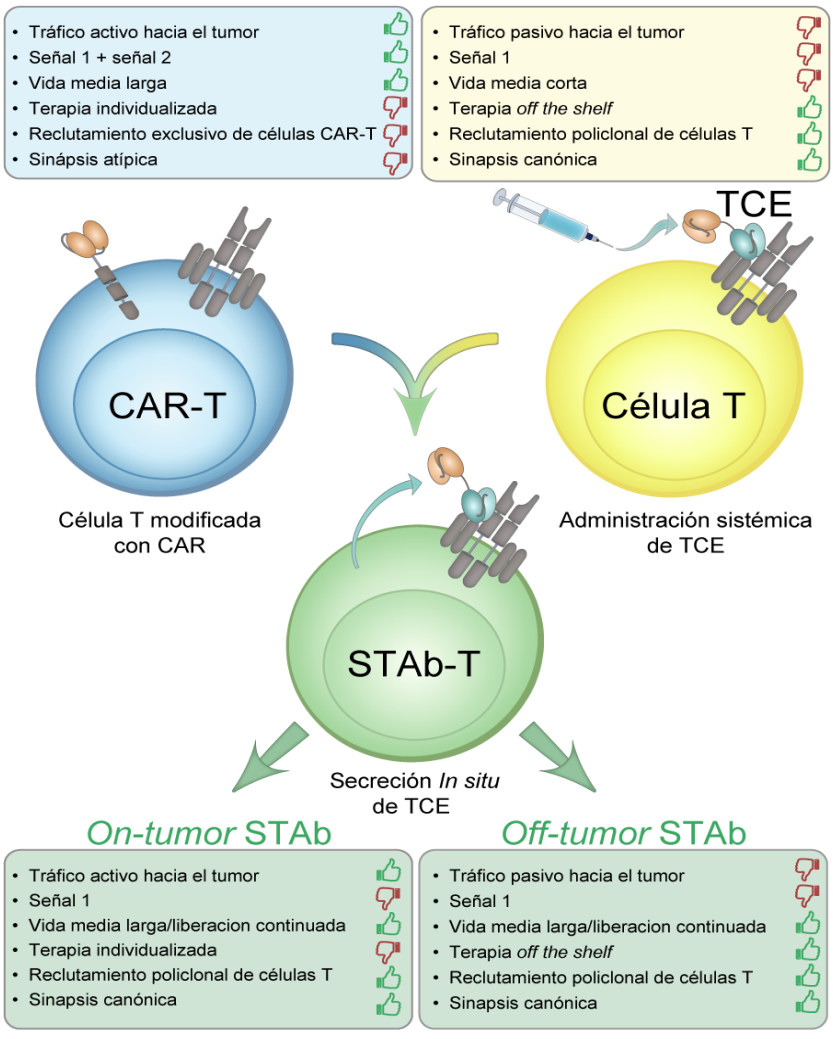

Figura 5. Ventajas y limitaciones de las estrategias de redirección de células T. Representación esquemática de las principales ventajas (pulgares arriba) y desventajas (pulgares abajo) de las estrategias de redirección de células T actuales, como son las células CAR-T (azul) y la administración sistémica de AcBis (amarillo), así como de la estrategias de nueva generación basadas en la secreción *in situ* de AcBis por parte de células modificadas genéticamente (STAb, verde). Las estrategias STAb se clasifican en *on-tumor* y *off-tumor*, dependiendo de si los TCEs son secretados intratumoralmente o en una localización distante del tumor. Figura modificada de (13).

La estrategia STAb permite una secreción constante de TCEs a largo plazo, lo que compensaría el rápido aclaramiento de moléculas tipo BiTE y permitiría alcanzar concentraciones terapéuticas efectivas (13). Por otro lado, la secreción *in vivo* reduciría los problemas asociados a la formulación y almacenamiento de los AcBis a largo plazo, evitando su agregación y deterioro (13, 53). Un aspecto muy relevante de la estrategia STAb es su capacidad para inducir, en contraposición con la terapia CAR-T, el reclutamiento policlonal de las células T no modificadas (9), lo que permitiría amplificar significativamente la respuesta anti-tumoral (9).

En el diseño de terapias STAb hay que tener en cuenta factores como el método de modificación genética, el tipo de célula a modificar o el formato del TCE secretado. El tipo de neoplasia y los AATs diana también son factores determinantes. Las terapias STAb se clasifican como *on-tumor y off-tumor* en función de si el TCE se secreta en el entorno tumoral o en localizaciones distantes.

3.1. Inmunoterapias STAb *on-tumor*

Una alternativa atractiva a la administración sistémica de TCEs, especialmente en el caso de tumores sólidos, es la secreción *in situ* por células modificadas con capacidad de migrar hacia el tumor (13). La secreción intratumoral de TCEs podría evitar los problemas de penetración tumoral, vida media sérica corta y toxicidad sistémica (13). En 2003 se demostró por primera vez la posibilidad de modificar células humanas para secretar un TCE anti-antígeno carcinoembrionario (CEA) x anti-CD3 en formato dAb funcionalmente activo. Los dAbs secretados eran capaces de redirigir y activar *in vitro* linfocitos T frente a células CEA^+ (54). Además, la inoculación intratumoral de células STAb retrasó significativamente el crecimiento tumoral en modelos de cáncer colorrectal humano en ratones inmunodeficientes. En un estudio posterior se describió la generación, mediante transducción lentiviral, de células STAb-T humanas secretoras de dAbs anti-CEA x anti-CD3 y se demostró que su administración intratumoral retrasaba significativamente el crecimiento de tumores humanos (55). Más recientemente, un estudio con células STAb-T secretoras de un BiTE anti-efrina A2 (EphA2) x anti-CD3 ha demostrado la capacidad de reclutar, *in vitro,* células T no modificadas frente al tumor

y de inducir potentes respuestas antitumorales *in vivo* en modelos de cáncer de pulmón (56).

El concepto de STAb *on-tumor* también puede utilizarse en el contexto de tumores hematológicos (57). De hecho, el éxito de las células CAR-T en el tratamiento de neoplasias de células B se atribuye, al menos parcialmente, a la mayor accesibilidad de las células T infundidas a las células leucémicas. En este sentido, se ha demostrado que la infusión de células STAb-T transducidas retroviralmente para secretar un TCE anti-CD19 x anti-CD3 en formato BiTE induce la regresión tumoral en modelos murinos de leucemia (58). En otro estudio se demostró cómo células STAb-T transfectadas con un mRNA que codifica un BiTE anti-CD19 x anti-CD3 tienen un efecto antitumoral superior al de las células CAR-T anti-CD19, induciendo remisión completa *in vivo* (57). También se ha descrito la generación de células STAb-T que secretan un BiTE anti-CD123 x anti-CD3 con capacidad de redirigir a los linfocitos T hacia las células $CD123^+$ e inducir regresiones en modelos de leucemia mieloide aguda (59). Todos estos estudios demuestran la eficacia de la estrategia STAb y la potencial utilidad de las células T como vehículos, aprovechando su capacidad de migrar hacia el tumor una vez infundidas, y secretar TCEs *in situ* (56). Por tanto, las células STAb-T no solo actúan como células efectoras, sino como factorías celulares de TCEs con potencial para reclutar todo el repertorio de células T circundante (56).

Existen numerosos factores a tener en cuenta a la hora de generar un producto terapéutico con células T, como el estadio madurativo o las subpoblaciones celulares a infundir. Así, se ha observado que los estadios menos diferenciados, como el de célula T de memoria central (TCM, del inglés *T Central Memory*) o célula T tipo *stem,* permiten una mejor expansión, persistencia *in vivo* y actividad antitumoral (60, 61). También se ha observado que los productos con una proporción más alta de células $CD8^+$ tienen mayor potencial citotóxico, pero menor persistencia que los productos con más células $CD4^+$ (57).

Podemos considerar otros tipos celulares como posibles factorías de anticuerpos en estrategias STAb *on-tumor*, entre los que destacan los macrófagos, debido a su capacidad de penetrar en el tumor y sobrevivir en el microambiente tumoral (62), aspectos en los que la célula T presenta ciertas desventajas. Otra alternativa atractiva

sería la utilización de células NK, ya que poseen actividad antitumoral intrínseca y es posible el uso de células NK alogénicas sin riesgo de desarrollar enfermedad injerto contra huésped (63). Dado que tienen una vida media más corta que la del linfocito T, las células NK podrían resultar de interés en escenarios en los que se pretenden reducir los posibles efectos adversos *on-target/off-tumor* (64). Finalmente, se han desarrollado estrategias STAb *on-tumor* que no derivan de células hematopoyéticas, como las basadas en el uso de células progenitoras mesenquimales (MSCs, del inglés *Mesenchymal Stem Cells*). El uso de MSCs es muy interesante debido a su fácil aislamiento, expansión y modificación genética (65). Además son células muy poco inmunogénicas, lo que permite su uso como terapia *off-the-shelf* (66). Sin embargo, esta estrategia no está exenta de riesgos, ya que las MSCs también se han implicado en procesos proangiogénicos y de inmunosupresión (67), pudiendo contribuir potencialmente al desarrollo del tumor primario y su diseminación (68).

3.2. Inmunoterapias STAb *off-tumor*

Como alternativa a la administración sistémica, las células STAb, pueden embeberse en matrices biocompatibles que les proporcionen los factores de crecimiento necesarios para la supervivencia del injerto *in vivo* (69). En este modelo, las células STAb se pueden implantar en localizaciones distantes al tumor, e incluso ser retiradas una vez obtenido el efecto terapéutico deseado. La primera demostración de este concepto se realizó a través de la modificación génica de MSCs para secretar un TCE anti-CEA x anti-CD3 en formato dAb y su posterior encapsulación en una matriz no inmunogénica, que fue implantada subcutáneamente en ratones (70). Mediante este sistema se consiguió una liberación prolongada de niveles terapéuticos del TCE durante aproximadamente seis semanas post-implantación. La liberación constante al torrente circulatorio indujo respuestas antitumorales *in vivo* (70). Esta estrategia podría utilizarse como terapia *off-the-shelf*, ya que, debido a la baja inmunogenicidad y a las propiedades inmunomoduladoras de las MSCs, podrían ser implantadas en cualquier paciente (71). Sin embargo, algunos estudios han demostrado que, a pesar de su baja inmunogenicidad, las MSC alogénicas no son completamente invisibles al sistema inmune (71). Por ello es importante desarrollar sistemas de encapsulación para que las

células STAb-MSC permanezcan viables y la liberación sistémica del TCE sea lo más prolongada posible. Estos sistemas de encapsulación celular están en constante evolución y diversos grupos han desarrollado estructuras basadas en matrices de alginato (72) o redes microvasculares (67, 73), que permiten una liberación prolongada de Acs.

Recientemente han surgido otras aproximaciones muy interesantes que utilizan vectores no celulares para inducir la secreción de TCEs *in situ*. Una de ellas se basa en el uso de RNA. De hecho, hay estudios que demuestran que la administración intravenosa de mRNAs modificados que codifican para TCEs anti-TAA x anti-CD3 (74) originan la secreción de TCEs e inducen la eliminación de xenoinjertos de carcinoma de ovario en modelos murinos humanizados. Otra aproximación se basa en el uso de mcDNA (del inglés, *minicircle DNA*) o vectores no virales de DNA que codifican TCEs. Se ha demostrado la capacidad de un mcDNA que codifica para un TCE anti-CD20 x anti-CD3 en formato BiTE para inducir respuestas antitumorales significativas en un modelo murino de linfoma B (75).

4. PERSPECTIVAS Y ESTRATEGIAS PARA MEJORAR EL EFECTO TERAPÉUTICO DE LAS CÉLULAS STAb-T

Las estrategias STAb han mostrado efectos terapéuticos prometedores en modelos preclínicos de tumores sólidos y hematológicos. Aun así, para trasladar estas terapias a la clínica es necesario desarrollar nuevas estrategias para mejorar su eficacia y seguridad. Los tumores sólidos constituyen uno de los retos más importantes. El microambiente tumoral dificulta el acceso de las células T, ya que está enriquecido en citoquinas, ligandos y receptores inmunosupresores que favorecen su hipofunción y agotamiento (76). Además, el microambiente favorece el reclutamiento de células capaces de bloquear respuestas inmunes anti-tumorales, como las células supresoras mieloides o las células T reguladoras (Tregs) (76). Respecto a las neoplasias hematológicas, las recidivas suponen una limitación importante (77).

4.1. Estrategias para mejorar la migración, persistencia y expansión de las células T en el tumor

Una de las principales limitaciones de la terapia celular adoptiva es la dificultad de las células T para infiltrar el tumor de forma eficiente. Estudios recientes han demostrado que la expresión intratumoral de ciertas quimiocinas como CCL2, CCL3, CCL4, CCL5, CXCL9 y CXCL10 incrementa la infiltración de células T en melanoma (78). Estos resultados han propiciado el desarrollo de estrategias destinadas a mejorar el tráfico de la célula T hacia el tumor, a través de la modificación para expresar receptores de quimiocinas (79, 80). Una vez que la célula T alcanza el tumor, es fundamental promover su persistencia y expansión para obtener un efecto anti-tumoral significativo (81). Esto se demostró con las células CAR-T de primera generación, carentes de dominio de co-estimulación (82, 83). La introducción de un dominio derivado de 4-1BB o de CD28 resultó en el aumento de la proliferación, la secreción de citoquinas y la resistencia a la apoptosis, lo que se tradujo en un incremento de la persistencia *in vivo* y de la eficacia terapéutica (82, 83). Por otra parte, aunque se ha demostrado en modelos preclínicos la eficacia anti-tumoral de células STAb-T secretoras de TCEs anti-CD19 x anti-CD3 en formato BiTE en tumores hematológicos (57), la provisión de señales de co-estímulo podría mejorar su eficacia en tumores sólidos (84). Así, se ha comprobado que la activación de células T por un TCE anti-EGFR x anti-CD3 en formato BiTE originó una población de células fenotípicamente agotadas, con capacidad proliferativa reducida y escasa persistencia, en comparación con células modificadas con un CAR anti-EGFRvIII de segunda generación (84). Estas diferencias podrían deberse al efecto de la co-estimulación mediada por 4-1BB (84).

En este contexto, nuestro grupo desarrolló una estrategia en la que la célula STAb-T secretaba de forma simultánea un TCE anti-CEA x anti-CD3 en formato dAb y un ligando de co-estímulo tumor-específico que comprendía la región extracelular de CD80 fusionada a un anticuerpo anti-CEA (85). La secreción simultánea de ambas moléculas por células STAb incrementó la actividad antitumoral en modelos de cáncer colorrectal humano en ratones (9). Más recientemente, se ha demostrado que la expresión de CD80 y del ligando de 4-1BB (4-1BBL) en la superficie de células STAb-T aumenta su actividad antitumoral *in vivo* (86). Además, la secreción de citoquinas, como IL-12 o IL-18, junto

con los TCEs, podría aumentar la potencia, expansión y persistencia *in vivo* de las células STAb-T, como se ha documentado con las células CAR-T (87-89). Por otra parte, para reducir la toxicidad asociada a la expresión constitutiva de las citoquinas, se han utilizado promotores que restringen su expresión a las células CAR-T activadas (90, 91). Por lo tanto, sería posible desarrollar sistemas similares para mejorar la eficacia de las células STAb-T.

4.2. Estrategias para evitar el agotamiento de las células T

El receptor de muerte celular programada 1 (PD-1) desempeña un importante papel en la inhibición de las respuestas inmunitarias mediadas por células T. El bloqueo de la interacción de PD-1 con su ligando PD-L1 puede inducir respuestas antitumorales prolongadas y reducir la disfunción de las células T en diversos tipos de tumores sólidos (92) y hematológicos (93). Varios AcMos anti-PD-1 y anti-PD-L1 han sido aprobados para uso clínico (7) y se ha demostrado en estudios preclínicos que la administración conjunta con células CAR-T (94, 95) o TCEs (96) puede mejorar su actividad antitumoral. Además, diversos trabajos han demostrado el potencial terapéutico de células CAR-T que secretan Acs anti-PD-1 o anti-PD-L1, algunas de las cuales se encuentran actualmente en ensayo clínico (97). Por otro lado, los avances en técnicas de edición genómica, como el sistema CRISPR-Cas9, han permitido desactivar el gen PD-1 en células T y CAR-T, inhibiendo el agotamiento celular (98). Todas estas aproximaciones podrían implementarse fácilmente en la terapia STAb-T para mejorar su eficacia terapéutica.

4.3. Estrategias para la prevención del escape tumoral

La presión selectiva de las inmunoterapias Ag-específicas conduce, en algunos casos, a la aparición o selección de células tumorales que no expresan el Ag diana y que, escapan al tratamiento, dando lugar a la aparición de recidivas (99). Este fenómeno se ha observado en pacientes con LLA-B tratados con células CAR-T anti-CD19, en los que un 10-20% de las recaídas son $CD19^-$ (26, 99). Parece que la pérdida del CD19 es menos frecuente en los pacientes tratados con *blinatumomab* (100). Se han propuesto varios mecanismos para explicar la pérdida del Ag diana, como la acumulación de mutaciones

genéticas y epigenéticas durante la progresión del tumor y/o la selección de variantes Ag-negativas debido a la presión inmunitaria (26). También se ha postulado que la trogocitosis, un proceso por el cual los linfocitos capturan fragmentos de la membrana plasmática de las células presentadoras de antígeno y los expresan en su propia superficie (101), ocurre tras la interacción de las células CAR-T con el CD19 expresado en la membrana de las células tumorales (102). La trogocitosis conduce a una pérdida reversible de Ag, que reduce la densidad de AAT en las células tumorales y, por tanto, su capacidad de ser reconocidas y eliminadas por las células CAR-T. Además, la transferencia de CD19 de las células leucémicas a las células CAR-T promueve la muerte por fratricidio de los linfocitos T y su agotamiento (102). Este fenómeno podría ser una característica general de las células CAR-T, ya que se ha observado con CARs específicos frente a diferentes Ags (102). Con respecto a las terapias de redirección de células T mediadas por BiTEs, hasta el momento no se han descrito mecanismos de trogocitosis del Ag diana, aunque son necesarios estudios adicionales para comprobar que no se produce dicho fenómeno en este contexto de redirección celular T.

Así pues, el desarrollo de aproximaciones que permitan evitar el escape de las células tumorales debido a la pérdida del Ag diana es una prioridad. Se han diseñado numerosas estrategias de redirección simultánea frente a dos Ags diferentes en modelos preclínicos de LLA-B y glioblastoma, administrando células CAR-T dirigidas a dos AATs distintos (77, 103), células T modificadas para expresar dos CARs diferentes en su superficie (CARs duales) o CAR biespecíficos (tándem CARs) (77, 103). En las terapias de redirección basadas en TCEs, la interacción simultáneamente con varios AATs ha demostrado una actividad antitumoral más potente que cuando se actúa frente a un AAT único (104, 105). Estas observaciones reflejan la importancia de desarrollar células STAb capaces de secretar TCEs con especificidades diferentes o incluso anticuerpos triespecíficos, con el fin de evitar el escape tumoral.

4.4. Estrategias basadas en nuevos formatos de anticuerpo

La ingeniería de Acs está en constante evolución con el objetivo de diseñar moléculas que mejoren la especificidad y los efectos inmunoestimuladores, al tiempo que reduzcan potenciales toxicidades. El diseño de TCEs debe ser preciso, ya que

numerosos estudios han demostrado fenómenos de activación y proliferación de células T independientes del Ag diana, debido probablemente a la agregación del TCE (106). Además de los dAbs y los BiTEs existen múltiples formatos de TCEs que se han utilizado para redirigir células T y que podrían ser considerados para su uso en el contexto de la terapia STAb. Un formato atractivo para las estrategias STAb-T *on-tumor* podría ser el LiTE (del inglés, *Light T cell Engager)*. Este TCE, que constituye una alternativa al formato BiTE, está formado por un sdAb específico para un AAT, fusionado en tándem a un scFv anti-CD3 (107). Debido a su menor tamaño (40 kDa) los TCEs en formato LiTE podrían alcanzar áreas del tumor no accesibles para moléculas más voluminosas. Se ha demostrado que un LiTE anti-EGFR x anti-CD3 induce la activación y la actividad citotóxica de células T específicamente frente a células tumorales $EGFR^+$ (107).

Otro diseño muy interesante es el ATTACK, un TCE que combina tres sdAbs específicos para un AAT unidos a un scFv anti-CD3. Este TCE es capaz de redirigir la célula T frente a células tumorales $EGFR^+$ con mayor eficacia que los BiTEs convencionales (108). Este formato podría reducir la potencial toxicidad asociada al tratamiento, ya que la combinación de múltiples dominios de unión anti-AAT de baja afinidad permitiría discriminar entre células que expresan bajos niveles del AAT (tejidos normales) y células que sobre-expresan el AAT (células tumorales) (108).

5. LA SINAPSIS INMUNOLÓGICA

Un aspecto fundamental a tener en cuenta con respecto a las estrategias de redirección de células T es la topología de la SI (109), estructura que contribuye de manera esencial a la activación e inducción de funciones efectoras. La interacción del TCR con el complejo péptido-MHC, expresado en la membrana de la célula diana, conduce a la formación de esta estructura altamente organizada, compuesta por complejos de activación supramoleculares (SMACs) concéntricos, que debe estar regulada con precisión para lograr una activación óptima de las células T (110). Un evento importante en la formación de la SI es la coalescencia de CD3 y la distribución distal de la F-actina, necesaria para lograr una activación adecuada de las células T (111) (**Figura 6**). Además, el correcto aclaramiento de la F-actina es importante para la secreción de gránulos líticos o citoquinas en la hendidura sináptica (112).

Se han llevado a cabo diversos estudios para tratar de comprender la estructura y funcionalidad de las SIs formadas tras la interacción de los CARs y los TCEs con el AAT expresado en la superficie de la célula diana. Así, se ha comprobado que las interacciones promovidas por CARs inducen un centro organizador de micro-túbulos eficiente y la secreción de gránulos líticos de manera incluso más rápida que en la SI canónica iniciada a través del TCR (113). Sin embargo, el citoesqueleto de F-actina no se aclara completamente del centro de la sinapsis y se forma una estructura multifocal desorganizada, que presenta diferencias importantes con respecto a la SI canónica iniciada por el TCR (28-30, 109). A diferencia de los CARs, los TCEs inducen la formación de SIs canónicas entre las células T y las células tumorales (44, 45). En la SI promovida por el TCR es determinante el número de moléculas MHC y la afinidad entre el complejo péptido-MHC y el TCR. En las SIs artificiales mediadas por un CAR o un TCE, influyen factores como la densidad, el tamaño y la estructura del AAT, la ubicación del epítopo (accesibilidad y distancia a la membrana celular) y la afinidad por el mismo (114). Otros factores potencialmente decisivos son la estructura, el formato (tamaño, geometría y valencia) y la densidad de la molécula que interacciona con el AAT (CAR o TCE) (**Figura**

6) (108). Sin embargo, son necesarios estudios adicionales para disponer de información más precisa sobre la topología espacial y temporal de las SIs artificiales (109).

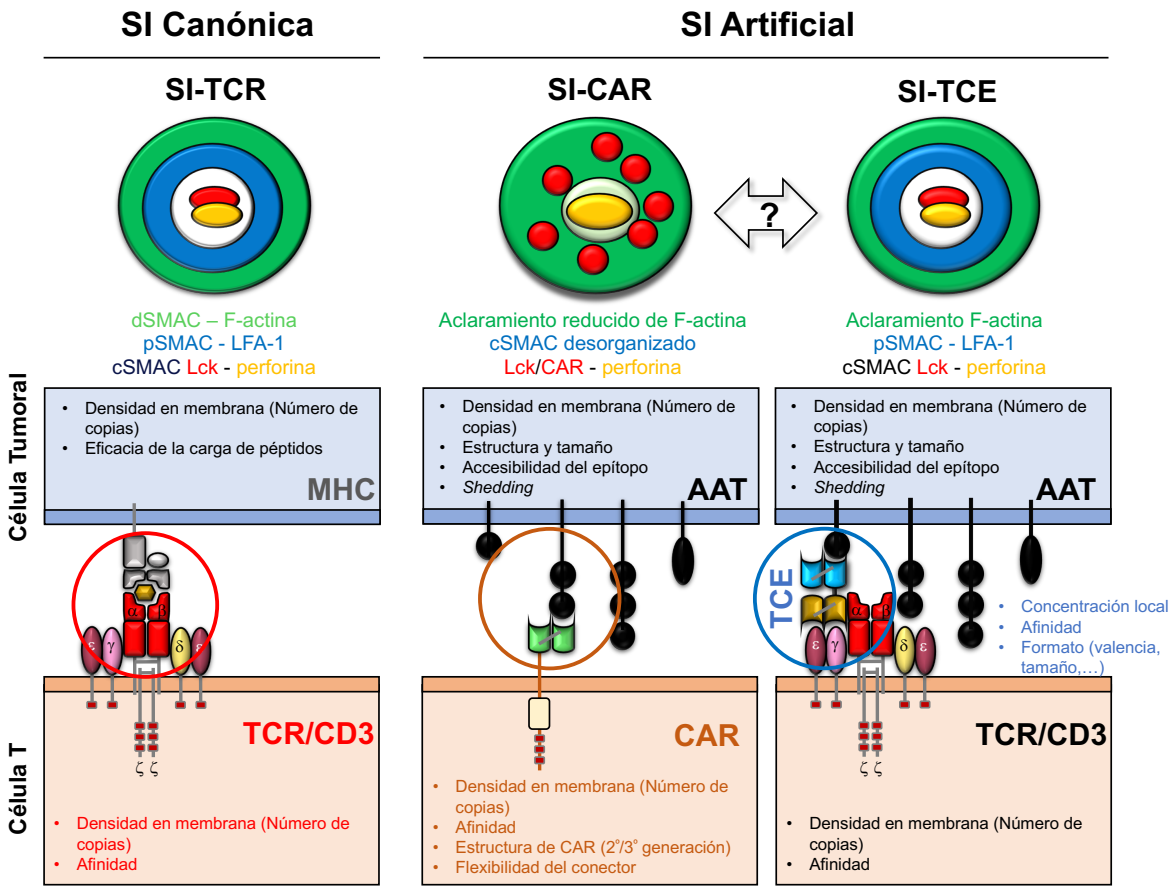

Figura 6. Factores que pueden afectar a la estructura de la sinapsis inmunológica. Topologías observadas en las SIs fisiológicas mediadas por el TCR (SI canónica) y en las SIs artificiales medidas por un CAR o un TCE. Se representa la organización del citoesqueleto y las moléculas de señalización y efectoras a lo largo de la interfaz de la SI establecida por la célula T y la célula diana. Las SIs mediadas por el TCR y por los TCEs presentan una característica morfología en "ojo de buey", mientras que las SIs mediadas por los CARs muestran una morfología desorganizada. Además, se indican diferentes factores que influyen en el ensamblaje de las SIs y la activación de las células T. Abreviaturas del inglés: cSMAC, *central SupraMolecular Activation Cluster*; dSMAC, *distal SupraMolecular Activation Cluster*; Lck, *Lymphocyte-specific protein tyrosine kinase*; MHC, *Major Histocompatibility Complex*; pSMAc, *peripheral SupraMolecular Activation Cluster*. Abreviaturas: AAT, Antígeno Asociado a Tumor. Figura modificada de (109).

OBJETIVOS

El objetivo general de este trabajo ha sido desarrollar una estrategia de inmunoterapia del cáncer basada en la secreción *in situ,* por linfocitos T modificados genéticamente (células STAb-T19), de un TCE anti-CD19 x anti-CD3 en formato BiTE (BiTE-19). Además, se ha comparado la eficacia de las células STAb-T19 con células CAR-T19 que expresan un CAR anti-CD19 de segunda generación (CAR-19). Para ello, se plantearon los siguientes objetivos específicos:

1. Diseño y generación de un vector lentiviral para la secreción del BiTE-19.
2. Generación de células STAb-T19, mediante la transducción de células T primarias y de la línea celular T Jurkat, y caracterización funcional del BiTE-19 secretado.
3. Evaluación *in vitro* de la activación y la actividad citotóxica de las células STAb-T19 frente a células tumorales $CD19^-$ y $CD19^+$: estudio comparativo con células CAR-T19.
4. Evaluación *in vitro de* la capacidad de las células STAb-T19 de realizar un reclutamiento policlonal de células T no modificadas genéticamente.
5. Análisis estructural de la sinapsis inmunológica y estudio de la señalización temprana inducida por el BiTE-19 y el CAR-19.
6. Evaluación *in vivo* de la eficacia terapéutica, a corto y largo plazo, de las células STAb-T19 en modelos animales: estudio comparativo con células CAR-T19.

PUBLICACIONES

CAPÍTULO I: Overcoming CAR-mediated CD19 downmodulation and leukemia relapse with T lymphocytes secreting anti-CD19 T cell engagers.

Belén Blanco[#], Ángel Ramírez-Fernández[#], Clara Bueno, Lidia Argemí-Muntadas, Patricia Fuentes, Óscar Aguilar-Sopeña, Francisco Gutierrez-Agüera, Samanta Romina Zanetti, Antonio Tapia-Galisteo, Laura Díez-Alonso, Alejandro Segura-Tudela, María Castellà, Berta Marzal, Sergi Betriu, Seandean L. Harwood, Marta Compte, Simon Lykkemark, Ainhoa Erce-Llamazares, Laura Rubio-Pérez, Anaïs Jiménez-Reinoso, Carmen Domínguez-Alonso, María Neves, Pablo Morales, Estela Paz-Artal, Sonia Guedán, Laura Sanz, María L. Toribio, Pedro Roda-Navarro, Manel Juan, Pablo Menéndez, Luis Álvarez-Vallina.

[#] Ambos autores han contribuido por igual

Cancer Immunology Research 2022 Apr 1; 10(4):498-511.

DOI: 10.1158/2326-6066.CIR-21-0853

Introducción:

Recientemente se han desarrollado inmunoterapias para el tratamiento de leucemias y linfomas de células B basadas en la redirección de linfocitos T mediante moléculas anti-CD19. Así, se han obtenido resultados clínicos notables tras la administración sistémica de TCEs anti-CD3 x anti-CD19 en formato BiTE y de terapias adoptivas con células CAR-T anti-CD19. Sin embargo, a pesar de una excelente tasa de respuestas, el 30-60 % de los pacientes recaen un año después del inicio del tratamiento. Como alternativa, se ha desarrollado la terapia STAb-T, basada en la modificación de las células T para secretar TCEs (células STAb-T).

Objetivos:

1. Diseño y generación de un vector lentiviral que codifica para un anticuerpo biespecífico anti-CD19 x anti-CD3 en formato BiTE (BiTE-19).
2. Generación de células STAb-T19 y caracterización funcional del BiTE-19 secretado.
3. Análisis estructural de la sinapsis inmunológica mediada por el BiTE-19 y el CAR-19.
4. Evaluación *in vitro* de la activación y la actividad citotóxica de las células STAb-T19 frente a células tumorales $CD19^+$: estudio comparativo con células CAR-T19.
5. Evaluación *in vitro de* la capacidad de las células STAb-T19 de realizar un reclutamiento policlonal de células T no modificadas genéticamente.
6. Evaluación *in vivo* de la eficacia terapéutica, a corto y largo plazo, de las células STAb-T19 en modelos murinos: estudio comparativo con células CAR-T19.

Conclusiones:

1. Las células STAb-T19 secretan BiTE-19 funcional, que induce la formación de sinapsis inmunológica canónicas.
2. Las células STAb-T19 son capaces de reclutar células T no modificadas (efecto *bystander*) e inducen una respuesta citotóxica más rápida y potente que las células CAR-T19.
3. Las células STAb-T19 previenen el escape de las células tumorales *in vitro* a ratios célula efectora:célula diana muy bajas, mientras que las células CAR-T19 no son

capaces de evitar el escape tumoral, asociado a una disminución rápida y drástica de la expresión de CD19 y de CAR tras la interacción entre ambas moléculas.

4. Ambas terapias evitan el desarrollo de la leucemia en modelos *in vivo* a corto plazo, pero sólo las células STAb-T19 previenen la recaída en modelos *in vivo* a largo plazo.

Publicación:

Overcoming CAR-Mediated CD19 Downmodulation and Leukemia Relapse with T Lymphocytes Secreting Anti-CD19 T-cell Engagers

Belén Blanco[1,2,3], Ángel Ramírez-Fernández[1,2], Clara Bueno[3,4,5], Lidia Argemí-Muntadas[6], Patricia Fuentes[7], Óscar Aguilar-Sopeña[8,9], Francisco Gutierrez-Agüera[3,4], Samanta Romina Zanetti[4], Antonio Tapia-Galisteo[10], Laura Díez-Alonso[1,2], Alejandro Segura-Tudela[1,2], Maria Castellà[11], Berta Marzal[11], Sergi Betriu[11], Seandean L. Harwood[6], Marta Compte[10], Simon Lykkemark[6], Ainhoa Erce-Llamazares[1,2], Laura Rubio-Pérez[1,2,12], Anaïs Jiménez-Reinoso[1,2], Carmen Domínguez-Alonso[1,2], Maria Neves[7], Pablo Morales[1], Estela Paz-Artal[1,8], Sonia Guedan[13], Laura Sanz[10], María L. Toribio[7], Pedro Roda-Navarro[8,9], Manel Juan[11,14,15,16], Pablo Menéndez[3,4,5,17,18], and Luis Álvarez-Vallina[1,2,3,6]

ABSTRACT

Chimeric antigen receptor (CAR)–modified T cells have revolutionized the treatment of CD19-positive hematologic malignancies. Although anti-CD19 CAR-engineered autologous T cells can induce remission in patients with B-cell acute lymphoblastic leukemia, a large subset relapse, most of them with CD19-positive disease. Therefore, new therapeutic strategies are clearly needed. Here, we report a comprehensive study comparing engineered T cells either expressing a second-generation anti-CD19 CAR (CAR-T19) or secreting a CD19/CD3-targeting bispecific T-cell engager antibody (STAb-T19). We found that STAb-T19 cells are more effective than CAR-T19 cells at inducing cytotoxicity, avoiding leukemia escape *in vitro*, and preventing relapse *in vivo*. We observed that leukemia escape *in vitro* is associated with rapid and drastic CAR-induced internalization of CD19 that is coupled with lysosome-mediated degradation, leading to the emergence of transiently CD19-negative leukemic cells that evade the immune response of engineered CAR-T19 cells. In contrast, engineered STAb-T19 cells induce the formation of canonical immunologic synapses and prevent the CD19 downmodulation observed in anti-CD19 CAR-mediated interactions. Although both strategies show similar efficacy in short-term mouse models, there is a significant difference in a long-term patient-derived xenograft mouse model, where STAb-T19 cells efficiently eradicated leukemia cells, but leukemia relapsed after CAR-T19 therapy. Our findings suggest that the absence of CD19 downmodulation in the STAb-T19 strategy, coupled with the continued antibody secretion, allows an efficient recruitment of the endogenous T-cell pool, resulting in fast and effective elimination of cancer cells that may prevent CD19-positive relapses frequently associated with CAR-T19 therapies.

Introduction

Potentially curative immunotherapies for B-cell leukemias have been based on redirecting the specificity and function of non-tumor-specific T cells with synthetic CD19-targeted cell–cell bridging molecules, such as membrane-anchored chimeric antigen receptors (CAR) or soluble bispecific antibodies (bsAb; ref. 1). Administration of anti-CD19 CAR-engineered autologous T (CAR-T19) cells and continuous infusion of the anti-CD19/CD3 bispecific T-cell engager (BiTE) blinatumomab (BLI) have demonstrated impressive complete

[1]Cancer Immunotherapy Unit (UNICA), Department of Immunology, Hospital Universitario 12 de Octubre, Madrid, Spain. [2]Immuno-Oncology and Immunotherapy Group, Instituto de Investigación Sanitaria 12 de Octubre (imas12), Madrid, Spain. [3]Red Española de Terapias Avanzadas (TERAV), Instituto de Salud Carlos III (RICORS, RD21/0017/0029), Madrid, Spain. [4]Josep Carreras Leukemia Research Institute, Barcelona, Spain. [5]Centro de Investigación Biomédica en Red-Oncología (CIBERONC), Instituto de Salud Carlos III, Madrid, Spain. [6]Immunotherapy and Cell Engineering Laboratory, Department of Engineering, Aarhus University, Aarhus, Denmark. [7]Centro de Biología Molecular Severo Ochoa CSIC-UAM, Madrid, Spain. [8]Department of Immunology, Ophthalmology and ENT, School of Medicine, Universidad Complutense, Madrid, Spain. [9]Lymphocyte Immunobiology Group, Instituto de Investigación Sanitaria 12 de Octubre (imas12), Madrid, Spain. [10]Molecular Immunology Unit, Hospital Universitario Puerta de Hierro Majadahonda, Majadahonda, Madrid, Spain. [11]Institut d'Investigacions Biomèdiques August Pi i Sunyer (IDIBAPS), Hospital Clínic, Barcelona, Spain. [12]Chair for Immunology UFV/Merck, Universidad Francisco de Vitoria (UFV), Pozuelo de Alarcón, Madrid, Spain. [13]Department of Hematology and Oncology, Institut d'Investigacions Biomèdiques August Pi i Sunyer (IDIBAPS), Hospital Clinic, Barcelona, Spain. [14]Servei d'Immunologia, Hospital Clínic de Barcelona, Barcelona, Spain. [15]Plataforma Immunoteràpia Hospital Sant Joan de Déu, Barcelona, Spain. [16]Universitat de Barcelona, Barcelona, Spain. [17]Department of Biomedicine, School of Medicine, Universitat de Barcelona, Barcelona, Spain. [18]Institució Catalana de Recerca i Estudis Avançats (ICREA), Barcelona, Spain.

Note: Supplementary data for this article are available at Cancer Immunology Research Online (http://cancerimmunolres.aacrjournals.org/).

B. Blanco and Á. Ramírez-Fernández contributed equally to this article.

Current address for M. Neves: Division of Clinical Genetics, Lund University, Lund 22184, Sweden.

Corresponding Authors: Luis Álvarez-Vallina, Cancer Immunotherapy Unit, Hospital Universitario 12 De Octubre, Madrid 28041, Spain. Phone: 34-917792773; Fax: 34-917792778; E-mail: lav.imas12@h12o.es; and Belén Blanco, bblanco.imas12@h12o.es

Cancer Immunol Res 2022;10:498–511

doi: 10.1158/2326-6066.CIR-21-0853

response rates in refractory/relapsed B-cell acute lymphoblastic leukemia (B-ALL; refs. 2, 3). However, despite this excellent clinical performance, disease recurrence/progression is eventually seen in 30% to 60% of patients after CAR-T19 cell therapy (4, 5). Relapses fall under two major types: CD19-positive (70%–80% of patients), typically linked to poor T-cell function, limited CAR T-cell persistence, and an overall low redirection of T cells (6), and CD19-negative (20%–30% of patients), where the disease recurs with antigen-negative variants enabling escape from CAR-T19 surveillance (4, 7). CAR-T19 therapy can also lead to reversible antigen loss through trogocytosis, a mechanism by which targeted antigens are transferred to T cells, thereby reducing both CD19 density on the tumor cell surface and CAR expression on T cells, resulting in T-cell fratricide and exhaustion (8). Approved CAR T-cell therapies rely on stable cell-surface CAR expression, whereas BiTE-mediated T-cell redirection is temporary and limited to the period of systemic infusion. As an alternative to BiTE infusion, T cells can be engineered to continuously secrete T cell–engaging bsAbs (STAb T cells) in order to compensate for their rapid blood clearance and achieve long-term therapeutically effective concentrations (9, 10). STAb T-cell therapy is under active preclinical investigation as an alternative to CAR T cells, and several groups have demonstrated encouraging therapeutic effects in preclinical models of B-ALL (11, 12). Here, we report a comparative study aimed at determining the efficacy of CD19-targeting engineered CAR T and STAb T cells in several *in vitro* and *in vivo* models of B-ALL. Although our results indicate that STAb-T19 therapy effectively controls tumor progression and can prevent the relapse frequently associated with CAR-T19 therapies in different *in vivo* models, further studies are needed to determine its ultimate clinical potential.

Materials and Methods

Cell lines and culture conditions

HEK293 (CRL-1573), HEK293T (CRL-3216), HeLa (CCL-2), Jurkat Clone E6-1 (TIB-152), Raji (CCL-86), NALM6 (CRL3273), and K562 (CCL-243) cells were obtained from the American Type Culture Collection. SEM (ACC546) cells were obtained from the DSMZ cell line bank. NALM6 and HeLa cells expressing the firefly luciferase (Luc) gene (NALM6^{Luc} and HeLa^{Luc}) have been described previously (13). HEK293, HEK293T, and HeLa cells were cultured in Dulbecco's modified Eagle medium (DMEM; catalog no. BE12-614F, Lonza) supplemented with 2 mmol/L L-glutamine (catalog no. 25030081, Life Technologies), 10% (vol/vol) heat-inactivated FBS (catalog no. F7524) and antibiotics (100 units/mL penicillin, 100 μg/mL streptomycin; catalog no. P4333; both from Sigma-Aldrich), referred to as DMEM complete medium. Jurkat, Raji, Nalm6, and K562 cells were cultured in RPMI-1640 (catalog no. 12-702Q, Lonza) supplemented with 2 mmol/L L-glutamine, heat-inactivated 10% FBS, and antibiotics, referred to as RPMI complete medium (RCM). SEM cells were cultured in Iscove's Modified Dulbecco's Medium (catalog no. 31980030, Thermo Fisher Scientific) supplemented with heat-inactivated 10% FCS and antibiotics. All the cell lines were grown at 37°C in 5% CO_2 for no longer than 1 month during experimental use and were routinely screened for mycoplasma contamination by PCR using the Mycoplasma Gel Detection Kit (catalog no. 90.021-4542, Biotools). Primary human B-ALL cells ($n = 3$) were obtained from patients' bone marrow (BM) samples after written informed consent, and the study was conducted in accordance with the Declaration of Helsinki. Mononuclear cells were isolated from BM samples by density gradient centrifugation using Ficoll-Paque (catalog no. 17-5446-52, Cytiva), washed, resuspended in FBS with 10% DMSO (catalog no. 317275, EMD Millipore) and stored in liquid nitrogen until use. B-ALL1 sample was an ETV6-RUNX1 t(12;21) B-ALL, and B-ALL2 sample a hypodiploid B-ALL. The sample used for generation of patient-derived xenograft (PDX) model was a high hyperdiploid B-ALL, obtained from the BM of a 3-year-old patient at diagnosis (prior to treatment) and blasts were sequentially expanded in NSG mice. Briefly, mice injected with 1×10^6 B-ALL cells were allowed to reach 85% blasts in BM. Then, mice were sacrificed, and blasts were obtained from tibiae and femurs and cryopreserved in FBS–10% DMSO until use.

Vector construction and preparation of lentivirus

To construct the expression vector pCDNA3.1-A3B1-OKT3, a synthetic gene (19-BiTE) encoding the human kappa light chain signal peptide L1 (14), the A3B1 scFv (V_L–V_H; ref. 13), a five-residue linker (G_4S), the OKT3 scFv (V_H–V_L; ref. 15), and a C-terminal polyHis tag was synthesized by GeneArt AG (Thermo Fisher Scientific), and subcloned as *Hind*III/*Xba*I into the plasmid pCDNA3.1 (catalog no. V79520, Thermo Fisher Scientific), using T4 DNA ligase (catalog no. M0202S, New England Biolabs). To generate the lentiviral transfer vector, the complete 19-BiTE gene (including signal peptide L1, A3B1 scFv (G_4S), OKT3 scFv, and polyHis tag) was synthesized by GeneArt AG and cloned as *Mlu*I/*BspE*I into the vector pCCL-EF1α-CAR19 (13), encoding a second-generation (CD8-BBζ) anti-CD19 CAR (19-CAR), to obtain the plasmid pCCL-EF1α-BiTE19. To construct the vector pCCL-EF1α-BiTE19-T2A-Tomato, a synthetic gene encoding the OKT3 scFv and T2A-Tomato was synthesized by GeneArt AG, and cloned as *Afe*I/*Bst*BI into the vector pCCL-EF1α-BiTE19. The plasmid pCCL-EF1α-CAR19-T2A-GFP has been previously described (16).

Lentivirus titration

All lentivirus stocks were normalized for p24 and RNA. The p24 concentration was determined by ELISA (catalog no. 632200, Takara), and the genomic lentiviral RNA by qRT-PCR (catalog no. 631235, Takara). In the case of 19-BBζ CAR-encoding lentivirus, functional titers (TU/mL) were determined by FACS analysis after limiting dilution in HEK293T cells, using an APC-conjugated $F(ab')_2$ fragment goat anti-mouse IgG $F(ab')_2$ fragment specific (catalog no. 115-006-072, Jackson ImmunoResearch Laboratories). Titration of 19-BiTE lentiviral preparations was performed by intracellular staining, as described below, of HEK293T cells after limiting dilution. Functional titers of 19-BBζ CAR and 19-BiTE-encoding lentiviruses carrying reporter genes were determined by flow cytometry by analyzing green fluorescence protein (GFP) or dTomato (dTO) expression, respectively, after limiting dilution in HEK293T cells.

T-cell transduction and culture conditions

Peripheral blood mononuclear cells (PBMC) were isolated from peripheral blood of volunteer healthy donors ($n = 15$) by density gradient centrifugation using lymphoprep (catalog no. AXS-1114544, Axis–Shield). All donors provided written informed consent in accordance with the Declaration of Helsinki. $CD3^+$ T cells were purified by negative selection using the Pan T-Cell Isolation Kit, human (catalog no. 130-096-535), and LS columns (catalog no. 130-042-401; both from Miltenyi Biotec, following the manufacturer's instructions. The purity of isolated populations was routinely >95%. Cells were then activated and expanded for 24 hours using anti-CD3/CD28 beads (catalog no. 111.31D, Dynabeads, Gibco) at 1:3 cell:bead ratio in RCM, at a concentration of 1×10^6 cells/mL. Twenty-four hours later, cells were left nontransduced (NT cells) or transduced with 19-CAR (CAR T cells) or 19-BiTE (STAb T cells) encoding lentiviruses at the indicated MOIs. A period of cell expansion of 6 to 8 days was necessary

before conducting experiments. Three different cell transductions using three different PBMC donors were used to conduct the experiments in triplicate. Alternatively, PBMCs obtained from Buffy coats provided by the Barcelona Blood and Tissue Bank on institutional review board approval (HCB/2018/0030) were activated in plates coated with 1 μg/mL anti-CD3 (OKT3; catalog no. 566685) and anti-CD28 (CD28.2; catalog no. 555725) antibodies (BD Biosciences) for 2 days and then were transduced with 19-BBζ CAR (CAR-T19 cells) or 19-BiTE (STAb-T19 cells) encoding lentiviruses at the indicated MOIs in the presence of 10 ng/mL IL7 (catalog no. 30-095-367) and 10 ng/mL IL15 (catalog no. 130-095-760; both from Miltenyi Biotec). T cells were expanded in RCM supplemented with IL7 and IL15 (10 ng/mL; Miltenyi Biotec) for up to 10 days.

Western blotting

Samples were separated under reducing conditions on 10% to 20% Tris-glycine gels (catalog no. XP10202BOX, Life Technologies), transferred onto PVDF membranes (catalog no. IPVH00010, Merck Millipore) and probed with anti-His mAb (catalog no. 34650, Qiagen; 200 ng/mL), followed by incubation with horseradish peroxidase (HRP)–conjugated goat anti-mouse (GAM) IgG, Fc specific (1:5,000 dilution; Sigma-Aldrich, see Supplementary Table S1). Visualization of protein bands was performed with Pierce ECL Western Blotting substrate (catalog no. 32134).

Enzyme-linked immunosorbent assay

To detect the 19-BiTE secreted to culture supernatants, human CD19:human Fc chimera (CD19:Fc; catalog no. 9269-CD-050, R&D Systems) was immobilized (5 μg/mL) on Maxisorp plates (catalog no. M9410-1CS, NUNC) overnight at 4°C. After washing and blocking, conditioned media were added and incubated for 1 hour at room temperature. Then, wells were washed 3 times with PBS–0.05% Tween20 (catalog no. P1379, Sigma-Aldrich) and 3 times with PBS (catalog no. 508002, Werfen), and anti-His mAb (Qiagen) was added (1 μg/mL). After washing, HRP-GAM IgG, Fc specific (1:2,000 dilution; Sigma-Aldrich) was added, and the plate was developed using tetramethylbenzidine (TMB; catalog no. T0440, Sigma-Aldrich).

T-cell proliferation assays

For primary T-cell proliferation assays, anti-CD3/CD28 beads were removed five days after lentiviral transduction, and activated T cells (A-T) were left resting for 24 hours at a concentration of 0.8×10^6 cells/mL. Then, transduced or nontransduced A-T were stained with 2.5 μmol/L Cell Trace Violet (catalog no. C34557, Life Technologies) and cocultured with freshly isolated T cells (nonactivated T cells, NA-T) from the same donor, previously stained with 2.5 μmol/L Cell Trace CFSE (catalog no. C34554, Life Technologies), and NALM6 or HeLa target cells at the indicated ratios. After 5 days, samples were stained with CD3-PE, CD4-APC, and CD8-APC-Cy7 (all from BD Biosciences; see Supplementary Table S1) and acquired in a FACSCanto flow cytometer. T-cell proliferation was analyzed using FCS Express 6 Plus Software (De Novo Software).

Cytokine secretion analysis

IFNγ secretion was analyzed by ELISA (catalog no. 950.000.096, Diaclone), following the manufacturer's instructions.

Cytotoxicity assays

For 48-hour cytotoxicity assays, transduced or nontransduced A-T cells were cocultured with or without freshly isolated NA-T cells and luciferase-expressing target cells ($NALM6^{Luc}$ or $HeLa^{Luc}$) at the indicated effector-to-target (E:T) ratios. As controls, NA-T cells were cultured with target cells. After 48 hours, supernatants were collected and stored at −20ºC for IFNγ secretion analysis, and 20 μg/mL D-luciferin (catalog no. E1602, Promega) was added before bioluminescence quantification using a Victor luminometer (PerkinElmer). Percent tumor cell viability was calculated as the mean bioluminescence of each sample divided by the mean of NA-T-target cell samples ×100. Specific lysis was established as 100% of cell viability. For cytotoxic studies using transwells, polycarbonate inserts (0.4 μmol/L pores; catalog no. CLS3381-1EA, Corning) were used. Luciferase-expressing targets cells (5×10^4) were plated on bottom wells with 1×10^5 NA-T cells, and A-T cells were added at the indicated ratios to inserts. Bioluminescence was quantified after 48 hours. In another set of experiments, transduced or nontransduced A-T cells were cocultured with or without freshly isolated NA-T cells and 1×10^5 tumor target cells (NALM6, SEM, or primary B-ALL cells) at the indicated E:T ratios. After 24 and 48 hours, cells were stained for 30 minutes at 4°C with CD3-PB, CD10-APC, CD19-PCy7, and 7-AAD (catalog no. 559925, BD Biosciences) in 50 μL PBS–0.5% FBS, in TruCount Absolute Counting Tubes (catalog no. 340334, BD Biosciences). Then, samples were diluted by adding 450 μL of PBS and gently mixed before proceeding to FACS analysis. Cytotoxicity was determined by analyzing the residual live (7-AAD^-) target cells. For real-time cytotoxicity assays, the xCELLigence RTCA DP system (Acea Biosciences) was used. 1×10^4 wild-type HEK293 or stably transfected CD19-expressing HEK293 cells were plated in an E-Plate 16 (catalog no. 05469813001, Acea Biosciences) and cultured at 37 °C and 5% CO_2. After 20 hours, NT-T, CAR-T19 or STAb-T19 cells were added at different E:T ratios and cell index values were measured every 15 minutes for 48 hours using RTCA Software 2.0 (Acea Biosciences). The percentage of specific lysis was calculated using the equation:

$$\text{Percentage} = [(\text{cell index of NT} - \text{cell index of CAR T cells})/(\text{cell index of NT})] \times 100$$

CD107a assays

NT-T, CAR-T19, or STAb-T19 cells (1×10^5) were cultured alone or coincubated with NALM6 or HeLa cells at a 2:1 E:T ratio in U-bottom 96-well plates, in the presence of anti-human CD107a-PE (BD Biosciences, see Supplementary Table S1). After 1 hour, 0.67 μL/mL monensin (BD GolgiStop, catalog no. 554724, BD Biosciences) was added, and cultures were continued for another 3 hours before CD3 staining and flow-cytometric analysis.

Flow cytometry

Antibodies used for flow cytometry analysis are detailed in Supplementary Table S1. DAPI (catalog no. D9542-10MG, Sigma-Aldrich) and 7-Aminoactinomycin D (7-AAD; cat. 559925, BD Biosciences) were used as viability markers. Cell-surface expression of 19-CAR was analyzed using an APC-anti-mouse IgG $F(ab')_2$; alternatively, CAR expression was estimated based on GFP expression. Cell surface–bound 19-BiTEs were detected with 1 μg/mL anti-6xHis tag-biotin mAb and PE-conjugated streptavidin (cat. 349023, BD Biosciences), or with APC-conjugated anti-His mAb. Intracellular 19-BiTE was detected using the Inside Stain Kit (cat. 130-090-477, Miltenyi Biotec) following the manufacturer's instructions, and APC-anti-His APC mAb. Alternatively, 19-BiTE was estimated based on dTO expression. Intracellular CD19 was detected using the Inside Stain Kit and PC5-conjugated anti-CD19 mAb. Cell acquisition was performed in a BD FACSCAnto II flow cytometer using BD FACSDiva software (both from BD Biosciences). Analysis was performed using FlowJo V10 software (Tree Star).

Immunofluorescence and confocal microscopy

Antibodies used for immunofluorescence and confocal microscopy analysis are detailed in Supplementary Table S1. For synapse studies, nontransduced or transduced T cells ($1–2 \times 10^5$) were coincubated for 15 minutes with Raji cells labeled with 10 μmol/L 7-amino-4-chloromethylcoumarin (CMAC; cat. C2110, Life Technologies), at 1:1 E:T ratio, on poly-L-lysine (cat. P4832, Sigma-Aldrich)–coated coverslips, at 37°C, 5% CO_2. For CD19 localization studies, NT-T, CAR-T19, or STAb-T19 cells (1×10^5) were coincubated with CMAC-labeled NALM6 cells at 2:1 E:T ratio in U-bottom 96-well plates, and after 2 hours, cocultures were incubated on poly-L-lysine–coated coverslips at 37°C, 5% CO_2. Then, cells were fixed with 4% paraformaldehyde (cat. P6148, Sigma-Aldrich) and permeabilized with 0.1% Triton X100 (cat. 9036-19-5, Sigma-Aldrich) at room temperature, as previously described (17). For synapse studies, samples were stained with mouse anti-CD3ε supernatant (1/2 dilution; T3b clone; kindly provided by Dr. Francisco Sánchez-Madrid, Hospital Universitario de la Princesa, Madrid, Spain) and Phalloidin-647 (1/200 dilution; cat. 10656353, Fisher Scientific) for 1 hour at room temperature. For CD19 localization studies, samples were stained with anti-CD3ε (T3b clone), anti-CD19 supernatant (1/2 dilution; BU12 clone; kindly provided by Dr. Francisco Sánchez-Madrid), and anti-CD107a (BioLegend) antibodies. Cells were then washed 3 times for 5 minutes with TBS (20 mmol/L tris pH 7.4, 150 mmol/L NaCl) and incubated with goat anti-mouse-Ig Alexa Fluor 488 (catalog no. A11029, Life Technologies) for 30 minutes at room temperature. Finally, coverslips were washed and mounted with Mowiol (catalog no. 81381, Sigma-Aldrich). Confocal sections of fixed samples were acquired using an SP-8 laser scanning laser confocal microscopy (Leica Microsystems). For 3D reconstructions, z-stacks through the complete synapse were acquired every 0.3 μm. Actin clearance was estimated by the ratio:area of central region of the synapse depleted of actin/complete area of the synapse, including the actin ring, in 3D images. CD3 coalescence and cSMAC formation were assessed by visual inspection of 3D images. 3D reconstruction and image quantitation were performed with ImageJ freeware (NIH).

In vivo B-ALL xenograft models

Nine-week-old NOD.Cγ-Prkdcscid-IL2rgtm1Wjl/SzJ mice (NSG; The Jackson Laboratory) were infused intravenously (i.v.) with 1×10^6 $NALM6^{Luc}$ cells, and after 2 days received 5×10^6 NT-T, CAR-T19 (10% 19-CAR^+), or STAb-T19 (10% 19-$BiTE^+$) cells. Tumor growth was evaluated weekly by bioluminescence imaging as previously described (18). Briefly, 150 mg/kg of D-luciferin (catalog no. E1605, Promega) was administrated intraperitoneally in 200 μL of sterile PBS. Animals were imaged 10 minutes after D-luciferin injection using the Xenogen IVIS Lumina II imaging system (Caliper Life Sciences). The photon flux emitted by the luciferase-expressing cells was measured as an average radiance (photons/sec/cm_2/sr). Imaging analysis was performed using the Living Image Software 3.2 (Caliper Life Sciences). Tumor burden and T-cell persistence were analyzed by flow cytometry in PB, obtained by facial vein puncture, at day 19, and in spleen and BM samples after euthanization. Human CD19 relative gene expression in BM was analyzed by qRT-PCR. Briefly, total RNA was isolated with the RNeasy Micro Kit (catalog no. 74004, Qiagen) and cDNA was synthesized using NZY First-Strand cDNA Synthesis Kit (catalog no. MB125, Nzytech). qRT-PCR was performed with LightCycler 480 SYBR Green I Master Kit (catalog no. 04707516001, Roche Diagnostics) on a LightCycler 480 system (Roche Diagnostics). Each sample was analyzed in triplicate, and fold-expression changes were calculated with the equation $2^{-\Delta Ct}$. Human succinate dehydrogenase gene expression was used to normalize. The following primers, synthesized by Roche Diagnostics, were used:

F-hSDHA (5′-TGGGAACAAGAGGGCATCTG-3′)
R-hSDHA (5′-CCACCACTGCATCAAATTCATG-3′)
F-hCD19 (5′-agagatatgtgggtaatggag-3′)
R-hCD19 (5′-ttgccacggtgacaataatac-3′)

Body weight was monitored over time. Animals showing endpoint weight loss or clinical signs of leukemic disease or xenogenic graft-versus-host disease (xGVHD) were euthanized. For studies in a B-ALL PDX model, 6- to 12-week-old NSG mice were irradiated (2 Gy) and i.v. transplanted with 1×10^6 $CD19^+CD22^+CD10^+$ B-ALL blasts. Mice were i.v.-infused 3 weeks later with 3 or 5×10^6 NT, CAR-T19, or STAb-T19 cells (percentage of 19-CAR^+ or 19-$BiTE^+$ is indicated). Tumor burden was followed by bleeding every 1 or 2 weeks and BM extraction from tibial aspirates at different time points, cell staining with CD3-PerCP/CD10-PCy7/CD19-BV421/CD45-AmCyan/HLA-ABC-APC and subsequent flow cytometry analysis. Mice were euthanized when they had >5% blasts in PB or when they developed signs of xGVHD. Tumor burden and effector T-cell persistence were analyzed in BM, PB, and spleen by flow cytometry after staining cells with CD3-PerCP/CD10-PCy7/CD19-BV421/CD45-AmCyan/HLA-ABC-APC. *CD19* mRNA expression in BM was analyzed by qPCR, as described above.

Statistical analysis

Results of experiments are expressed as mean ± standard deviation (SD). Graphics and the statistical tests indicated in figure legends were done with Prism 6 (GraphPad Software).

Ethical issues

In vivo studies with the NALM6 cell line–derived xenograft model were carried out at CBM-SO in accordance with the guidelines of the Animal Experimentation Ethics Committee of the Spanish National Research Council. *In vivo* studies with the B-ALL PDX model were performed in the Barcelona Biomedical Research Park. All procedures were performed in compliance with the institutional animal care committee of the Barcelona Biomedical Research Park (DAAM7393).

Results

Engineered STAb-T19 cells efficiently secrete anti-CD19/CD3 BiTE and promote the formation of canonical immunologic synapses

This study was performed using engineered T cells expressing either a second-generation (CD8TM-4-1BB-CD3ζ) anti-CD19 CAR (13) or an anti-CD19/CD3 BiTE (referred to as 19-CAR or 19-BiTE, respectively), both using the clinically validated anti-CD19 A3B1 scFv (refs. 13, 16, 19; Supplementary Fig. S1). The 19-BiTE has a 6xHis-tag for immunodetection. Both constructs were cloned under the control of the EF1α promoter in both monocistronic and T2A-based bicistronic (19-BBζ-T2A-GFP and 19-BiTE-T2A-tdTo) lentiviral vectors (ref. 20; Supplementary Fig. S1). Gene transfer of 19-CAR and 19-BiTE vectors into primary human T cells was achieved with both lentiviral vector systems. The 19-BiTE was efficiently secreted by transduced primary human T cells (STAb-T19) with the expected molecular weight of 55 kDa (**Fig. 1A**). The secreted 19-BiTE specifically recognized plastic-immobilized human CD19 Fc chimeric protein (CD19-Fc; Supplementary Fig. S2A), and target cells expressing either cognate antigen (CD3 or CD19; Supplementary Fig. S2B). 19-BiTE intracellular expression and positive surface staining (decoration) of STAb-T19 cells was

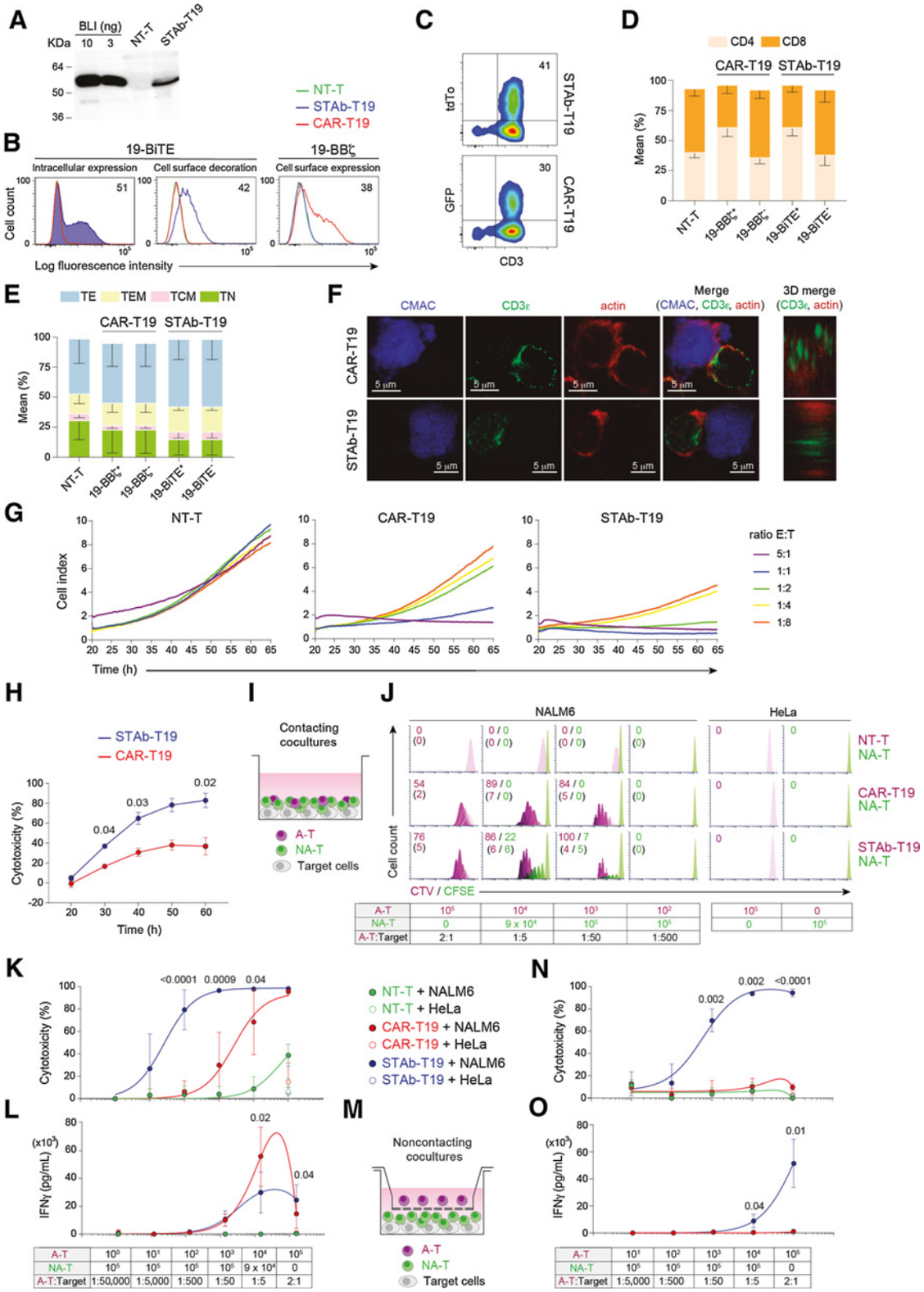

observed with an anti–His-tag mAb, indicating that secreted BiTEs bound to the CD3 complexes on the T-cell surface (**Fig. 1B**; Supplementary Fig. S2C and S2D). The percentage of 19-CAR$^+$ T cells was determined by labeling with a polyclonal Fab-targeting antibody (**Fig. 1B**; Supplementary Fig. S2E). Comparable transduction efficiencies were observed according to the percentage of tdTo$^+$ or GFP$^+$ cells (**Fig. 1C**; Supplementary Fig. S2F and S2G). Jurkat T cells were transduced at the same multiplicity of infection (MOI), albeit with more homogeneous expression profiles than primary T cells (Supplementary Fig. S2H). Lentivirus-transduced primary T cells that were 19-CAR$^+$ or 19-BiTE$^+$ showed a higher proportion of CD4$^+$ than CD8$^+$ T cells (**Fig. 1D**). The relative distribution of naïve, central memory, effector memory, and effector T-cell subsets was similar in nontransduced (NT)-T cells and in CAR-T19 and STAb-T19, with the most prevalent subset being effector T cells (**Fig. 1E**).

Following interaction with CD19$^+$ Raji cells, primary STAb-T19 cells organized a canonical immunologic synapse (IS), with normal filamentous (F)-actin–containing distal supramolecular activation cluster (dSMAC) and accumulation of CD3ε at the central SMAC (cSMAC; **Fig. 1F**; Supplementary Fig. S3A-S3E). In contrast, CAR-T19 cells formed a noncanonical IS with disperse clusters of CD3ε, and F-actin not properly cleared from the central area of interaction (**Fig. 1F**; Supplementary Fig. S3A–S3E). In an impedance-based real-time cytotoxicity assay, STAb-T19 cells were found to mediate rapid reduction of CD19$^+$ target cell viability (Supplementary Fig. S4A) at all E:T ratios, whereas CAR-T19 cells showed a lesser cytotoxic effect that required higher E:T ratios (**Fig. 1G**). When displayed as the percentage of cytotoxicity at several time points, STAb-T19 cells were significantly more effective than CAR-T19 cells (**Fig. 1H**). In contrast, CD19$^+$ cells cocultured with NT-T cells (**Fig. 1G**), or CD19$^-$ cells cocultured with NT-T, CAR-T19 or STAb-T19 cells (Supplementary Fig. S4C), displayed similar viability kinetics to those of target cells cultured alone (Supplementary Fig. S4B). Furthermore, analysis of CD107a staining showed higher degranulation activity in STAb-T19 cells compared with CAR-T19 cells following stimulation with CD19$^+$ targets (Supplementary Fig. S5).

STAb-T19 cells recruit bystander T cells and induce a more potent and rapid cytotoxic response than CAR-T19 cells

To assess STAb-T19 cell ability to recruit bystander T cells, we designed different *in vitro* coculture assays. NT or lentivirus-transduced activated T cells (A-T), or mixtures of A-T and freshly isolated T cells (nonactivated T cells, NA-T) from the same healthy donor were cocultured with CD19$^+$ or CD19$^-$ cells at a constant 2:1 T cell:target cell ratio (**Fig. 1I**). The A-T (NT-T, CAR-T19, or STAb-T19) were mixed with NA-T cells at different proportions (from 1/10 to 1/100,000) while keeping a constant total number of 1×10^5 effector T cells. When stimulated with NALM6 cells in a direct cell–cell contact context (**Fig. 1I**), the STAb-T19 cells proliferated efficiently and exhibited a higher percentage of dividing cells than CAR-T19 at the different A-T:target ratios (**Fig. 1J**). Importantly, STAb-T19 cells efficiently stimulated bystander NA-T cells to proliferate in the presence of NALM6 cells (**Fig. 1J**). This ability to recruit bystander NA-T cells allowed STAb-T19 cells to induce 100% lysis of tumor cells even at the 1:50 A-T:target ratio (**Fig. 1K**). Around 80% and 30% of specific target cell lysis persisted at 1:500 and 1:5,000 A-T:target ratios, respectively (**Fig. 1K**). The cytotoxic capacity of CAR-T19 cells rapidly declined as the A-T:target ratio decreased, from 60% lysis of NALM6 cells at a 1:5 A-T:target ratio to no apparent lysis at the 1:500 A-T:target ratio (**Fig. 1K**). In this context, the secretion of IFNγ by CAR-T19 cells was higher than in STAb-T19 cells (**Fig. 1L**). No significant proliferation or IFNγ secretion was observed when NA-T cells were mixed with NT-T cells and NALM6 cells (**Fig. 1I–L**); however, some degree of cytotoxicity was observed at the highest E:T ratio, attributable to allogeneic T-cell–activation against target cells (13). Transwell assays were used to further demonstrate that STAb-T19 cells were able to recruit bystander NA-T cells to CD19$^+$ cells. CD19$^+$ or CD19$^-$ target cells were plated with NA-T cells in the bottom well, and NT-T, CAR-T19, or STAb-T19 cells were plated in the insert well (**Fig. 1M**). Tumor cell killing (**Fig. 1N**) and IFNγ secretion (**Fig. 1O**) were totally dependent on the presence of STAb-T19 cells in the insert well, indicating that secreted 19-BiTEs effectively redirected the cytotoxicity of NA-T cells to CD19$^+$ targets. T cell lysis (70%) was induced at a STAb-T19:NA-T ratio of 1:50 and an overall E:T ratio of 2:1 in this transwell setup, demonstrating an efficient recruitment of bystander T cells by STAb-T19 cells (**Fig. 1N**).

STAb-T19 cells prevent leukemia escape *in vitro*

We next studied the ability of B-ALL cells to escape from immune control by coculturing CAR-T19 and STAb-T19 cells with NALM6 cells at low E:T ratios. STAb-T19 cells completely eliminated all leukemia cells, even at the 1:16 E:T ratio (**Fig. 2A**). By contrast,

Figure 1.

Comparative *in vitro* study of engineered STAb-T19 and CAR-T19 cells. **A,** Western blot detection of secreted 19-BiTE in the conditioned media from lentivirus-transduced human primary T cells (STAb-T19). Conditioned media from nontransduced T cells (NT-T) and media containing blinatumomab (BLI) were used as negative and positive controls, respectively. One representative experiment of three is shown. **B,** Representative analysis of intracellular and cell surface–bound 19-BiTE (decoration), and cell surface–expressed 19-CAR in NT-T and engineered CAR-T19 and STAb-T19 cells by flow cytometry. One representative experiment out of three independent experiments is shown. The numbers represent the percentage of cells staining positive for the indicated marker. **C,** Percentage of reporter protein expression in STAb-T19 cells (tdTo) and CAR-T19 cells (GFP). One representative transduction out of three performed is shown. **D** and **E,** Percentage of CD4$^+$ and CD8$^+$ T cells (**D**) and naïve (T_N), central memory (T_{CM}), effector memory (T_{EM}), and effector (T_E) T cells (**E**) among NT-T, CAR-T19, or STAb-T19 cells 7 days after transduction (means ± SD of three independent experiments are shown). **F,** Representative images of immunologic synapse (IS) assembly by primary CAR-T19 and STAb-T19 cells stimulated for 15 minutes with CMAC (blue)-labeled CD19$^+$ cells, stained for CD3ε and actin at the mature IS, with IS topology obtained from 3D reconstructions of regions of interest in confocal stacks. **G** and **H,** Real-time cell cytotoxicity assay with HEK-293^{CD19} target cells cocultured with NT-T, CAR-T19, or STAb-T19 cells at the indicated E:T ratios, and cell index values determined every 15 minutes for 65 hours using an impedance-based method (**G**) and percentage lysis normalized to NT-T cells (E:T ratio = 0.5:1; **H**), presented from one representative experiment performed in duplicate. **I,** Schematic representation of the direct contact coculture system used to study the ability of secreted 19-BiTE to induce bystander T-cell proliferation. **J,** Bystander T-cell proliferation after 5 days of coculture, with percentage of dividing cells and the number of cell divisions in parentheses. The total E:T ratio was constant (2:1), but the ratios A-T:target and A-T:NA-T varied as indicated. One representative experiment from three independent experiments is shown. **K,** Cytotoxicity induced by varying numbers of A-T and NA-T cells from the same donor cocultured with NALM6^{Luc} or HeLa^{Luc} target cells for 48 hours, maintaining a constant 2:1 E:T ratio, measured by adding D-luciferin to detect bioluminescence. Data are shown as mean ± SD from four replicates. Significance was calculated by an unpaired Student *t* test. **L,** IFNγ secretion was determined by ELISA. Data are mean ± SD of three independent experiments. Significance was calculated by an unpaired Student *t* test. **M,** Cocultures were performed in a noncontacting transwell system; NALM6^{Luc} or HeLa^{Luc} target cells and NA-T cells were plated in the bottom well and A-T cells (NT-T, CAR-T19, or STAb-T19) in the insert well. **N** and **O,** After 48 hours, the percentage of cytotoxicity (**N**) was determined by luciferase assay, and IFNγ secretion (**O**) was determined by ELISA. Data are shown as mean ± SD from three and four replicates, respectively. Significance was calculated by an unpaired Student *t* test.

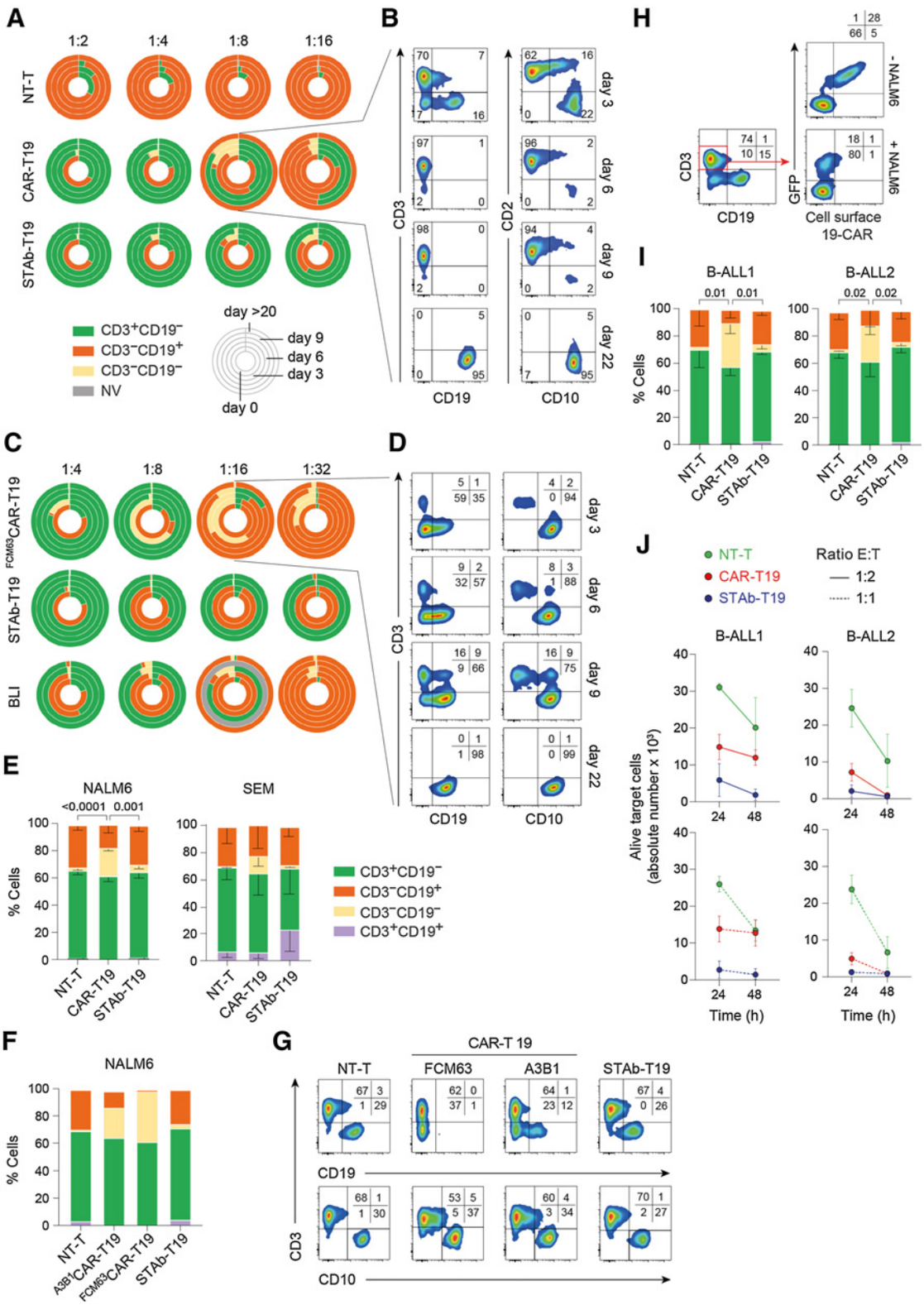

CAR-T19 cells did not eliminate $CD19^+$ cells at E:T ratios of 1:8 or lower, where leukemia cells persisted with a partial downmodulation of CD19 (**Fig. 2A** and **B**; Supplementary Fig. S6). In some cases, NALM6 cells had almost completely lost surface expression of CD19 by day 6 (which continued to day 9; **Fig. 2B**; Supplementary Fig. S6). Preincubation of NALM6 cells with A3B1 scFv only partially blocked the binding of the J3.119 antibody, suggesting that they recognize nonoverlapping epitopes on CD19 (Supplementary Fig. S7). Furthermore, CD10 remained unchanged in NALM6 cells (**Fig. 2B**). Thereafter, leukemia cells progressed and recovered surface expression of CD19, suggesting that antigen downmodulation functions as an escape mechanism against CAR-T19 pressure (**Fig. 2A** and **B**; Supplementary Fig. S6). The CD19 downmodulation effect was even more pronounced when NALM6 cells were cocultured with CAR-T19 cells bearing an anti-CD19 FMC63 scFv-based 4-1BBζ CAR (^{FMC63}CAR-T19; ref. 13), which also failed to control tumor cell growth at the lowest rates analyzed (1:16 and 1:32; **Fig. 2C** and **D**). Two different 19-BiTEs, either *in situ*–secreted A3B1 BiTE or exogenously added HD37 BiTE (a.k.a. blinatumomab, BLI), were not associated with a loss of CD19 expression (**Fig. 2C**). Importantly, STAb-T19 cells were more effective than the addition of BLI to the coculture, as *in situ*–secreted A3B1 BiTE eliminated leukemic cells even at a 1:32 ratio, whereas NALM6 cells persisted after exogenous administration of BLI at the two lower ratios (**Fig. 2C**). This is likely explained by the fact that STAb-T19 cells continuously secrete and display a stable quantity of 19-BiTE decoration, whereas exogenously administered BLI is cleared from the cell surface in a relatively short period of time (Supplementary Fig. S8).

Next, CAR-T19 and STAb-T19 cells were cocultured at 2:1 E:T ratio with two B-ALL cell lines (NALM6 and SEM) and two primary B-ALL cells (B-ALL1 and B-ALL2) for 2 hours. Both B-ALL cell lines showed a rapid decrease of surface CD19 expression after coculture with CAR-T19 cells (**Fig. 2E**). CD19 reduction was more intense when NALM6 cells were cocultured with ^{FMC63}CAR-T19 cells, whereas CD10 expression was unchanged (**Fig. 2F** and **G**). Concomitantly, the 19-CAR was profoundly downmodulated from CAR-T19 cell surface after encountering $CD19^+$ cells, whereas the expression of CD3 was unaffected (**Fig. 2H**). A significant CD19 downmodulation was also observed in cocultures of primary B-ALL cells with CAR-T19 cells (**Fig. 2I**). In contrast, CD19 was not lost after coculture of STAb-T19 cells with either B-ALL cell lines or primary B-ALL cells (**Fig. 2E–I**). We next assessed the cytotoxic activity of CAR-T19 and STAb-T19 cells against primary B-ALL cells. STAb-T19 cells were able to eliminate nearly 100% of the primary B-ALL blasts after 24 hours, whereas CAR-T19 cells exerted a weaker cytotoxic effect (B-ALL1) or required 48 hours to kill 100% of tumor cells (B-ALL2; **Fig. 2J**; Supplementary Table S2).

Leukemia escape is associated with rapid and drastic CAR-mediated CD19 downmodulation

To more carefully study the mechanism of leukemia escape, NALM6 cells were cocultured for 2 hours at a 1:1 E:T ratio with lentivirus-transduced Jurkat T cells homogeneously expressing high amounts of A3B1-based 19-CAR (J-CAR-T19) or 19-BITE (J-STAb-T19; Supplementary Fig. S2H). Although NALM6 cells showed a rapid and intense downmodulation of CD19 (**Fig. 3A**), the 19-CAR disappeared completely from the J-CAR-T19 cell surface (**Fig. 3B**). Membrane CD19 was not reduced in NALM6 after coculture with J-STAb-T19 cells (**Fig. 3A**). In order to locate CD19, NALM6 cells were cocultured with effector T cells, costained for CD19 and the lysosomal marker LAMP1, and analyzed by confocal microscopy. In cocultures with J-CAR-T19 cells, a reduction of cell-surface CD19 (**Fig. 3C**) and a clear colocalization of intracellular CD19 in lysosomes (**Fig. 3C** and **D**) was observed. The presence of CD19 in lysosomes was much lower in target cells cocultured with either J-STAb-19 or nontransduced Jurkat cells (**Fig. 3C** and **D**).

STAb-T19 cells are as effective as CAR-T19 cells in short-term *in vivo* models

To study the *in vivo* antitumor effects of CAR-T19 and STAb-T19 cells in a xenograft model, 1×10^6 $NALM6^{Luc}$ cells were injected intravenously (i.v.) in NSG mice, followed 2 days later by 5×10^6 primary T cells (NT-T, CAR-T19, or STAb-T19), where 19-CAR^+ or 19-$BITE^+$ T cells accounted for 10% of the infused T cells (5×10^5; **Fig. 4A**). Mice receiving NT-T cells were sacrificed within the first three weeks due to leukemia progression, whereas CAR-T19– and STAb-T19–treated mice effectively controlled $NALM6^{Luc}$ cells (**Fig. 4B** and **C**).

Notably, in contrast to STAb-T19–treated mice, 2 of the 6 mice that received CAR-T19 cells developed early cases of severe xenogeneic graft-versus-host disease (xGvHD) and had to be euthanized before week 5 (**Fig. 4B** and **D**). Flow cytometry analysis confirmed the bioluminescence imaging data, with an absence of leukemia cells in peripheral blood (PB), BM and spleen in mice treated with either CAR-T19 or STAb-T19 cells (**Fig. 4E**). qRT-PCR analysis confirmed the absence of CD19 transcripts in BM from both groups (**Fig. 4F**). Regarding T-cell persistence, we found a marked expansion of $CD3^+$ cells in PB, spleen, and BM in both groups (**Fig. 4G**), which could be a consequence of the xGvHD. In a more clinically relevant PDX model (**Fig. 4H**), NSG mice were i.v.-injected with 1×10^6 primary B-ALL cells homogeneously expressing CD19, CD22, and CD10 (**Fig. 4I**), followed 3 weeks later by i.v. infusion of 5×10^6 T cells (**Fig. 4H**), where 19-CAR^+ or 19-$BITE^+$ T cells comprised 10% of the infused T cells. An aggressive leukemia progression was observed in both BM (96.7% ± 0.5% on week 4) and PB (2.2 ± 1.3% and

Figure 2.

Leukemia escape from immune pressure. **A** and **B,** NALM6 cells were cocultured with NT-T, CAR-T19, or STAb-T19 cells at the indicated E:T ratios, and the relative percentage of $CD3^+CD19^-$, $CD3^-CD19^+$, and $CD3^-CD19^-$ cells were measured by FACS. **A,** Results are shown as the mean of three independent experiments. **B,** Representative FACS dot plots of the CAR-T19 1:8 E:T ratio sample. Gray, nonviable (NV), in which number of cells in the culture was <500. **C** and **D,** NALM6 coculture as in **A–B**, with CAR-T19 bearing the anti-CD19 FMC63 scFv (^{FMC63}CAR-T19), STAb-T19, or with NT-T cells in the presence of 100 ng/mL blinatumomab (BLI). One representative experiment out of two is shown. Dot plots (**D**) showing the cell populations cocultured at a 1:16 E:T ratio. **E,** The percentages of $CD3^+CD19^-$, $CD3^-CD19^+$, and $CD3^-CD19^-$ and $CD3^+CD19^+$ NALM6 or SEM cell lines after 2 hours of coculture with A-T cells at a 2:1 E:T ratio. The results are means of 3 ± SD similar experiments. **F** and **G,** The percentages of $CD3^+CD19^-$, $CD3^-CD19^+$, $CD3^-CD19^-$, and $CD3^+CD19^+$ NALM6 cells after coculture with NT-T cells, CAR-T19 cells bearing the anti-CD19 FMC63 scFv (^{FMC63}CAR-T19) or the anti-CD19 A3B1 (^{A3B1}CAR-T19), or STAb-T19 cells. **H,** Representative dot plots showing the downmodulation of 19-CAR in ^{A3B1}CAR-T19 cells after 2 hours of coculture with NALM6 cells. One representative experiment out of three independent experiments is shown. **I,** The percentage of $CD3^+CD19^-$, $CD3^-CD19^+$, $CD3^-CD19^-$, and $CD3^+CD19^+$ primary human B-ALL cells from two different patients (B-ALL1 and B-ALL2, >90% of $CD19^+$ B-ALL blasts) after coculture with primary A-T cells at a 2:1 E:T ratio. The results are means ± SD of 3 similar experiments. **J,** The number of alive ($7AAD^-$) target B-ALL1 and B-ALL2 cells determined after 24- and 48-hour coculture with primary NT-T, CAR-T19, or STAb-T19 cells at 1:2 and 1:1 E:T ratios. Results are shown as mean ± SD from 3 experiments. Significance was calculated by an unpaired Student *t* test.

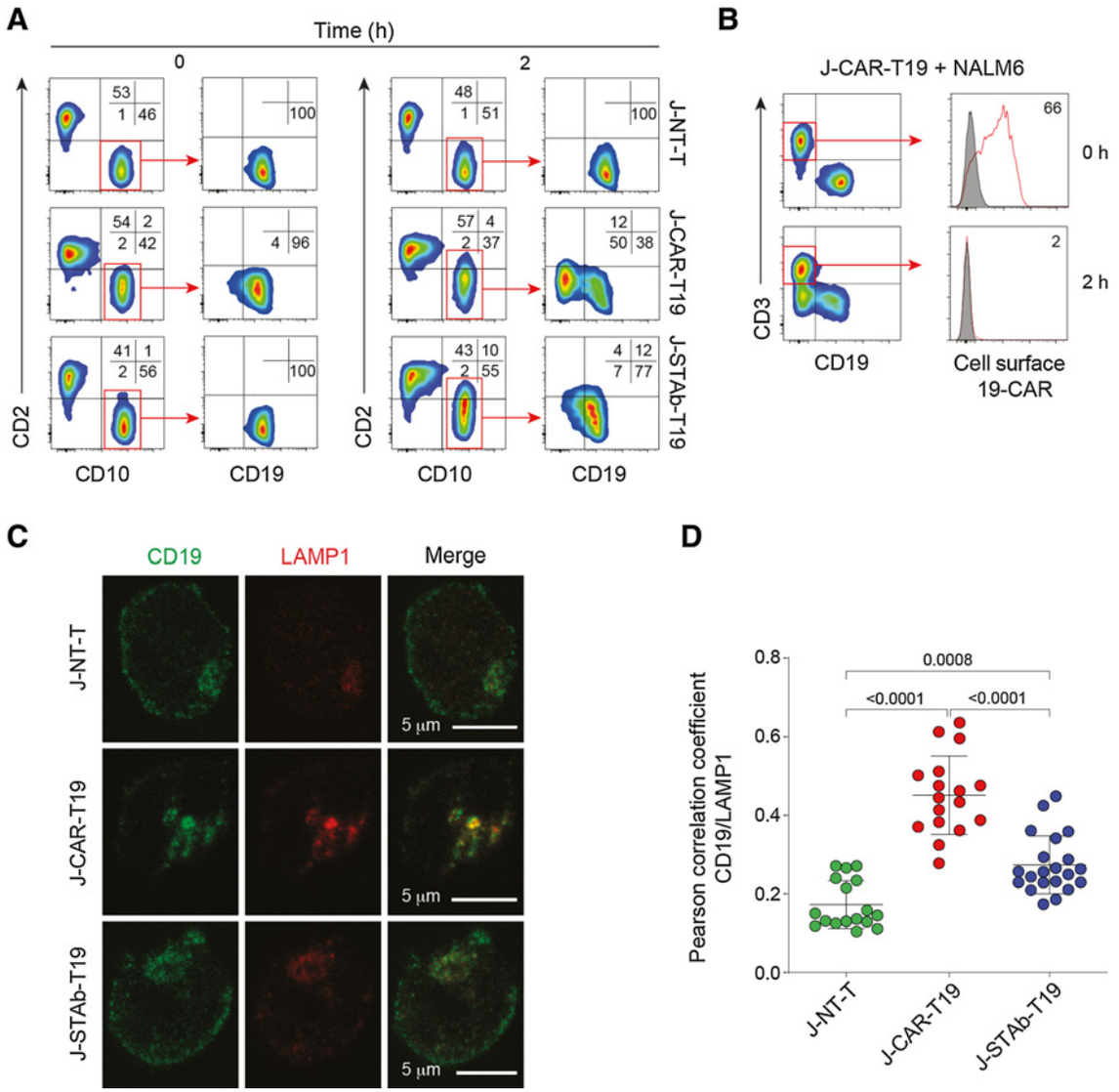

Figure 3.

CAR-T19 cells induced CD19 downmodulation and degradation. NALM6 cells were cocultured for 2 hours at a 1:1 E:T ratio with nontransduced Jurkat cells (J-NT), J-CAR-T19, or J-STAb-T19 cells. **A,** Representative dot plots showing CD2, CD19, and CD10 expression. **B,** Analysis of 19-CAR expression. **C,** Representative images of CD19 and LAMP1 cellular localization in NALM6 cells cocultured with J-NT-T, J-CAR-T19, or J-STAb-T19 cells. **D,** Pearson coefficients' for CD19 and LAMP1 colocalization assessment in NALM6 cells in the indicated cocultures. Dots represent the analyzed cells in one experiment representative of two performed. Mean ± SD values are shown. The *P* values were calculated with one-way ANOVA with Tukey multiple comparison tests.

12.1% ± 11.6%, on weeks 2 and 4, respectively) in NT-T cell–treated mice (**Fig. 4J** and **K**), that were euthanized 4 weeks after T-cell infusion due to the severity of the disease. In contrast, mice treated with CAR-T19 and STAb-T19 cells effectively controlled B-ALL growth for 8 weeks, when the mice were euthanized because of xGvHD (**Fig. 4J** and **K**). To exclude the presence of $CD19^-$ blasts, CD10 expression was analyzed by flow cytometry, and no $CD19^-CD10^+$ cells were detected in BM from CAR-T19– and STAb-T19–treated mice (**Fig. 4L**). T cells expanded progressively in PB, BM, and spleen, especially in the CAR-T19 group (**Fig. 4M**). These studies clearly showed that STAb-T19 cells are as effective as CAR-T19 cells in short-term *in vivo* models.

STAb-T19 cells prevent the leukemia relapse in long-term *in vivo* models

To test whether STAb-T19 cells can prevent escape *in vivo*, as observed *in vitro*, we modeled leukemia relapse by infusing lower doses of T cells to delay the onset of xGVHD and extend the observational window. NSG mice were i.v.-infused with 1×10^6 primary B-ALL cells from the same patient (**Fig. 4H** and **I**), followed 3 weeks later by i.v. infusion of 3×10^6 T cells [NT-T, CAR-T19 (5×10^5 19-CAR^+) or STAb-T19 (5×10^5 19-$BiTE^+$); **Fig. 5**A]. NT-T–treated mice rapidly developed leukemia, as shown by the increase in the percentage of blasts in PB early during week 2 and were sacrificed at week 5 (**Fig. 5B**). Both CAR-T19 and STAb-T19 groups initially controlled disease

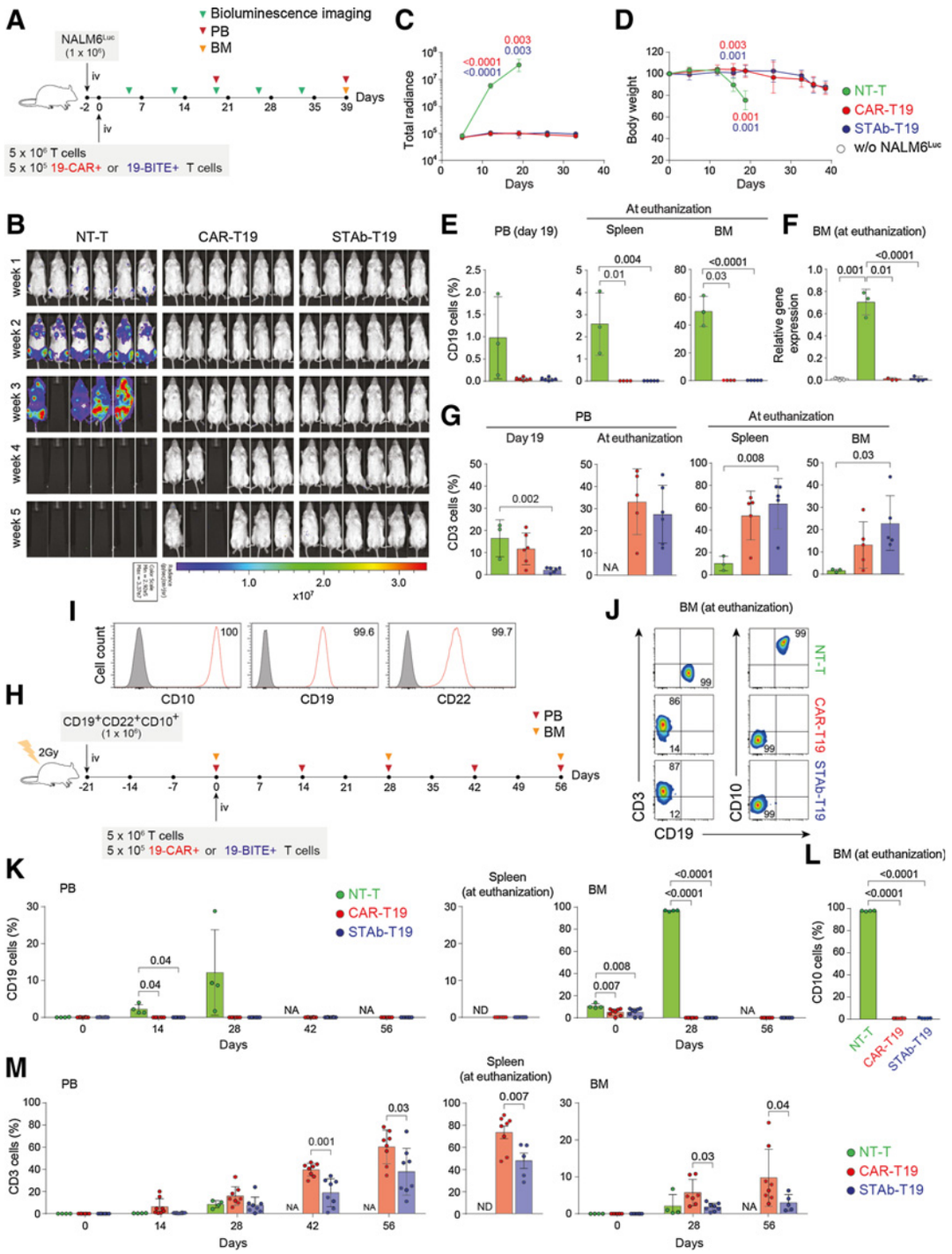

Figure 4.

In vivo antitumor efficacy of STAb-T19 cells. **A,** Timeline of cell line–derived xenograft murine model of NSG mice ($n = 6$/group) receiving i.v. NALM6^{Luc} cells followed by NT-T, CAR-T19, or STAb-T19 cells. **B,** Bioluminescence images showing disease progression. **C,** Total radiance quantification at the indicated time points. **D,** Change in body weight over time. **E,** Detection by FACS of B-ALL cells (CD19$^+$) cells in PB at day 19, and in spleen and BM at euthanization. **F,** Relative mRNA expression of *CD19* in BM at euthanization. **G,** T-cell (CD3$^+$) persistence in PB at days 19 and 39, and in spleen and BM at euthanization. Data are shown as mean ± SD. **H,** Timeline of PDX murine model of NSG mice receiving i.v. CD19$^+$ CD22$^+$ CD10$^+$ B-ALL blasts followed NT-T ($n = 4$), CAR-T19 ($n = 8$), or STAb-T19 ($n = 8$) cells. **I,** CD10, CD19, and CD22 expression in primary human B-ALL cells with the percentage of positive cells. **J,** Representative dot plots showing human T cells and B-ALL cells in BM of mice at day 56 after infusion. **K,** Percentage of CD19$^+$ leukemic cells in PB, spleen, and BM at indicated time points. **L,** Percentage of CD10$^+$ leukemic cells in BM at euthanization. **M,** Human T-cell persistence over time in PB, spleen, and BM at the indicated time points. Data are shown as mean ± SD; each dot represents an independent mouse. Significance was calculated by an unpaired Student *t* test. NA, not applicable; ND, not determined.

progression (**Fig. 5B**). However, blasts in PB of CAR-T19–treated mice gradually increased from week 4, and mice were euthanized when they reached 5% CD19$^+$ blasts in PB, whereas no blasts were detected in STAb-T19–treated mice by week 15 (**Fig. 5B**). Accordingly, analyses of spleen and BM showed complete leukemia control in STAb-T19–treated mice, whereas blasts were found in CAR-T19–treated mice (**Fig. 5C**). qRT-PCR confirmed the absence of CD19 transcripts in BM from STAb-T19–treated mice (**Fig. 5D**). The presence of CD19-negative blasts in BM was excluded by flow cytometry analysis of CD10 expression (**Fig. 5E**). Regarding T-cell expansion and persistence, percentages of CD3$^+$ cells in PB were lower than those observed in the groups that received 5 × 10^6 T cells (**Figs. 4M**; **5F** and **G**), although CAR-T19 cells (CD3$^+$GFP$^+$) and STAb-T19 cells (CD3$^+$tdTo$^+$) at week 2 comprised nearly 10% of the peripheral T cells (**Fig. 5H**). Consistent with these antileukemic results and absence of xGvHD, a very significant disease-free and overall survival benefit was observed for the mice that had been treated with STAb-T19 cells ($P = 0.005$; **Fig. 5I**).

Discussion

In this study, we demonstrate that engineered T cells expressing soluble anti-CD19/CD3 BiTEs are more effective than engineered CAR T cells expressing a membrane-anchored second-generation anti-CD19 CAR at inducing specific cytotoxicity, preventing tumor escape *in vitro*, and leukemia relapse *in vivo*. STAb-T19 cells redirect bystander T cells efficiently, leading to a more rapid and effective cytotoxic activity, even at very low E:T ratios. This demonstrates that *in situ*–secreted anti-CD19/CD3 BiTEs efficiently decorate CD3 on the surface of bystander T cells, converting them into efficient leukemia killers. Notably, unlike CAR-T19 cells, STAb-T19 cells are able to achieve a high cytotoxic effect at E:T ratios in which IFNγ secretion is low. This could imply that an effective treatment with STAb-T19 cells might require lower doses than those used with CAR-T19 cells and could be of particular relevance in such cases where it is not possible to generate an adequate number of CAR T cells due to the lymphopenic status of many multitreated patients or due to manufacturing problems (21). Therefore, a reduction in

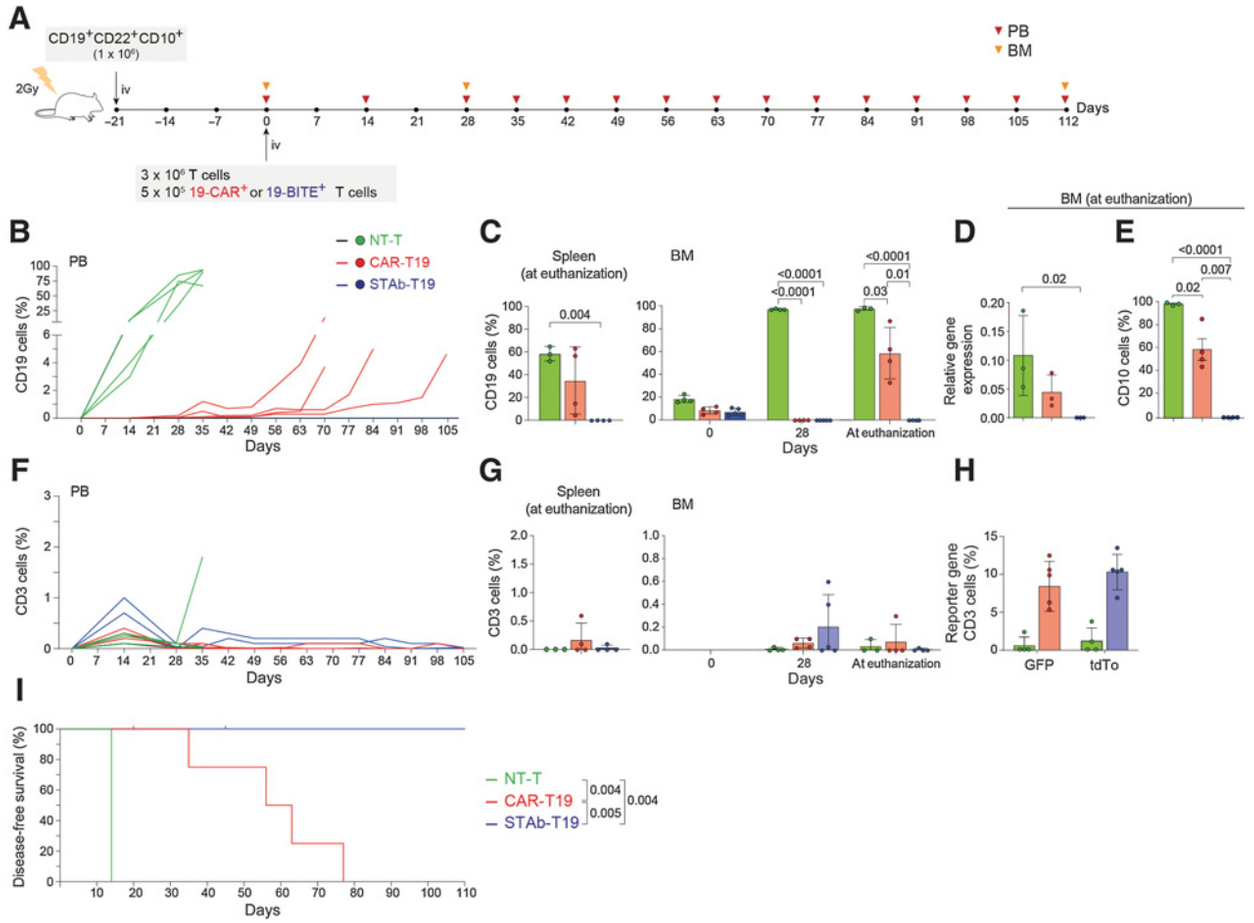

Figure 5.

STAb-T19 cells, but not CAR-T19, prevent relapse in a PDX murine model. **A,** Timeline of NSG mice transplanted with human primary CD19$^+$ CD22$^+$ CD10$^+$ B-ALL blasts followed by NT-T ($n = 4$), CAR-T19 ($n = 5$), or STAb-T19 ($n = 5$) cells. **B,** Percentage of B-ALL cells (CD19$^+$) in PB over time; each line represents an independent mouse. **C,** Percentage of human B-ALL cells in spleens and BM of NT-T, CAR-T19, and STAb-T19–treated mice at the indicated time points post-infusion. **D,** Relative mRNA expression of *CD19* in BM at euthanization, and (**E**) percentage of CD10$^+$ leukemic cells in BM at euthanization. **F,** Human T-cell (CD3$^+$) persistence over time in PB of each individual mouse. **G,** Percentage of human T cells (CD3$^+$) in spleen and BM at the indicated time points, and (**H**) percentage of human CD3$^+$ cells expressing reporter genes (GFP or tdTo). Data are shown as mean ± SD; each dot represents an independent mouse. Significance was calculated by an unpaired Student *t* test. **I,** Disease-free survival curve according to the percentage of CD19$^+$ B-ALL cells in PB. Significance was calculated by a log-rank test.

the therapeutically effective cell number may increase the number of patients who would benefit from STAb T-cell therapy, and significantly reduce the cost of the treatment. In addition, disease progression during the manufacturing period may, in some circumstances, preclude CAR T-based therapies (21), in which case the requirement for a lower number of cells and the accordingly shortened manufacturing time would be advantageous.

STAb-T19 cells, contrary to CAR-T19 cells, prevent *in vitro* tumor escape even at 1:32 E:T ratio. Leukemia escape is associated with rapid and drastic CAR-mediated CD19 downmodulation, alongside an intense loss of T-cell surface CAR. It has been reported that the density of the targeted antigen plays an important role in the modulation of CAR T cell–activation, which occurs only if a threshold density is reached (22). Therefore, the partial or complete loss of CD19 could explain the reduced cytotoxic activity of CAR-T19 cells. Importantly, this CAR-mediated CD19 downmodulation is also observed in engineered T cells expressing a second-generation CAR containing an scFv derived from the anti-CD19 clone FMC63, which has been used to generate the four FDA-approved anti-CD19 CAR T therapies (2). Furthermore, our data indicate that the rapid CAR-mediated internalization is associated with lysosome-mediated CD19 degradation. This leads to the emergence of a subpopulation of leukemic cells that transiently decrease CD19 expression and evade the immune response of CAR-T19 cells. Subsequently, when the CAR-mediated selective pressure is reduced or disappears, leukemia cells progress and recover CD19 expression. The rate of CD19 internalization upon binding to soluble anti-CD19 antibodies varies considerably (23, 24) and, in fact, has been shown that only a small fraction of an FMC63 scFv-based monovalent molecule bound to the surface is internalized (25). This suggests that membrane anchoring of the anti-CD19 scFv through the CAR is instrumental to induce CD19 internalization and could explain why we did not observe internalization following BiTE-mediated interaction. This phenomenon of CD19 downmodulation after CAR-T19 cell interaction, which has not been previously characterized, may have a major impact *in vivo*. Although both strategies show similar efficacy in short-term (40–60 days) mouse models, there is a drastic difference between the two CD19-targeted therapies in a long-term (over 100 days) PDX mouse model. In the long-term mouse model, STAb-T19 cells efficiently eradicated leukemia cells, whereas leukemia relapsed after CAR-T19 therapy. Most *in vivo* models used to study the efficacy of CAR T therapies in which complete remission is achieved are conducted with short- to intermediate-length windows of observation (13, 26, 27), which may lead to an underestimation of the risk of relapse after CAR-T19–based treatment.

In addition to CD19, CARs also undergo a rapid downmodulation after antigen engagement. Indeed, ligand-induced downmodulation is a common feature of antigen receptors such as TCR (28). CAR downmodulation has been reported to occur due to ubiquitination and lysosomal degradation (29) and leads to attenuation of the tumor killing ability of CAR T cells (29–31). In contrast, we did not observe such a drastic reduction of CD3 expression after BiTE-mediated interactions. Although the CAR- and BiTE-mediated T-cell redirection strategies are conceptually similar, they are very distinct in their implementation. CARs are artificial type I transmembrane proteins with variable modular architecture, which directly interacts with CD19, whereas soluble Fc-free BiTEs establish bridges between two type I transmembrane proteins, CD19 and the CD3ε subunit of the TCR/CD3 complex (5). Moreover, our findings support previous studies showing that, whereas CAR-T19 cells form noncanonical disorganized ISs (32–34), anti-CD19/CD3 BiTEs induce the formation of canonical ISs (35, 36), which promote efficient degranulation and prevent the CD19 downmodulation and degradation observed in CAR-mediated interactions. In summary, the absence of CD19 downmodulation in the STAb-T19 strategy, coupled with the continued secretion of BiTEs, allows a rapid recruitment of the endogenous T-cell pool, resulting in a fast and efficient elimination of cancer cells, which may prevent the leukemia relapse that is frequently associated with CAR-T19 therapies. Further studies are needed to fully evaluate the therapeutic capacity and toxicity profile of STAb-T19 cells in a clinical setting.

Authors' Disclosures

S. Guedan reports grants from the Spanish Ministry of Science and Innovation during the conduct of the study; grants from Spanish Ministry of Science and Innovation, Innovative Medicines Initiative 2, La Caixa, and Asociación Española contra el Cancer outside the submitted work; and she has received research funding from Gilead and Roche and personal honoraria from Gilead, Novartis, and Bristol-Myers Squibb. M. Juan reports a patent for EP3865513A1 pending. P. Menéndez reports grants from Onechain ImmunoTx during the conduct of the study and is the founder of Onechain Immnunotherapeutics, a spin-off company from the Josep Carreras Leukemia Research Institute. L. Álvarez-Vallina reports grants from CRIS Cancer Foundation, Carlos III Health Institute, Spanish Association Against Cancer, and Spanish Ministry of Science and Innovation during the conduct of the study; and cofounder of Leadartis, a spin-off focused on unrelated interest. No disclosures were reported by the other authors.

Authors' Contributions

B. Blanco: Conceptualization, resources, supervision, funding acquisition, investigation, methodology, writing–original draft, writing–review and editing. **A. Ramírez-Fernández:** Investigation, methodology, writing–original draft. **C. Bueno:** Resources, supervision, funding acquisition, investigation, methodology, writing–review and editing. **L. Argemí-Muntadas:** Investigation, methodology, writing–review and editing. **P. Fuentes:** Resources, investigation, methodology, writing–review and editing. **Ó. Aguilar-Sopeña:** Investigation and methodology. **F. Gutierrez-Agüera:** Validation, investigation, and methodology. **S.R. Zanetti:** Investigation, methodology, writing–review and editing. **A. Tapia-Galisteo:** Investigation and methodology. **L. Díez-Alonso:** Investigation and methodology. **A. Segura-Tudela:** Investigation and methodology. **M. Castellà:** Investigation and methodology. **B. Marzal:** Investigation and methodology. **S. Betriu:** Investigation and methodology. **S.L. Harwood:** Investigation, methodology, writing–review and editing. **M. Compte:** Investigation and methodology. **S. Lykkemark:** Investigation and methodology. **A. Erce-Llamazares:** Investigation and methodology. **L. Rubio-Pérez:** Investigation and methodology. **A. Jiménez-Reinoso:** Investigation and visualization. **C. Domínguez-Alonso:** Investigation and methodology. **M. Neves:** Investigation and methodology. **P. Morales:** Investigation and methodology. **E. Paz-Artal:** Investigation and methodology. **S. Guedan:** Investigation and methodology. **L. Sanz:** Funding acquisition, investigation, methodology, writing–review and editing. **M.L. Toribio:** Resources, funding acquisition, methodology, writing–review and editing. **P. Roda-Navarro:** Resources, funding acquisition, methodology, writing–review and editing. **M. Juan:** Resources, funding acquisition, investigation, methodology, writing–review and editing. **P. Menéndez:** Resources, supervision, funding acquisition, methodology, writing–review and editing. **L. Álvarez-Vallina:** Conceptualization, resources, formal analysis, supervision, funding acquisition, validation, investigation, writing–original draft, writing–review and editing.

Acknowledgments

We thank R. Vilella for generating and providing the A3B1 antibody, F. Sánchez-Madrid for reagents, and the staff of the fluorescence microscopy facility of the Complutense University of Madrid for assistance with the confocal microscopy. We thank CRIS Cancer Foundation, CERCA/Generalitat de Catalunya, and Fundació Josep Carreras-Obra Social la Caixa for core support. Financial support for this work was obtained from the European Research Council (CoG-2014-646903, PoC-2018-811220, to P. Menéndez); the Spanish Ministry of Science and Innovation (PID2019-105623RB-I00, to M.L. Toribio; SAF2016-75656-P and RTC-2017-5944-1, to P. Roda-Navarro; SAF-2019-108160-R, to

P. Menéndez; and SAF2017-89437-P, PID2020-117323RB-100, and PDC2021-121711-100, to L. Álvarez-Vallina), partially supported by the European Regional Development Fund (ERDF); the Carlos III Health Institute (ISCIII, PI20/01030, to B. Blanco; PI20/00822 to C. Bueno; PI16/00357 and PI19/00132 to L. Sanz; PICI14/122, PI13/676, PIE13/33, and PI18/775, to M. Juan; DTS20/00089, to L. Álvarez-Vallina), partially supported by the ERDF; the Obra Social La Caixa (LCF/PR/HR19/52160011, to P. Menéndez), CatSalut, Fundació La Caixa (CP042702, to M. Juan); the Spanish Association Against Cancer (AECC CICPF18030TORI, to M.L. Toribio; AECC 19084, to L. Álvarez-Vallina); Fundación Uno Entre Cien Mil, and Fundación Ramón Areces to M.L. Toribio; and the CRIS Cancer Foundation (FCRIS-IFI-2018 and FCRIS-IFI-2020, to L. Álvarez-Vallina). ISCIII-RICORS is supported within the Next Generation EU program (Plan de Recuperación, Transformación y Resiliencia). S. Guedan has received funding from the Spanish Ministry of Science and Innovation under a Ramon y Cajal grant (RYC2018-024442-I). A. Tapia-Galisteo was supported by predoctoral fellowship from Comunidad Autónoma de Madrid (PEJD-2018- PRE/BMD-8314). L. Díez-Alonso was supported by a Rio Hortega fellowship from the ISCIII (CM20/00004). L. Rubio-Pérez was supported by a predoctoral fellowship from the Immunology Chair, Universidad Francisco de Vitoria/Merck. C. Domínguez-Alonso was supported by a predoctoral fellowship from the Spanish Ministry of Science and Innovation (PRE2018-083445). M. Neves was supported by a grant from Portuguese Foundation for Science and Technology (SFRH/BD/136574/2018).

The costs of publication of this article were defrayed in part by the payment of page charges. This article must therefore be hereby marked *advertisement* in accordance with 18 U.S.C. Section 1734 solely to indicate this fact.

Received October 7, 2021; revised December 6, 2021; accepted February 9, 2022; published first February 14, 2022.

References

1. Blanco B, Compte M, Lykkemark S, Sanz L, Alvarez-Vallina LT. Cell-redirecting strategies to 'STAb' tumors: beyond CARs and bispecific antibodies. Trends Immunol 2019;40:243–57.
2. Frigault MJ, Maus MV. State of the art in CAR T cell therapy for CD19+ B cell malignancies. J Clin Invest 2020;130:1586–94.
3. Romero D. Haematological cancer: blinatumomab facilitates complete responses. Nat Rev Clin Oncol 2018;15:200.
4. Xu X, Sun Q, Liang X, Chen Z, Zhang X, Zhou X, et al. Mechanisms of relapse after CD19 CAR T-cell therapy for acute lymphoblastic leukemia and its prevention and treatment strategies. Front Immunol 2019;10:2664.
5. Blanco B, Ramirez-Fernandez A, Alvarez-Vallina L. Engineering immune cells for in vivo secretion of tumor-specific T cell-redirecting bispecific antibodies. Front Immunol 2020;11:1792.
6. Maude SL, Frey N, Shaw PA, Aplenc R, Barrett DM, Bunin NJ, et al. Chimeric antigen receptor T cells for sustained remissions in leukemia. N Engl J Med 2014; 371:1507–17.
7. Shah NN, Fry TJ. Mechanisms of resistance to CAR T cell therapy. Nat Rev Clin Oncol 2019;16:372–85.
8. Hamieh M, Dobrin A, Cabriolu A, van der Stegen SJC, Giavridis T, Mansilla-Soto J, et al. CAR T cell trogocytosis and cooperative killing regulate tumour antigen escape. Nature 2019;568:112–6.
9. Blanco B, Holliger P, Vile RG, Alvarez-Vallina L. Induction of human T lymphocyte cytotoxicity and inhibition of tumor growth by tumor-specific diabody-based molecules secreted from gene-modified bystander cells. J Immunol 2003;171:1070–7.
10. Compte M, Blanco B, Serrano F, Cuesta AM, Sanz L, Bernad A, et al. Inhibition of tumor growth in vivo by in situ secretion of bispecific anti-CEA x anti-CD3 diabodies from lentivirally transduced human lymphocytes. Cancer Gene Ther 2007;14:380–8.
11. Velasquez MP, Torres D, Iwahori K, Kakarla S, Arber C, Rodriguez-Cruz T, et al. T cells expressing CD19-specific engager molecules for the immunotherapy of CD19-positive malignancies. Sci Rep 2016;6:27130.
12. Liu X, Barrett DM, Jiang S, Fang C, Kalos M, Grupp SA, et al. Improved anti-leukemia activities of adoptively transferred T cells expressing bispecific T-cell engager in mice. Blood Cancer J 2016;6:e430.
13. Castella M, Boronat A, Martin-Ibanez R, Rodriguez V, Sune G, Caballero M, et al. Development of a novel anti-CD19 chimeric antigen receptor: a paradigm for an affordable CAR T cell production at academic institutions. Mol Ther Methods Clin Dev 2019;12:134–44.
14. Haryadi R, Ho S, Kok YJ, Pu HX, Zheng L, Pereira NA, et al. Optimization of heavy chain and light chain signal peptides for high level expression of therapeutic antibodies in CHO cells. PLoS One 2015; 10:e0116878.
15. Compte M, Alvarez-Cienfuegos A, Nunez-Prado N, Sainz-Pastor N, Blanco-Toribio A, Pescador N, et al. Functional comparison of single-chain and two-chain anti-CD3-based bispecific antibodies in gene immunotherapy applications. Oncoimmunology 2014;3:e28810.
16. Zanetti SR, Romecin PA, Vinyoles M, Juan M, Fuster JL, Camos M, et al. Bone marrow MSC from pediatric patients with B-ALL highly immunosuppress T-cell responses but do not compromise CD19-CAR T-cell activity. J Immunother Cancer 2020;8:e001419.
17. Harwood SL, Alvarez-Cienfuegos A, Nunez-Prado N, Compte M, Hernandez-Perez S, Merino N, et al. ATTACK, a novel bispecific T cell-recruiting antibody with trivalent EGFR binding and monovalent CD3 binding for cancer immunotherapy. Oncoimmunology 2017;7:e1377874.
18. Cuesta-Mateos C, Fuentes P, Schrader A, Juarez-Sanchez R, Loscertales J, Mateu-Albero T, et al. CCR7 as a novel therapeutic target in t-cell PROLYMPHOCYTIC leukemia. Biomark Res 2020;8:54.
19. Ortiz-Maldonado V, Rives S, Castella M, Alonso-Saladrigues A, Benitez-Ribas D, Caballero-Banos M, et al. CART19-BE-01: a multicenter trial of ARI-0001 cell therapy in patients with CD19(+) relapsed/refractory malignancies. Mol Ther 2021;29:636–44.
20. Velasco-Hernandez T, Zanetti SR, Roca-Ho H, Gutierrez-Aguera F, Petazzi P, Sanchez-Martinez D, et al. Efficient elimination of primary B-ALL cells in vitro and in vivo using a novel 4-1BB-based CAR targeting a membrane-distal CD22 epitope. J Immunother Cancer 2020; 8:e000896.
21. Graham C, Jozwik A, Pepper A, Benjamin R. Allogeneic CAR-T cells: More than ease of access? Cells 2018;7:155.
22. Majzner RG, Mackall CL. Tumor antigen escape from CAR T-cell therapy. Cancer Discov 2018;8:1219–26.
23. Sapra P, Allen TM. Internalizing antibodies are necessary for improved therapeutic efficacy of antibody-targeted liposomal drugs. Cancer Res 2002; 62:7190–4.
24. Horton HM, Bernett MJ, Pong E, Peipp M, Karki S, Chu SY, et al. Potent in vitro and in vivo activity of an Fc-engineered anti-CD19 monoclonal antibody against lymphoma and leukemia. Cancer Res 2008; 68:8049–57.
25. Du X, Beers R, Fitzgerald DJ, Pastan I. Differential cellular internalization of anti-CD19 and -CD22 immunotoxins results in different cytotoxic activity. Cancer Res 2008;68:6300–5.
26. Scarfo I, Ormhoj M, Frigault MJ, Castano AP, Lorrey S, Bouffard AA, et al. Anti-CD37 chimeric antigen receptor T cells are active against B- and T-cell lymphomas. Blood 2018;132:1495–506.
27. Ormhoj M, Scarfo I, Cabral ML, Bailey SR, Lorrey SJ, Bouffard AA, et al. Chimeric antigen receptor T cells targeting CD79b show efficacy in lymphoma with or without cotargeting CD19. Clin Cancer Res 2019;25: 7046–57.
28. Liu H, Rhodes M, Wiest DL, Vignali DA. On the dynamics of TCR:CD3 complex cell surface expression and downmodulation. Immunity 2000;13: 665–75.
29. Li W, Qiu S, Chen J, Jiang S, Chen W, Jiang J, et al. Chimeric antigen receptor designed to prevent ubiquitination and downregulation showed durable anti-tumor efficacy. Immunity 2020;53:456–70.
30. Davenport AJ, Jenkins MR, Cross RS, Yong CS, Prince HM, Ritchie DS, et al. CAR-T cells inflict sequential killing of multiple tumor target cells. Cancer Immunol Res 2015;3:483–94.
31. Walker AJ, Majzner RG, Zhang L, Wanhainen K, Long AH, Nguyen SM, et al. Tumor antigen and receptor densities regulate efficacy of a chimeric

antigen receptor targeting anaplastic lymphoma kinase. Mol Ther 2017;25:2189–201.
32. Mukherjee M, Mace EM, Carisey AF, Ahmed N, Orange JS. Quantitative imaging approaches to study the CAR immunological synapse. Mol Ther 2017;25:1757–68.
33. Davenport AJ, Cross RS, Watson KA, Liao Y, Shi W, Prince HM, et al. Chimeric antigen receptor T cells form nonclassical and potent immune synapses driving rapid cytotoxicity. Proc Natl Acad Sci U S A 2018;115:E2068–76.
34. Watanabe K, Kuramitsu S, Posey AD Jr, June CH. Expanding the therapeutic window for CAR T cell therapy in solid tumors: the knowns and unknowns of CAR T cell biology. Front Immunol 2018;9:2486.
35. Offner S, Hofmeister R, Romaniuk A, Kufer P, Baeuerle PA. Induction of regular cytolytic T cell synapses by bispecific single-chain antibody constructs on MHC class I-negative tumor cells. Mol Immunol 2006;43:763–71.
36. Kouhestani D, Geis M, Alsouri S, Bumm TGP, Einsele H, Sauer M, et al. Variant signaling topology at the cancer cell-T-cell interface induced by a two-component T-cell engager. Cell Mol Immunol 2021;18:1568–70.

Supplemental Material

Overcoming CAR-mediated CD19 downmodulation and leukemia relapse with T lymphocytes secreting anti-CD19 T cell engagers

Supplementary Figures

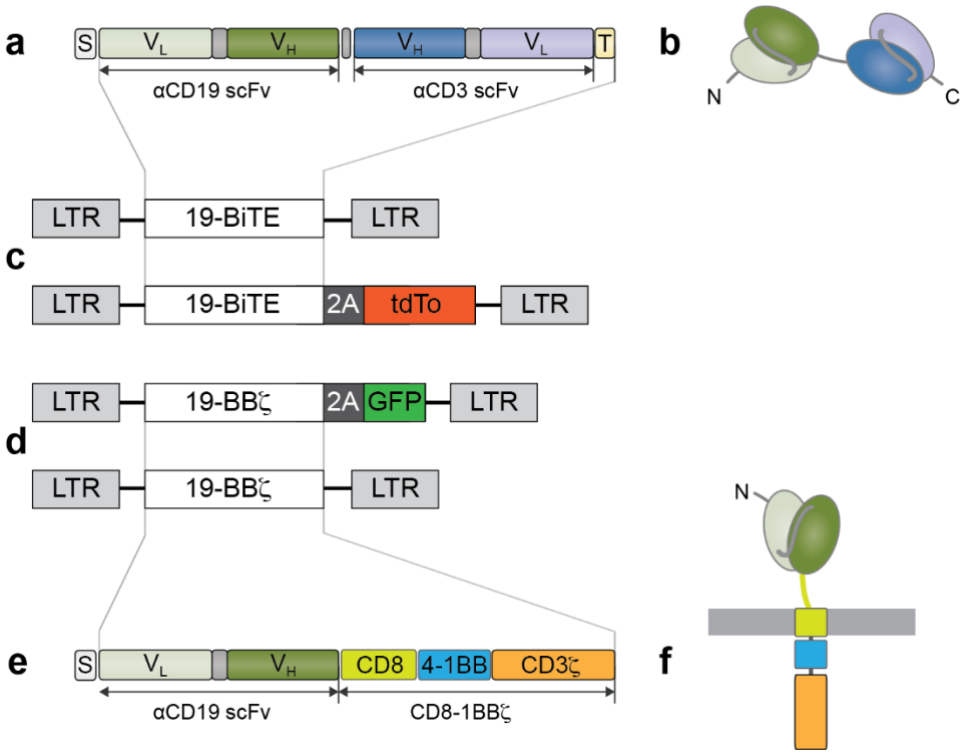

Supplementary Figure 1. **19-BiTE and 19-BBζ structures.** Schematic diagrams showing the genetic (a) and domain structure (b) of the 19-BiTE, bearing a signal peptide from the human *k* light chain signal peptide (white box), the anti-CD19 A3B1 scFv gene (green boxes), the anti-CD3 OKT3 scFv gene (blue boxes), and the His tag (yellow box). (c) Two different constructs were designed, one containing the tdTomato (tdTo) reporter gene following the 2A sequence from *Thosea asigna* virus. (d) Two different 19-BBζ constructs were designed, one containing the GFP reporter gene following the 2A sequence; (e) genetic and (f) domain structures of the A3B1 scFv-CD8α-4BB-CD3ζ, are shown.

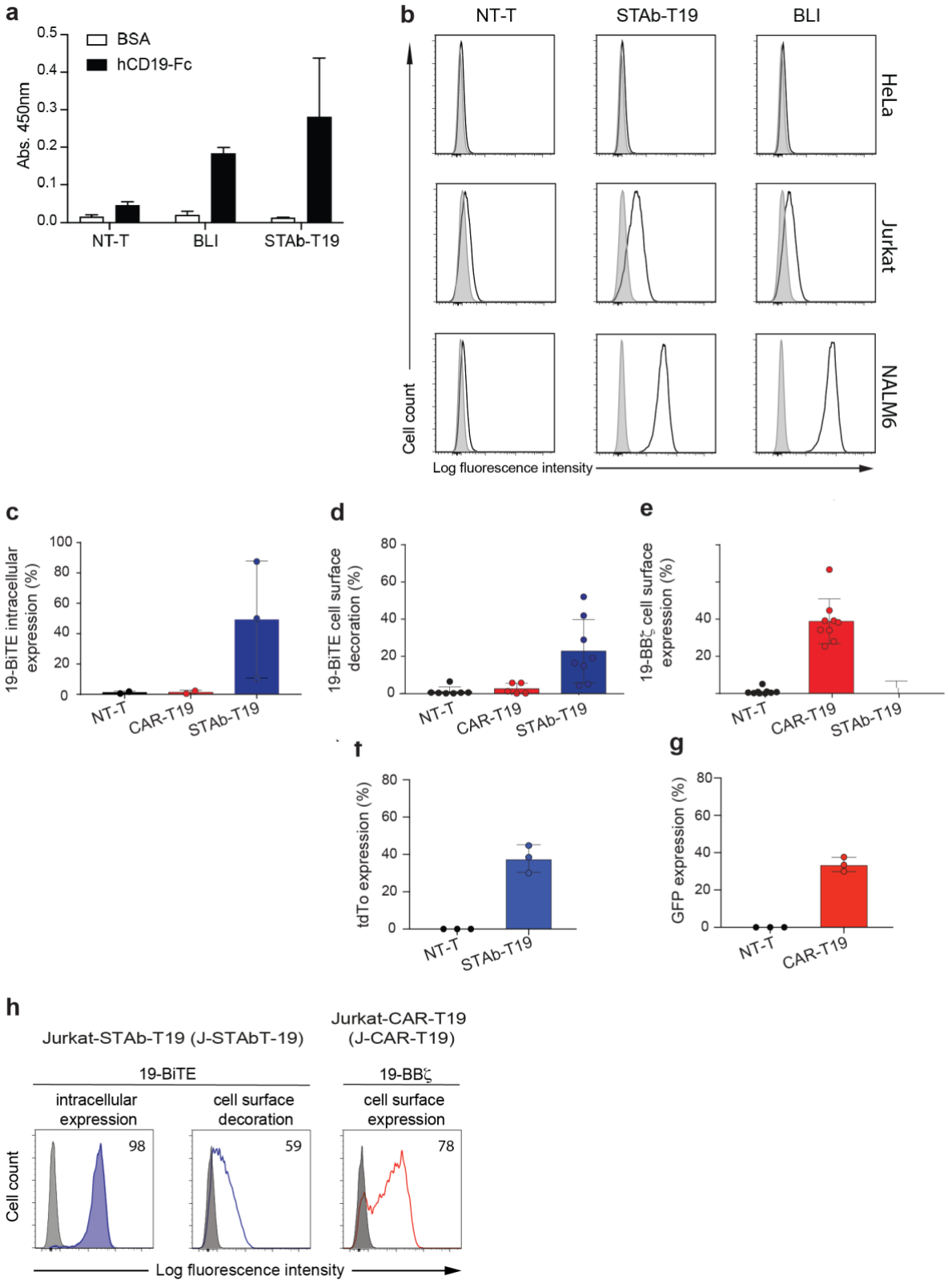

Supplementary Figure 2. Functionality of secreted 19-BiTE and transduction efficiency studies. (a) Detection of soluble functional 19-BiTE in the conditioned media from non-transduced primary T cells (NT-T) or transduced with pCCL-EF1α-BiTE19 lentiviral vector

(STAb-T19) by ELISA against plastic-immobilized human CD19-Fc chimera (hCD19) or BSA; purified blinatumomab (BLI, 100 ng/ml) was used as control. Data are mean ± SD of three independent experiments (b) The functionality of secreted 19-BiTE was demonstrated by FACS on $CD3^{-}CD19^{-}$ HeLa, $CD3^{+}CD19^{-}$ Jurkat or $CD3^{-}CD19^{+}$ NALM6 cells, using purified BLI (100 ng/ml) as control. Histograms are representative of three independent experiments. Activated human primary T cells were either untransduced (NT-T), transduced with the lentiviral vectors pCCL-EF1α-BiTE19 or pCCL-EF1α-CAR19 (c,d,e), or transduced with the reporter gene-encoding lentiviral vectors pCCL-EF1α-BiTE19-tdTo or pCCL-EF1α-CAR19-GFP vectors (f, g); intracellular 19-BiTE (c), cell-surface bound 19-BiTE (d), 19-BBζ CAR (e), tdTo (d) and GFP (e) expression are shown; results are mean ± SD of at least three different transductions. (h) Intracellular and cell surface-bound 19-BiTE on Jurkat T cells lentivirally transduced with pCCL-EF1α-BiTE19 (J-STAb-T19), and cell surface expression of 19-BBζ on transduced Jurkat T cells with pCCL-EF1α-CAR19 (J-CAR-T19).

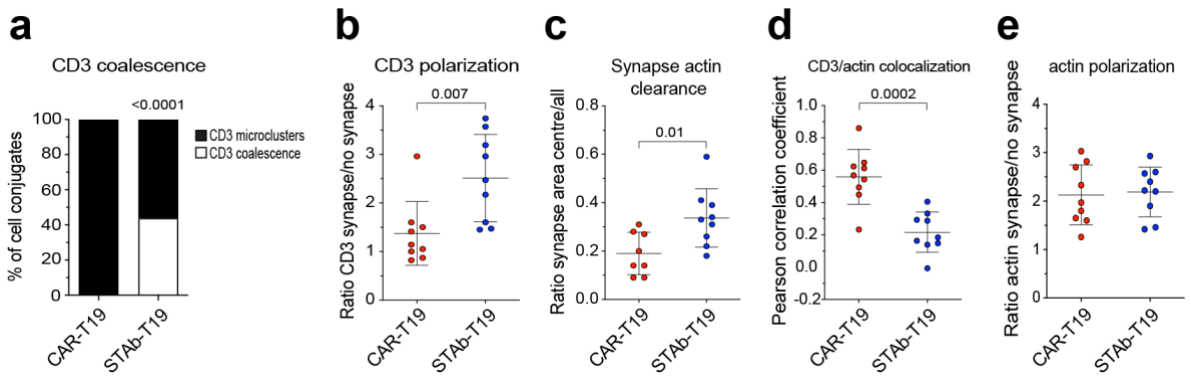

Supplementary Figure 3. Characteristics of immunological synapse (IS) on primary STAb-T19 and CAR-T19 cells. Primary CAR-T19 and STAb-T19 cells were stimulated for 15 minutes with Raji cells. (a) Graph representing the percentage of cell conjugates showing peripheral CD3 microclusters or cSMAC formation by CD3 coalescence. Contingency tests were performed in the comparison. Graphs representing (b) CD3 polarization, (c) actin polarization, (d) CD3/actin co-localization and (e) actin clearance at the IS in each cell. Symbols indicate individual cells (n = 9) analyzed and the black line the average value. Samples were compared by an ordinary one-way ANOVA with a Tukey's multiple comparison test. Data are mean ± SD of nine replicates from one representative experiment out of two.

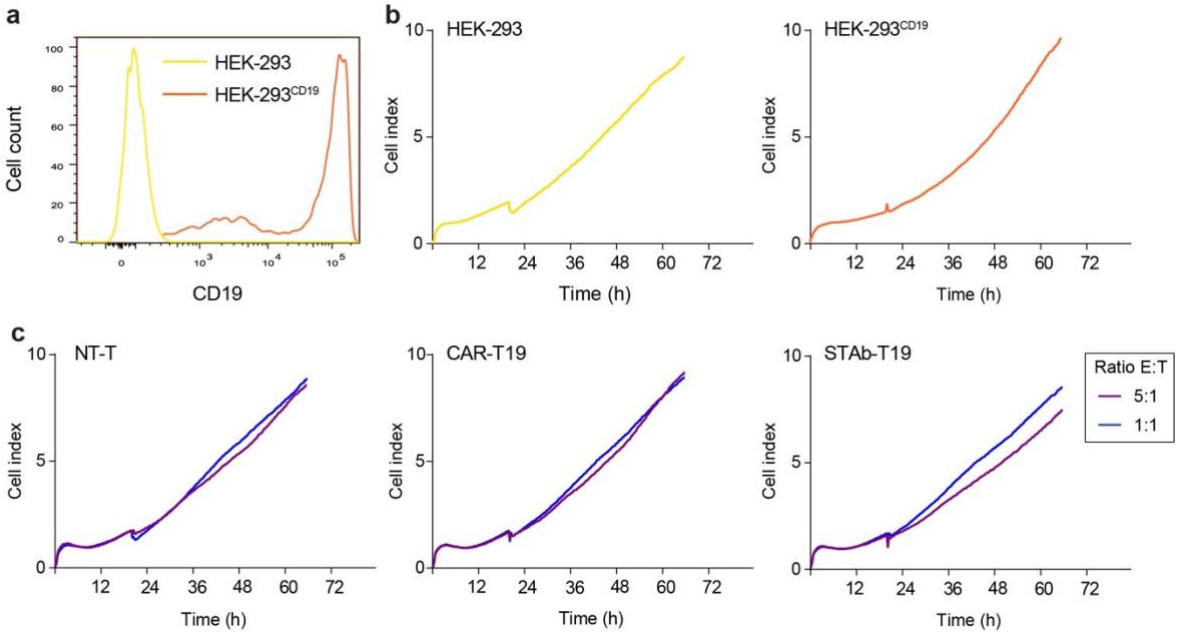

Supplementary Figure 4. Real-time cell cytotoxicity assay. (a) CD19 expression on HEK-293 and HEK-293^{CD19} cells, and (b) cell viability kinetics over time of both cell lines cultured alone. (c) Cell viability kinetics of HEK-293 cells co-cultured with primary NT-T, CAR-T19 or STAb-T19 cells at different E:T ratios (5:1 and 1:1). Cell Index values were determined over 65 hours with measurements taken at 15 min intervals and normalized. Results from one of two experiments performed in duplicate are shown.

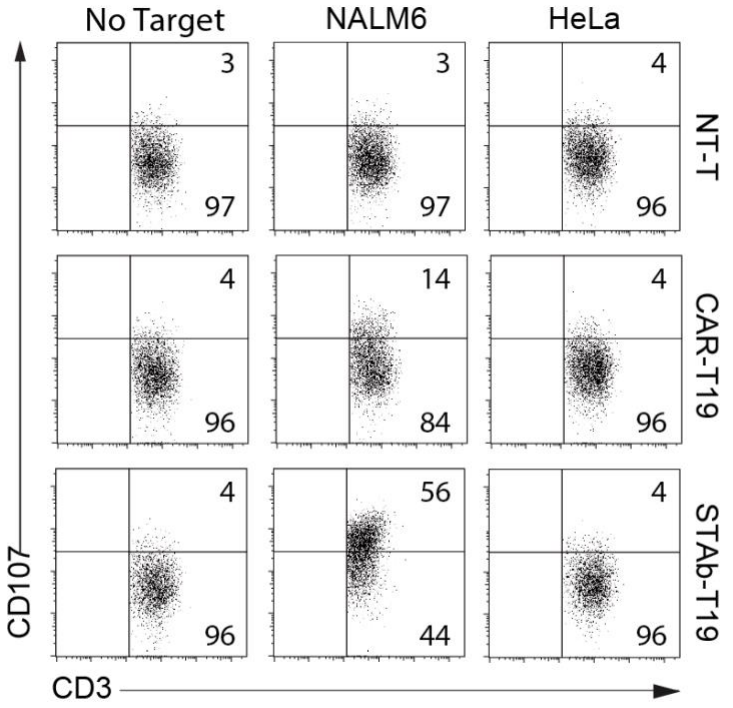

Supplementary Figure 5. CD107a expression. Primary NT-T, CAR-T19 or STAb-T19 cells were incubated alone or after exposure to $CD19^+$ (NALM6) or $CD19^-$ (HeLa) target cells at a 2:1 E:T ratio for 4 hours. The percentage of positive cells is displayed. One representative experiment out of three independent experiments is shown.

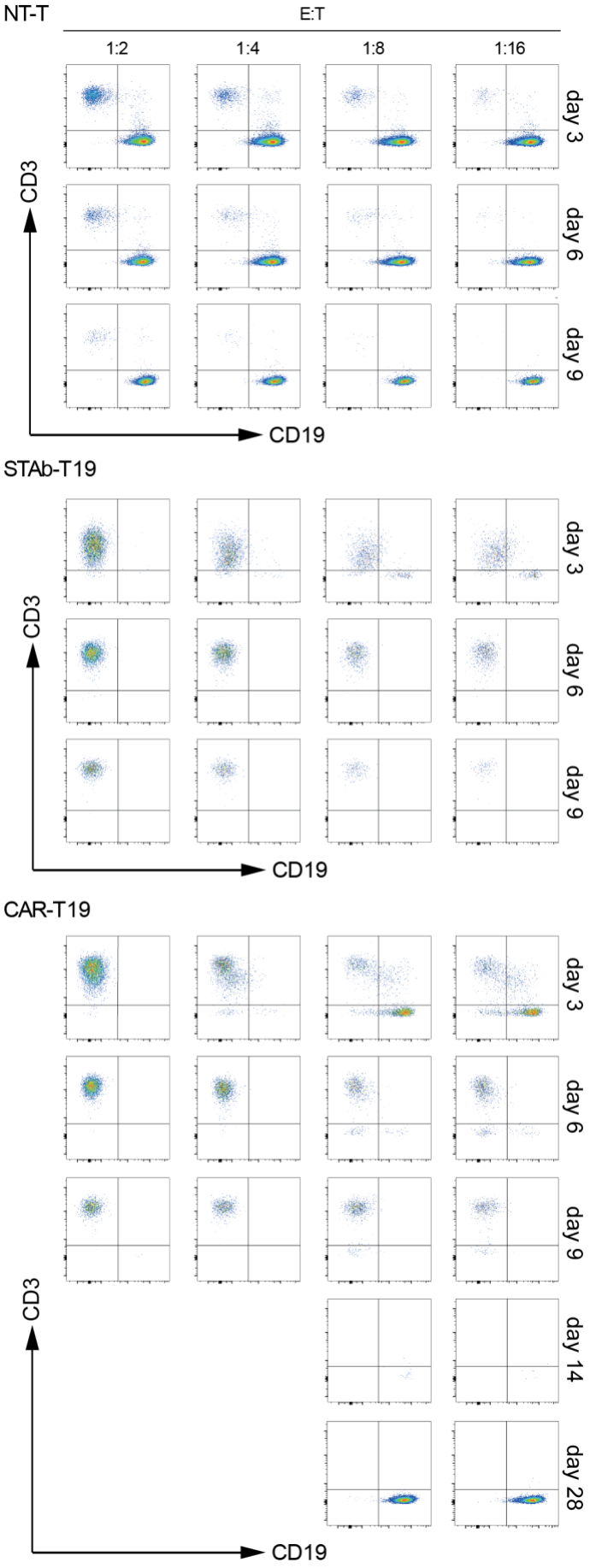

Supplementary Figure 6. Leukemia escape from immune pressure. NALM6 cells were co-cultured with primary NT-T, CAR-T19 or STAb-T19 cells at the indicated E:T ratios, and the expression of CD3 and CD19 was analyzed at time 0 and after 3, 6, 9, 14 and 28 days. Representative dot plots of one of three replicate experiments are shown.

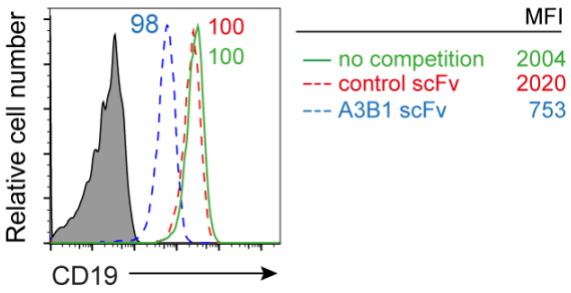

Supplementary Figure 7. Competition study of the anti-CD19 J3.119 and A3B1 antibodies. Percentage of $CD19^{+}$ NALM6 cells and mean fluorescence intensity (MFI) after labeling with PC5-conjugated J3.119 mAb in the presence or absence of the indicated competitors. One representative experiment out of three independent experiments is shown.

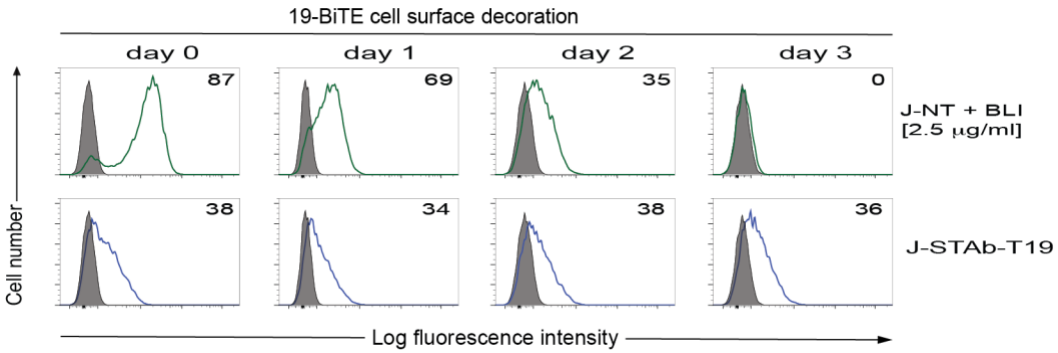

Supplementary Figure 8. Stability of cell surface-bound 19-BiTE. Non-transduced Jurkat cells (JN-T) incubated with 2.5 µg/ml blinatumomab (BLI), and pCCL-EF1α-BiTE19 transduced J-STAb-T19 cells (J-STAb-T19) were cultured for the indicated period of time and the level of cell surface-bound 19-BiTE determined by flow cytometry. One representative experiment out of three independent experiments is shown.

Supplementary Tables

Supplementary Table 1. Antibodies used for flow cytometry analysis and immunofluorescence and confocal microscopy.

FLOW CYTOMETRY	**MONOCLONAL ANTIBODIES - *in vitro* studies**				
	Target	Conjugation	Clone	Supplier	Catalog number
	human CD2	PE	S5.2	BD Biosciences[1]	347597
	human CD3	FITC	UCHT1	BD Biosciences	561806
	human CD3	PE	SK7	BD Biosciences	345765
	human CD3	APC	UCHT1	BD Biosciences	561810
	human CD3	PB	UCHT1	Beckman Coulter[2]	B49204
	human CD4	PE	MEM-241	Immunotools[3]	21270044
	human CD8	PE-Cy7	RPA-T8	BD Biosciences	557746
	human CD10	APC	HI10a	BD Biosciences	340923
	human CD19	PC5	J3.119	Beckman Coulter	A66328
	human CD19	PC7	J3.119	Beckman Coulter	IM3628
	human CD69	PE	L78	BD Biosciences	341652
	human CD107	PE	H4A3	BD Biosciences	555801
	human CD45RA	V500	HI100	BD Biosciences	561640
	human CCR7	BV421	150503	BD Biosciences	562555
	6xHis tag	Biotin	HIS.H8	Invitrogen[4]	MA1-21315-BTIN
	His	APC	GC11-8F3.5.1	Miltenyi Biotec[5]	130-119-782
	MONOCLONAL ANTIBODIES - *in vivo* studies				
	Target	Conjugation	Clone	Supplier	Catalog number
	human CD3	PerCP	SK7	BD Biosciences	347344
	human CD10	PECy7	HI10a	BD Biosciences	341092
	human CD19	BV421	HIB19	BD Biosciences	562440
	human CD22	APC	HIB22	BD Biosciencies	562860
	human CD45	AmCyan	2D1	BD Biosciences	339203
	human HLA-ABC	APC	G46-2.6	BD Biosciencies	562006
	POLYCLONAL ANTIBODIES				
	Antibody	Conjugation		Supplier	Catalog number
	goat anti-mouse IgG $F(ab')_2$	APC		Jackson ImmunoResearch[6]	115-136-072

IMMUNOFLUORESCENCE AND CONFOCAL MICROSCOPY	**PRIMARY ANTIBODIES**				
	Target	Conjugation	Clone	Supplier	
	human CD3	-	T3b	F. Sánchez Madrid[7]	
	human CD19	-	BU12	F. Sánchez Madrid	
	human CD107a	Alexa647	1DB4	Biolegend	328612
	SECONDARY ANTIBODIES				
	Antibody	Conjugation		Supplier	
	goat anti-mouse-Ig	Alexa 488		Invitrogen	10357742

[1] BD Biosciences, San Jose, CA, USA

[2] Beckman Coulter, Marseille Cedex, France

[3] Immunotools, Friesoythe, Germany

[4] Invitrogen, Rockford, IL, USA

[5] Miltenyi Biotec, Bergisch Gladbach, Germany

[6] Jackson ImmunoResearch, West Grove, PA, USA

[7] Dr. Francisco Sánchez-Madrid, Hospital Universitario de la Princesa, Madrid, Spain

Supplementary Table 2. Statistical analysis of cytotoxicity studies with primary B-ALL cells and primary T cells.

B-ALL1	Ratio E:T	*p* CAR-T19 vs. NT-T	*p* STAb-T19 vs. NT-T	*p* STAb-T19 vs. CAR-T19
24 h	1:1	0.0108	0.0002	0.0139
	1:2	0.0100	0.0078	0.054
48 h	1:1	0.7698	0.0069	0.0173
	1:2	0.2165	0.0028	0.0034

B-ALL2	Ratio E:T	*p* CAR-T19 vs. NT-T	*p* STAb-T19 vs. NT-T	*p* STAb-T19 vs. CAR-T19
24 h	1:1	0.0064	0.008	0.0446
	1:2	0.0150	0.0105	0.0433
48 h	1:1	0.1474	0.1475	0.9584
	1:2	0.1523	0.1436	0.4228

CAPÍTULO II: Synapse topology and downmodulation events determine the functional outcome of anti-CD19 T cell-redirecting strategies.

Ángel Ramírez-Fernández[#], Óscar Aguilar-Sopeña[#], Laura Díez-Alonso, Alejandro Segura-Tudela, Carmen Domínguez-Alonso, Pedro Roda-Navarro, Luis Álvarez-Vallina, Belén Blanco.

[#] Ambos autores han contribuido por igual

Oncoimmunology 2022; Mar 23; 11(1):2054106.

DOI: 10.1080/2162402X.2022.2054106

Introducción:

Numerosos estudios han demostrado la eficacia clínica de la terapia CAR-T y diversos trabajos han confirmado la capacidad de las células STAb-T para inducir repuestas antitumorales *in vivo*. Sin embargo, apenas hay estudios que investiguen la estructura de la SI formada tras las interacciones mediadas por CARs y TCEs. En este trabajo, hemos estudiado en profundidad la estructura de las "SIs artificiales" inducidas por ambas estrategias de redirección de células T frente a CD19, centrándonos en la expresión y dinámica de moléculas relevantes para la señalización y activación celular.

Objetivos:

1. Generación de células Jurkat STAb-T19 y caracterización funcional del BiTE-19 secretado.
2. Análisis estructural de la SI.
3. Estudio de la señalización temprana inducida por el TCR, *blinatumomab*, BiTE-19 y CAR-19.
4. Estudio de la expresión en membrana y tráfico de las moléculas CAR-19, CD19 y CD3.

Conclusiones:

1. El BiTE-19 secretado por las células Jurkat STAb-T19 reconoce el complejo TCR/CD3 de las células T y "decora" su superficie, lo que les permite unirse específicamente a CD19 humano de manera tan eficiente como las células Jurkat CAR-T19.
2. El BiTE-19 secretado por las células Jurkat STAb-T19 induce la formación de SIs canónicas, similares a las promovidas por el TCR, con acumulación de F-actina en la zona distal (dSMAC) y coalescencia de CD3 en la zona central (cSMAC). Por el contrario, el CAR-19 promueve SIs desorganizadas, con cúmulos dispersos de CD3 y una disposición difusa de la F-actina.
3. Las células Jurkat STAb-T19 muestran cinéticas de activación de PLCγ1 y ERK1/2 similares a las observadas en células Jurkat no transducidas estimuladas a través de su TCR. Por el contrario, las células Jurkat CAR-T19 generan una señalización más transitoria.

4. La interacción CAR-19:CD19 origina una reducción de CD19 en la membrana de las células diana, así como una rápida y drástica disminución de CAR-19 en la superficie de las células T. Ambas moléculas son internalizadas y se localizan en el compartimento lisosomal.
5. Tras la interacción de las células Jurkat STAb-T19 con células $CD19^+$ se produce una disminución moderada de la expresión de CD3 en membrana debido, al menos parcialmente, a la captación de CD3 por las células $CD19^+$.

Publicación:

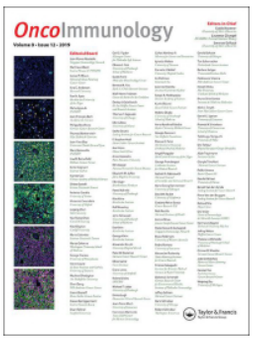

OncoImmunology

ISSN: (Print) (Online) Journal homepage: https://www.tandfonline.com/loi/koni20

Synapse topology and downmodulation events determine the functional outcome of anti-CD19 T cell-redirecting strategies

Ángel Ramírez-Fernández, Óscar Aguilar-Sopeña, Laura Díez-Alonso, Alejandro Segura-Tudela, Carmen Domínguez-Alonso, Pedro Roda-Navarro, Luis Álvarez-Vallina & Belén Blanco

To cite this article: Ángel Ramírez-Fernández, Óscar Aguilar-Sopeña, Laura Díez-Alonso, Alejandro Segura-Tudela, Carmen Domínguez-Alonso, Pedro Roda-Navarro, Luis Álvarez-Vallina & Belén Blanco (2022) Synapse topology and downmodulation events determine the functional outcome of anti-CD19 T cell-redirecting strategies, OncoImmunology, 11:1, 2054106, DOI: 10.1080/2162402X.2022.2054106

To link to this article: https://doi.org/10.1080/2162402X.2022.2054106

ONCOIMMUNOLOGY
2022, VOL. 11, NO. 1, e2054106 (11 pages)
https://doi.org/10.1080/2162402X.2022.2054106

Taylor & Francis
Taylor & Francis Group

ORIGINAL RESEARCH

OPEN ACCESS Check for updates

Synapse topology and downmodulation events determine the functional outcome of anti-CD19 T cell-redirecting strategies

Ángel Ramírez-Fernández[a,b#], Óscar Aguilar-Sopeña[c,d#], Laura Díez-Alonso[a,b], Alejandro Segura-Tudela[a,b], Carmen Domínguez-Alonso[a,b], Pedro Roda-Navarro[c,d], Luis Álvarez-Vallina[a,b,e], and Belén Blanco[a,b,e]

[a]Cancer Immunotherapy Unit (UNICA), Department of Immunology, Hospital, Universitario 12 de Octubre, Madrid, Spain; [b]Immuno-Oncology and Immunotherapy Group, Instituto de Investigación Sanitaria 12 de Octubre (imas12), Madrid, Spain; [c]Department of Immunology, Ophthalmology and ENT, School of Medicine, Universidad Complutense, Madrid, Spain; [d]Lymphocyte Immunobiology Group, Instituto de Investigación Sanitaria 12 de Octubre (imas12), Madrid, Spain; [e]Red Española de Terapias Avanzadas (TERAV), Instituto de Salud Carlos III (RICORS, RD21/0017/0029), Madrid, Spain

ABSTRACT

Cancer immunotherapy strategies based on the endogenous secretion of T cell-redirecting bispecific antibodies by engineered T lymphocytes (STAb-T) are emerging as alternative or complementary approaches to those based on chimeric antigen receptors (CAR-T). The antitumor efficacy of bispecific anti-CD19 × anti-CD3 (CD19×CD3) T cell engager (BiTE)-secreting STAb-T cells has been demonstrated in several mouse models of B-cell acute leukemia. Here, we have investigated the spatial topology and downstream signaling of the artificial immunological synapses (IS) that are formed by CAR-T or STAb-T cells. Upon interaction with CD19-positive target cells, STAb-T cells form IS with structure and signal transduction, which more closely resemble those of physiological cognate IS, compared to IS formed by CAR-T cells expressing a second-generation CAR bearing the same CD19-single-chain variable fragment. Importantly, while CD3 is maintained at detectable levels on the surface of STAb-T cells, indicating sustained activation mediated by the secreted BiTE, the anti-CD19 CAR was rapidly downmodulated, which correlated with a more transient downstream signaling. Furthermore, CAR-T cells, but not STAb-T cells, provoke an acute loss of CD19 in target cells. Such differences might represent advantages of the STAb-T strategy over the CAR-T approach and should be carefully considered in order to develop more effective and safer treatments for hematological malignancies.

ARTICLE HISTORY
Received 4 November 2021
Revised 23 February 2022
Accepted 11 March 2022

KEYWORDS
CD19$^+$ B cell malignancies; T cell-redirecting strategies; STAb; BiTE; CAR; leukemia relapse

Introduction

In the past few years, immunotherapeutic strategies based on the redirection of T cells toward cell-surface tumor-associated antigens (TAAs), such as adoptive cellular therapy with chimeric antigen receptor (CAR)-modified T cells or administration of bispecific antibodies (bsAbs), have revolutionized the treatment landscape of hematologic malignancies.[1] CARs are synthetic receptors consisting of an extracellular antigen-binding domain, usually a single-chain fragment variable (scFv) antibody, a transmembrane domain, and a T cell-activating domain, most often the intracellular signaling region of the CD3 linked to a costimulatory sequence (from CD28 or 4–1BB molecules).[2] Four anti-CD19 CAR-T cell therapies [3–5] and one anti-BCMA (B cell maturation antigen) CAR-T cell therapy [5] have been approved by the US Food and Drug Administration (FDA) for the treatment of patients with relapsed or refractory (R/R) B cell malignancies and multiple myeloma, respectively. Despite high complete response rates, 30–60% of patients relapse after anti-CD19 CAR-T cell therapy [6] and its application in solid tumors remains challenging.[7]

BsAbs are artificial molecules designed to bridge two different epitopes, usually a cell surface TAA and the CD3 chain of the TCR/CD3 complex,[8] resulting in T cell cytokine secretion and cytotoxic effector functions.[8,9] An anti-CD19 × anti-CD3 bispecific T cell engager (BiTE), blinatumomab, has been approved by the FDA for the treatment of R/R and minimal residual disease-positive B-cell acute lymphoblastic leukemia (B-ALL).[10,11] A potential advantage of bsAbs over CAR-T cells is their ability to achieve the polyclonal recruitment of bystander T cells. However, the need for continuous intravenous administration to overcome their short serum half-life [12] and their inability to actively traffic to tumors [13,14] represent major disadvantages compared to CAR-T therapy.[1] In addition, despite the impressive responses observed with blinatumomab,[13,15,16] 44% of patients relapse after initial response.[14]

Although no clinical data directly comparing CAR-T cells and blinatumomab treatments are available, data suggest that CAR-T cells achieve greater antitumor efficacy and a more prolonged antileukemic response,[17,18] presumably due to their long-term persistence (up to 39 months).[3] By contrast, blinatumomab short half-life is associated with shorter relapse-free survival.[18] Moreover, CAR-T therapy has been proved to be more efficient than blinatumomab in patients with high tumor burden or with extramedullary disease (EMD),[18]

CONTACT Belén Blanco bblanco.imas12@h12o.es Cancer Immunotherapy Unit (UNICA), Department of Immunology, Hospital Universitario 12 de Octubre, Avenida de Córdoba s/n, 28041 Madrid, Spain; Pedro Roda-Navarro proda@med.ucm.es; Luis Álvarez-Vallina lav.imas12@h12o.es
[#]These authors contributed equally
Supplemental data for this article can be accessed on the publisher's website

which could be related to the potential of CAR-T cells to actively traffic to extramedullary leukemia deposits,[18] whereas there is no evidence of blinatumomab's ability to cross the blood–brain barrier.[18] In addition, higher complete response rates in pediatric patients have been achieved with CAR-T treatment.[17]

In an attempt to overcome the drawbacks and combine the advantages of both strategies, another immunotherapy approach, based on the *in situ* secretion of **T** cell-redirecting bs**Ab**s (STAb) by genetically modified T cells, is emerging. Thus, *in vivo* secretion of the T cell-redirecting bsAb might result in constant effective concentrations, compensating for the rapid renal clearance of small-sized antibody fragments [19] and, importantly, in STAb strategies T cell recruitment is not restricted to engineered T cells, as in the case of CAR-T cell approaches. The polyclonal recruitment by bsAbs of both engineered and unmodified bystander T cells, present at the tumor site, might lead to a significant boost in antitumor T cell responses.[20] We and others have previously shown that STAb-T cells mediate potent antitumor responses *in vivo* in several animal models,[21–24] but whether the STAb-T strategy might be more effective than CAR-T therapy has remained poorly studied. In particular, a relevant issue concerns the structure of the immune synapse (IS) formed by the CAR-TAA or bsAbs-TAA interactions. It has been reported that the IS initiated by CARs exhibits major differences to the canonical TCR-initiated IS in effector T cells, conforming a disorganized multifocal signaling cluster structure and giving rise to shorter interactions,[25–28] but further studies are needed to more precisely define the impact of non-classical IS in the functional capacity and cytotoxic potential of CAR-T cells. Contrary to CARs, Fc-free T cell-redirecting bsAbs are able to induce the formation of a classical IS between T cells and tumor cells.[29] Indeed, BiTE-initiated IS has been reported to be identical in structure and molecular composition to TCR-induced IS.[30,31]

We have recently demonstrated that engineered primary human T cells secreting a CD19xCD3 bsAb (STAb-T19) are more effective than engineered T cells bearing a second-generation CAR with the same anti-CD19 clone (CAR-T19) in several *in vivo* models of B-ALL.[28] Interestingly, we observed that the secreted BiTE mediated the organization of a canonical IS between primary T cells and $CD19^+$ cells, whereas CAR-T19 cells formed a noncanonical and disorganized IS.[28] Here, we have further studied the topology of the IS induced by both anti-CD19 T cell-redirecting strategies, with special emphasis on the expression and dynamics of relevant molecules for cell signaling and activation.

Material and methods

Cell lines and culture conditions

HEK293T (CRL-3216) cells were cultured in Dulbecco's modified Eagle's medium (DMEM) (Lonza, Walkersville, MD, USA) supplemented with 2 mM L-glutamine (Life Technologies, Paisley, UK), 10% (vol/vol) heat-inactivated fetal bovine serum (FBS), and antibiotics (100 units/mL penicillin, 100 µg/mL streptomycin) (both from Sigma-Aldrich, St. Louis, MO, USA), referred to as DMEM complete medium (DCM). Jurkat Clone E6-1 (TIB-152), Raji (CCL-86), and NALM6 (CRL3273) (CCL243) cells were maintained in RPMI-1640 (Lonza) supplemented with 2 mM L-glutamine, heat-inactivated 10% FBS, and antibiotics, referred to as RPMI complete medium (RCM). All cell lines were obtained from the American Type Culture Collection (Rockville, MD, USA) and were grown at 37°C and 5% CO_2. All cell lines were routinely screened for mycoplasma contamination by PCR using the Mycoplasma Gel Detection Kit (Biotools, Madrid, Spain).

Preparation of lentiviral particles and transduction

The lentiviral vectors pCCL-EF1α-BiTE19,[28] containing the human kappa light chain signal peptide L1,[32] the A3B1 scFv (VL-VH),[33] a five-residue linker (G4S), the OKT3 scFv (VH-VL) [34] and a C-terminal polyHis tag, and pCCL-EF1-CAR19,[33] encoding a second-generation (CD8-BBζ) anti-CD19 CAR (19-CAR),[33] was used. To produce lentiviral particles, HEK293T cells were transfected with the transfer vector (pCCL-EF1α-BiTE19 or pCCL-EF1-CAR19) together with packaging plasmids. In brief, HEK293T cells (6×10^6) were plated 24 hours before transfection in 10 cm dishes. At the time of transfection, 6.9 µg transfer vector (pCCL-EF1α-BiTE19 or pCCL-EF1α-CAR19), 3.41 µg pMDLg/pRRE (Addgene, 12251), 1.7 µg pRSV-Rev (Addgene, 12253), and 2 µg envelope plasmid pMD2.G (Addgene, 12259) were diluted in serum-free DMEM. 35 µg linear polyethyleneimine (PEI) molecular weight 25,000 (Polysciences, 23966–1) was added to the mixture and incubated for 20 minutes at room temperature. After incubation, DNA-PEI complexes were added onto the cells cultured in 7 mL of complete DMEM. Media were replaced 4 hours later.

Viral supernatants were collected 48 hours later and clarified by centrifugation and filtration using a 0.45-µm filter. Viral supernatants were concentrated using ultracentrifugation at 26,000 rpm for 2 hours 30 minutes. Virus-containing pellets were resuspended in complete XVivo15 media (Lonza, Walkersville, MD, USA) and stored at −80°C until use.

Functional titers (TU/ml) were determined by FACS analysis after limiting dilution in Jurkat cells, as specified in the flow cytometry section. Jurkat cells at a concentration of 1×10^6 cells/ml cells were left untransduced (nontransduced, J-NT-T cells) or transduced with 19-CAR (J-CAR-T19 cells) or 19-BiTE (J-STAb-T19 cells) encoding lentivirus at the indicated Multiplicity of Infection (MOI). A period of cell expansion of 6–8 days was carried out before conducting experiments.

Viral copy number

The copy number of integrated lentiviruses in J-NT-T, J-CAR-T19, and J-STAbT19 cells was determined by qPCR with the Lenti-X Provirus Quantitation kit (Takara Bio Inc, Saint Germain, France) following the manufacturer´s instructions.

Western blotting

For analysis of CAR and BiTE expression, samples were lysed for 5 minutes in an ice-cold RIPA buffer (Sigma-Aldrich) with 5 mM EDTA and a 1x Halt Protease Inhibitor Cocktail

(ThermoFisher-Pierce Biotechnology, Rockford, IL, USA), centrifuged at 11,000 g for 10 minutes at 4°C and soluble fractions were collected; for analysis of BiTE secretion, culture supernatants were collected. 15 μg of protein or 16 μl of supernatant was were separated under reducing conditions on 10–20% Tris-glycine gels (Life Technologies, Carlsbad, CA, USA), transferred onto Immobilon-PVDF membranes (Merck Millipore, Tullagreen, Carrigtwohill, Ireland) and probed with mouse antihuman CD247 mAb (1:1000) (BD Biosciences) or anti-His mAb (Qiagen, Hilden, Germany) (200 ng/ml), followed by incubation with horseradish peroxidase (HRP)-conjugated goat antimouse (GAM) IgG, Fc specific (1:5000) (Sigma-Aldrich).

HRP-conjugated mouse anti-actin mAb (1:50,000) was used as loading control. Visualization of protein bands was performed with Pierce ECL Western Blotting substrate. Blots were scanned and quantified using a Bio-Rad ChemiDoc MP Imaging System.

For analysis of T cell signaling, J-CAR-T19 and J-STAb-T19 cells were incubated at 37°C with Raji cells at a Jurkat-Raji ratio of 10:1 for the indicated times. J-NT-T cells were incubated with non-loaded Raji cells or Raji cells loaded for 1 hour with 5 nM blinatumomab (BLI) (Amgen Inc, Thousand Oaks, California) or 1 μg/mL *Staphylococcus aureus* Enterotoxin-E (SEE) (Toxin Technologies, Sarasota, FL, USA). The stimulation time 0 minutes corresponds to J-NT-T cells mixed with Raji cells at room temperature, which were immediately centrifuged and lysed. Samples were lysed for 30 minutes in an ice-cold lysis buffer containing 20 mM Tris-HCl pH 7.5; 1% NP-40; 0.2% Triton X-100 (Sigma-Aldrich); 2 mM EDTA; 150 mM NaCl; 1.5 mM $MgCl_2$; 5 mM β-glicerolphosphate; 1x protease inhibitor cocktail; 1 mM NaF; 1 mM PMSF; 1 mM Na_3VO_4 and 1 mM Sodium pyrophosphate. Lysates were then centrifuged at 10,000 rpm for 10 minutes at 4°C, and soluble fractions were collected, mixed with 6x Laemmli buffer (Alfa Aesar, Haverhill, MA, USA) containing 20% β-mercaptoethanol, boiled at 95°C for 5 minutes, and resolved in 10% SDS-PAGE acrylamide gels. Resolved proteins were transferred to Immobilion PVDF membranes, which were blocked with blocking buffer (LI-COR Bioscience, Lincoln, NE, USA), incubated overnight with rabbit anti-phospho-Y783-PLCγ1, anti-PLCγ1, anti-phospho-T202/T204-ERK1/2, or mouse anti-ERK1/2 primary antibodies (all from Cell Signaling Technology, Beverly, MA, USA) and incubated for 30 minutes with IRDye 680-conjugated goat-antirabbit (GAR) and IRDye 800-conjugated GAM (Miltenyi Biotec). All blots were scanned, and fluorescence was quantified with an Odyssey Infrared Imager (LI-COR). Densitometry of images was done with Image Studio Freeware (LI-COR). When necessary, blots were striped in 50 ml containing 2% SDS; 12.5% Tris-HCl pH 6.8 and 0.7% β-mercaptoethanol for 30 minutes at 50°C.

Flow cytometry

The following mAbs against human proteins were used: PE-conjugated anti-CD2 (clone S5.2), APC-conjugated anti-CD3 (clone UCHT1), and APC-conjugated anti-CD10 (clone HI10a) from BD Biosciences (San Jose, CA, USA) and PC7-conjugated anti-CD19 (clone J4.119) from Beckman Coulter (Marseille Cedex, France). DAPI (SigmaAldrich) was used as a viability marker. Cell surface expression of 19-CAR was analyzed using an APC-conjugated GAM IgG $F(ab')_2$ (Jackson ImmunoResearch, West Grove, PA, USA). Cell surface-bound 19-BiTE was detected with APC-conjugated anti-His mAb (clone GG11-8F3.5.1, Miltenyi Biotec), and intracellular BiTE was detected with APC-conjugated anti-His mAb after cell fixation and permeabilization with Inside Stain kit (Miltenyi Biotec). Cell acquisition was performed in a BD FACSCanto II flow cytometer using BD FACSDiva software (both from BD Biosciences, San Jose, CA, USA). Analysis was performed using FlowJo V10 software (Tree Star, Ashland, OR, USA).

Immunofluorescence and confocal microscopy

For synapse studies, Jurkat NT-T, CAR-T19, and STAb-T19 cells were incubated for 15 minutes on Poly-L-lysine (Sigma-Aldrich)-coated coverslips at 37°C with Raji cells at a Jurkat: Raji ratio of 1:1. Where indicated, Raji cells were loaded for 1 hour with 5 nM BLI or 1 μg/mL SEE. In order to properly find cell conjugates, Raji cells were pre-incubated with the fluorescent tracker chloromethyl derivative of aminocoumarin (CMAC) 1 μM (Molecular Probes, Eugene, OR, USA). Jurkat: Raji cell conjugates (200.000 cells each) were fixed with 4% paraformaldehyde in PBS for 5 minutes at room temperature, permeabilized with 0.1% Triton X-100 (Sigma Aldrich) for 5 minutes at room temperature, and blocked with 10 μg/ml human gamma globulin (Sigma-Aldrich) for 20 minutes at room temperature. Samples were stained with mouse anti-CD3ε mAb (T3b clone; kindly provided by Dr. Francisco Sánchez-Madrid, Hospital Universitario de la Princesa, Madrid, Spain) and with Phalloidin-647 (Molecular Probes) (for F-actin detection) for 1 hour at room temperature. Cells were then washed with TBS (50 mM Tris-HCl, pH 7.4 150 mM NaCl) and incubated with an Alexa 488-conjugated GAM secondary antibody (Molecular Probes) at room temperature for 30 minutes. Finally, samples were washed with TBS and distilled water before being mounted with Mowiol medium (Sigma-Aldrich). Confocal sections of fixed samples were acquired using an SP-8 laser scanning confocal microscopy (Leica Microsystems, Wetzlar, Germany), with a 60×/1.35 oil immersion objective. CMAC, Alexa 488, and phalloidin-647 were excited by 405, 488, and 633 nm laser lines, respectively. Image acquisition was performed using a Leica HyVolution system and an automatically optimized image resolution of 40 nm/pixel. For 3D reconstructions, z-stacks through the complete IS were acquired every 0.3 μm. F-actin clearance was estimated by the ratio of the area of the central region of the IS depleted of F-actin versus the complete area of the IS including the actin ring in 3D images. Assessment of CD3 coalescence at the cSMAC was assessed by visual inspection of the 3D images and using criteria shown in supplementary Figure 2. 3D reconstruction and image quantitation were performed using ImageJ freeware (National Institutes of Health, Rockville, MD, USA).

For 19-CAR and CD3 localization studies, J-NT-T, J-CAR-T19, or J-STAb-T19 cells (1×10^5) were co-cultured for 2 hours with CMAC-labeled NALM6 cells at a 2:1 E:T

ratio in U-bottom 96-well plates. Co-cultures were then incubated on poly-L-lysine-coated coverslips at 37°C, 5% CO_2 and fixed and permeabilized as described above. 19-CAR localization at the lysosomal compartment was assessed by staining with GAMIgG F(ab')$_2$-biotin (Jackson ImmunoResearch) followed by streptavidin-Alexa Fluor 594 (Life Technologies-Thermo Fisher Scientific, Carlsbad, CA, USA) and mouse anti-CD107a (IDB4 clone)-Alexa Fluor 647 (Biolegend, San Diego, CA, USA). CD3 localization was determined by staining with mouse anti-CD3ε (T3b clone) followed by GAM-Alexa-488. All samples were mounted with Mowiol (Sigma-Aldrich) as described above. Confocal sections were acquired using the SP-8 scanning laser confocal microscopy equipped as described. CMAC, Alexa 488, Alexa 594, and Alexa 647 were excited by 405, 488, 594, or 633 nm laser lines, respectively. Image acquisition was automatically optimized with the Leica software to get an image resolution of 58 nm/pixel. In the case of 19-CAR localization, Z-stacks through the cell were acquired every 0.8 µm. Colocalization was estimated by Pearson correlation coefficients obtained in complete stacks of cells (Figure 2b, c). CD3ε uptake by target cells shown in Figure 3e was estimated as the ratio of the signal of CD3ε in NALM6 cells and JK cells after subtracting the background. Analysis was implemented in ImageJ freeware.

Statistical analysis

Results of experiments are expressed as mean ± standard deviation (SD). Graphics and the statistical tests indicated in figure legends were performed using Prism 6 (GraphPad Software, USA).

Results

Generation and characterization of anti-CD19 Jurkat CAR-T and STAb-T cells

Jurkat T cells were transduced at different multiplicities of infection (MOI) with lentiviruses encoding a second-generation (CD8-BBζ) anti-CD19 CAR (19-CAR) or an anti-CD19 × anti-CD3 BiTE (19-BiTE) (Figure 1a), and the relationship between the number of vector integrations and transgene expression was analyzed. Vector copy number (VCN) was found to be similar in both cases, between 1 and 5 copies for 19-CAR-transduced Jurkat T cells (J-CAR-T19) and between 1 and 7 for 19-BiTE-infected Jurkat T cells (J-STAb-T19) (Fig. S1a). The intracellular levels of both proteins were similar, as determined by Western blotting, with a clear correlation between MOI and both 19-CAR expression (Fig. S1b) and 19-BiTE expression and secretion (Fig. S1c,d). The percentage of 19-CAR-positive cells among J-CAR-T19 cells varied between 65% and 100% according to the VCN increase, and a VCN-dependent surface staining of J-STAb-T19 cells was observed as well, ranging from 16% to 78%, indicating that secreted 19-BiTEs were bound to the CD3 complexes on the T cell surface (Fig. S1e). Jurkat T cells transduced at MOI 5 were selected for use in subsequent studies since VCN was <5 copies per genome in both J-CAR-T19 and J-STAb-T 19 cells, and the 19-CAR and 19-BiTE expression levels were homogeneous and stable.

Importantly, the process of cis-/trans-decoration of the TCR/CD3 complex by the secreted 19-BiTE (Figure 1a and Fig. S1e) results in specific adhesion of J-STAb-T19 cells to plastic immobilized CD19, almost as efficient as observed with 19-CAR expressing cells (Figure 1b). T cell activation was further reflected by expression of the activation marker CD69 when J-CAR-T19 or J-STAb-T19 cells were co-cultured with $CD19^+$ target cells (Figure 1c).

Topology of the immune synapses induced by Jurkat CAR-T19 and STAb-T19 cells

To study the assembly of 19-CAR- and 19-BiTE-mediated IS, J-CAR-T19 and J-STAb-T19 cells were co-cultured with CD19-expressing Raji cells. As controls, non-transduced Jurkat cells (J-NT-T) were co-cultured with unloaded (non-activated control) or with BLI- or SEE-loaded Raji cells (activation controls). Jurkat:Raji cell conjugates were stained for filamentous (F)-actin and CD3ε to evaluate the organization of the distal and central supramolecular activation clusters, dSMAC and cSMAC, respectively. Confocal 3D microscopy was implemented to visualize the central F-actin clearance, with the typical actin ring at the dSMAC, and the coalescence of CD3ε microclusters at the cSMAC occurring in the mature IS (Fig. S2). All conditions, including CAR-T19 cells, recruited CD3ε to the IS. However, while J-STAb-T19 cells cleared F-actin and formed the cSMAC by CD3 coalescence in a similar way to J-NT-T cells stimulated by SEE or BLI, CAR-T19 cells formed a disorganized IS with disperse CD3 clusters and a diffuse organization of F-actin (Figure 1d-f). These data showed that 19-BiTE, but not 19-CAR, allows the organization of a canonical IS and confirm our previous results obtained with engineered primary T cells.[28]

Early signaling during J-CAR-T19 and J-STAb-T19 cell activation

In order to assess if the differences observed in synapse topology might have functional consequences, the early signaling triggered upon J-CAR-T19 and J-STAbT19 interaction with $CD19^+$ Raji cells was studied. As activation controls, J-NT-T cells were stimulated with BLI- or SEE-loaded Raji cells. As negative control, J-NT-T cells were incubated with Raji cells alone. PLCγ1 and ERK1/2 activation was analyzed by Western blot due to their important role in early activation signaling downstream the TCR/CD3. Interestingly, J-STAb-T19 cells showed PLCγ1 and ERK1/2 activation kinetics similar to J-NT-T cells stimulated with SEE or BLI. However, J-CAR-T19 cells showed a more transient signaling compared to J-STAb-T19 cells and control stimulation conditions (Figure 1g,h and Fig. S3).

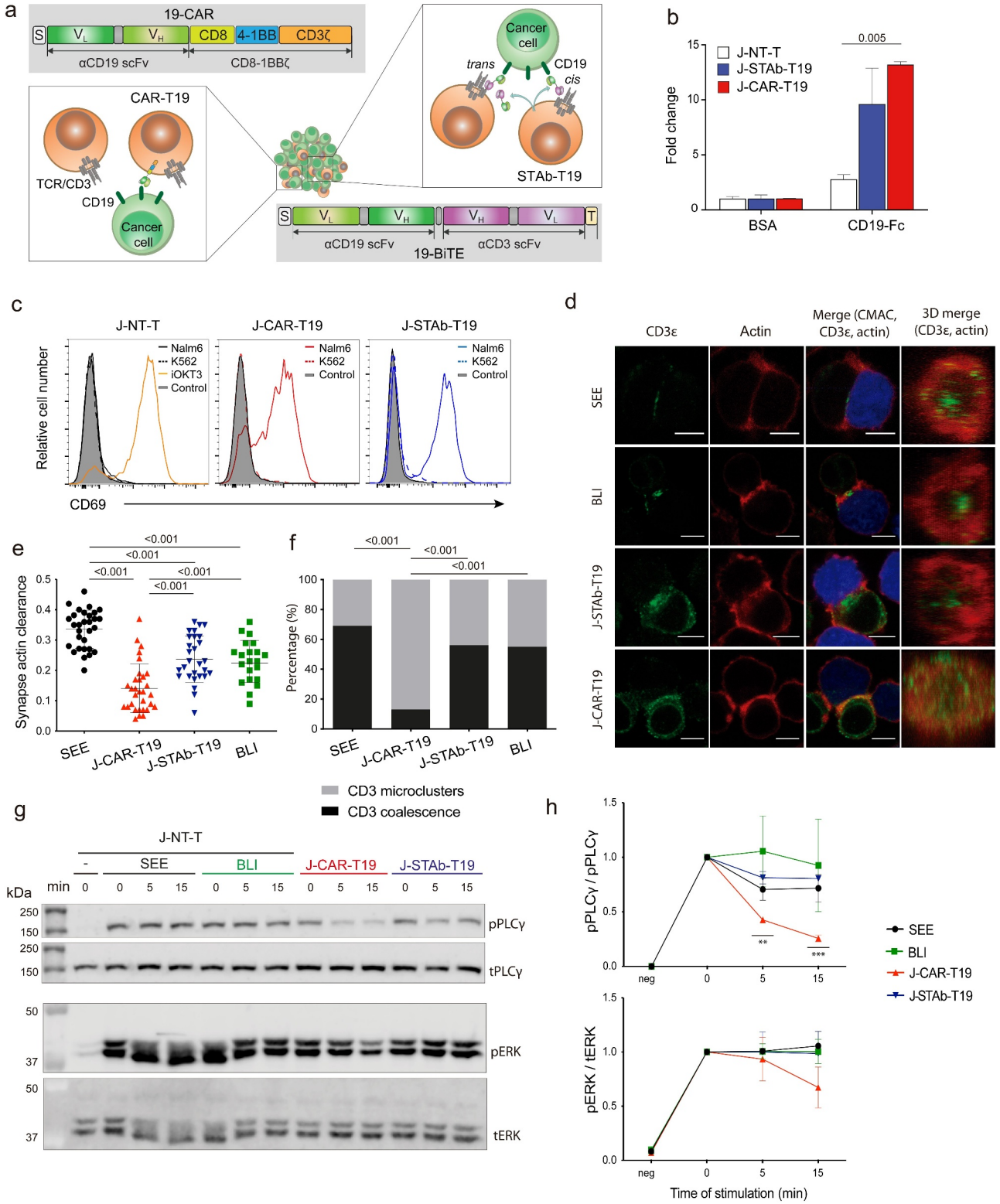

Figure 1. Functional characterization, IS assembly, and early signaling in J-CART19 and J-STAb-T19 cells. (a) Schematic representation of 19-CAR and 19-BiTE constructs and CAR-T19 and STAb-T19 cells. Whereas in the CAR-T strategy, only genetically engineered 19-CAR-expressing cells are able to interact with target cells, the 19-BiTE secreted by STAb-T cells can achieve a polyclonal recruitment of the complete T cell pool, including engineered and not engineered T cells. (b) Adhesion of J-NT-T, J-CAR-T19 and J-STAb-T19 cells to plastic-immobilized BSA or human CD19 (CD19-Fc). (c) CD69 expression by J-NT-T, J-CAR-T19 or J-STAb-T19 cells cocultured with $CD19^{-}$ K562, $CD19^{+}$ NALM6 target cells or plastic immobilized anti-CD3 mAb (iOKT3) for 24 hours. (d-h) J-NT-T, J-STAb-T19 and J-CAR-T19 cells were cocultured for the indicated minutes (min) with Raji cells. As activation controls, J-NT-T cells were incubated with $CD19^{+}$ Raji cells loaded with SEE or blinatumomab 5 nM (BLI). (d) Distribution of CD3ε and actin at the mature IS in representative cell conjugates of Jurkat cells interacting with Raji cells labelled with CMAC (blue). The green (CD3ε) and red (actin) channels, as well as the merged images, are shown. Scale bar corresponds to 5 µm. The IS topology obtained from the 3D reconstructions of region of interest placed at the IS in confocal stacks containing the red and the green channels are shown. (e) The graph represents the actin clearance at the IS in each sample, estimated as the fraction of actin cleared area as explained in material and methods. Symbols in each sample indicate individual cells analyzed and the black line the average value. Samples were compared by an ordinary one-way ANOVA with a Tukey's multiple comparison test. (f) Graph representing the percentage of cell conjugates showing peripheral CD3 microclusters or cSMAC formation by CD3 coalescence. Contingency tests were performed in each possible comparison. Analysis from three independent experiments is shown. (g) Western blot for quantification of PLCγ1 and ERK1/2 activation. (h) Phosphorylated fraction of the molecules analyzed in (g), normalized to the maximum fraction found in 0 minutes (min). Mean ± SD from three independent experiments is shown. Samples were compared by a paired two-tailed Student t-test.

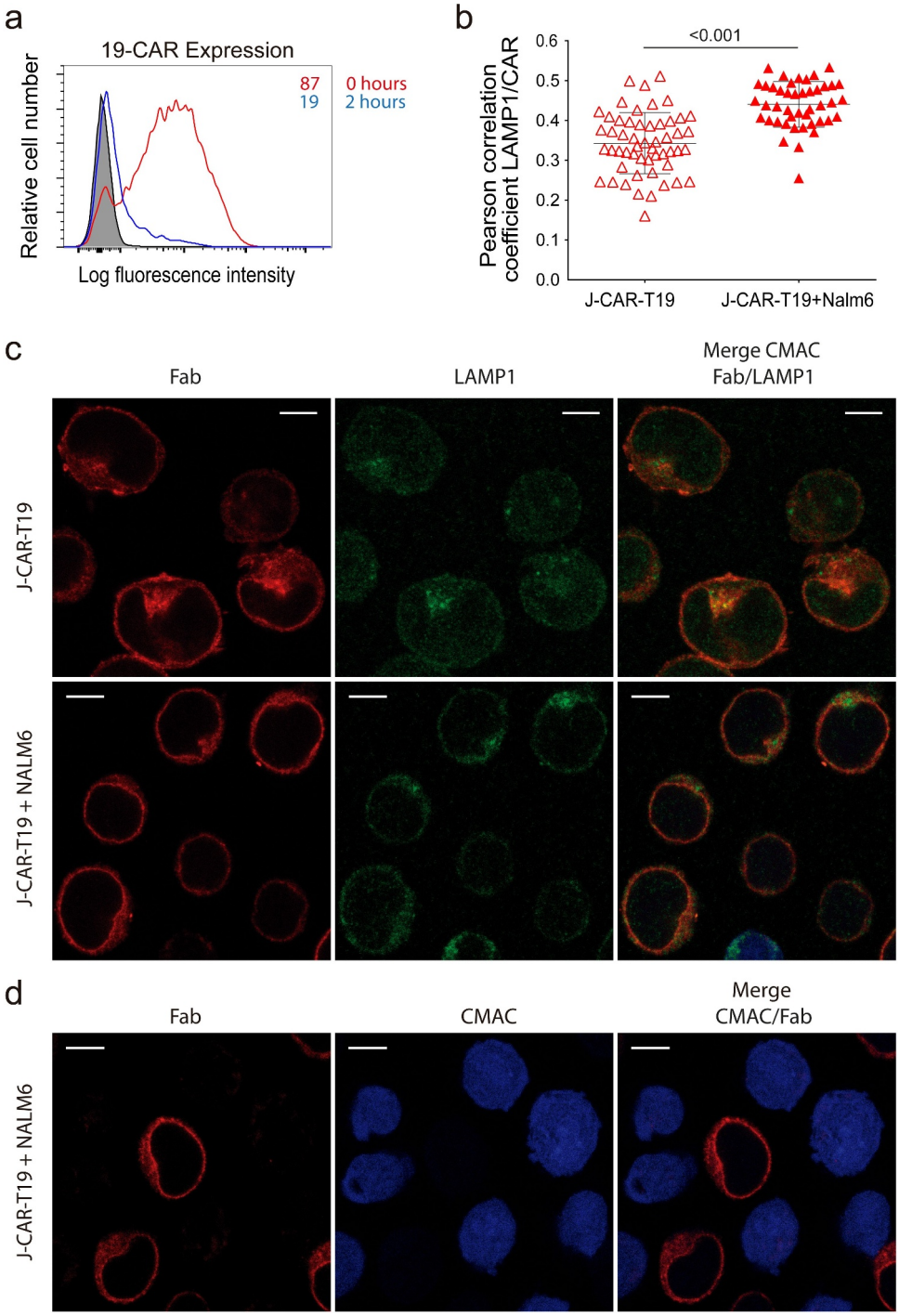

Figure 2. CAR downmodulation and fate upon antigen engagement. (a) J-CART-19 cells were co-cultured for 2 hours at a 2:1 E:T ratio with NALM6 cells and stained with an antimouse Fab antibody. 19-CAR expression by J-CAR-T19 cells before and after the coculture was analyzed by flow cytometry. Percentages of 19-CAR positive cells are indicated. (b-d) J-CAR-T19 cells and CMAC-labeled NALM6 cells were cocultured for 2 hours at 2:1 E:T ratio, stained with antibodies against mouse Fab and LAMP1, and analyzed by confocal microscopy. (b) Pearson's coefficients and (c) representative images of cellular colocalization of 19-CAR and LAMP1 in J-CAR-T19 cells after 2-hour culture. The green (LAMP1) and red (Fab) channels, as well as the merged images, are shown. The scale bar corresponds to 5 µm. Dots in graphs represent the Pearson´s coefficient in the individual cells analyzed, and the black line the average value of one representative experiment out of two. Samples were compared by and unpaired t-test. (d) Representative images showing the absence of 19-CAR uptake by NALM6 target cells. One experiment out of three is shown.

Modulation and trafficking of cell surface 19-CAR and CD3 molecules

Duration of signal transduction could also be related to the presence of adequate levels of the activating molecules on the T cell surface. Interestingly, as we had previously reported,[28] a rapid and drastic 19-CAR downmodulation occurs after interaction with $CD19^+$ cells (Figure 2a), which might account for the shorter signaling observed in J-CAR-T19 cells. In an attempt to define the fate of the 19-CAR molecules, J-CAR-T19 cells were cultured alone or with $CD19^+$ NALM6 cells for 2 hours and co-stained with antibodies against mouse Fab (Fab), for 19-CAR detection, and against the lysosome-associated

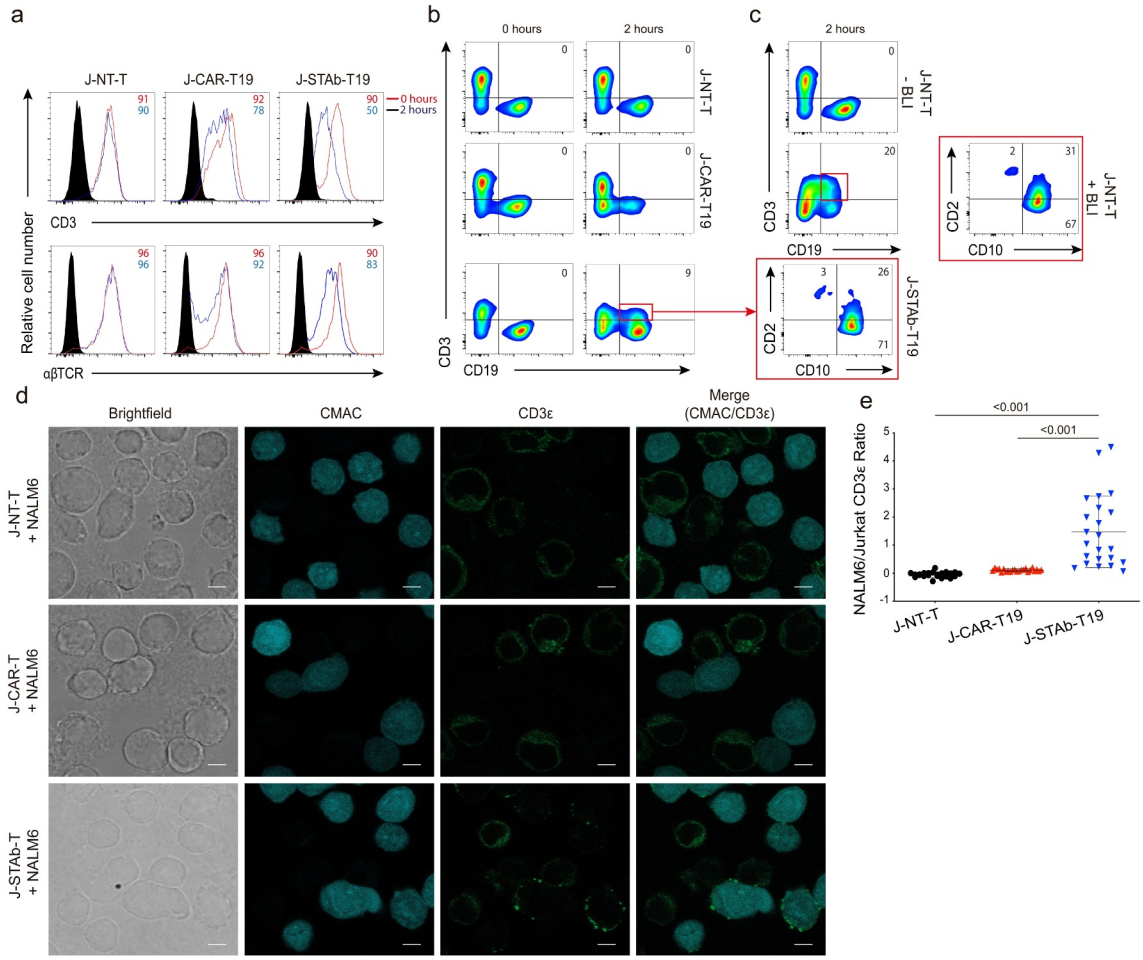

Figure 3. 19-BiTE-mediated CD3 uptake by target cells. (a,b) J-NT-T, J-CAR-T19 or J-STAb-T19 cells were co-cultured for 2 hours at a 2:1 E:T ratio with CMAC-labeled NALM6 cells. (a) Analysis, by flow cytometry, of CD3 and TCR expression on J-NT-T, J-CAR-T19 and J-STAB-T19 cells before and after the co-culture; one representative experiment out of three is shown. (b) Analysis of CD3/CD19 and CD2/CD10 co-expression at 0 and 2 hours after co-culture; one representative experiment out of three is shown. (c) J-NT-T cells were co-cultured for 2 hours at a 2:1 E:T ratio with CMAC-labeled NALM6 cells in the presence of 100 ng/ml BLI. CD3/CD19 and CD2/CD10 co-expression was analyzed before and after the coculture; one representative experiment out of three is shown. (d) Representative images of CD3 localization in both Jurkat and CMAC labeled-NALM6 cells after the coculture. The cyan (CMAC), green (CD3ε) and bright field channels, as well as the merged images of cyan and green, are shown. Scale bar corresponds to 5 µm. (e) Ratio of NALM6/Jurkat cell CD3 signal after 2 hours of co-culture. Dots represent the individual cells analyzed, and the black line the average value of one representative experiment out of two. Samples were compared by a one-way ANOVA with a Tukey's multiple comparison test.

membrane glycoprotein 1 (LAMP1). The analysis by confocal microscopy showed an increase in the colocalization of 19-CAR and LAMP1 in J-CAR-T19 cells cocultured with NALM6 cells, compared to J-CAR-T19 cells cultured alone (Figure 2b,c), indicating the traffic of 19-CAR to the lysosomal compartment after the interaction with the target antigen. 19-CAR was not detected on the cell surface nor in cellular compartments of $CD19^+$ target cells after the coculture (Figure 2d), suggesting that 19-CAR downmodulation in J-CAR-T19 cells is not due to 19-CAR uptake by NALM6 cells upon interaction.

Following 19-BiTE-mediated engagement with $CD19^+$ target cells, a reduced cell surface detection of CD3 was observed in J-STAb-T19 cells, which is more pronounced than that observed in J-CAR-T19 cells cocultured in the same conditions with NALM6 cells (Figure 3a). This cell surface CD3 decrease was concomitant with a modest TCR downmodulation (Figure 3b). Interestingly, the reduction in CD3 expression from J-STAb-T19 cells paralleled the increase in cell surface detection of CD3 on NALM6 cells and the emergence of a $CD19^+CD10^+CD3^+$ subpopulation, suggesting that CD3 is transferred to leukemia cells following 19-BiTE-mediated interactions (Figure 3b). The CD3 uptake by $CD19^+$ target cells was also observed in cocultures of NALM6 cells with J-NT-T cells in the presence of BLI (Figure 3c). To further address these observations, J-NT-T, J-CAR-T19, or J-STAb-T19 cells were cocultured with CMAC-labeled NALM6 target cells for 2 hours, labeled with anti-CD3 mAb and analyzed by confocal microscopy. When co-cultured with J-STAb-T19 cells, CD3 aggregates were observed at the NALM6 cell surface, which were not observed when NALM6 was cocultured with J-NT-T or J-CAR-T19 cells (Figure 3d,e), suggesting that CD3 trogocytosis [35] occurred after the 19-BiTE-mediated interaction. This could explain, at least in part, the higher reduction in CD3 cell surface expression observed in J-STAb-T19 cells, compared to J-NT-T and J-CAR-T19 cells. On the other hand, a decrease in CD19 expression on NALM6 target cell surface upon interaction with J-CAR-T cells was observed (Figure 3b), as previously described.[28]

Discussion

We have recently reported the generation of STAb-T19 cells secreting a previously uncharacterized anti-CD19 × anti-CD3 BiTE and demonstrated their potent antitumor activity in relevant *in vivo* B-ALL models when compared to CAR-T cells expressing a cell surface CD19-targeted second-generation CAR.[28] Interestingly, we observed significant differences in the topology of 19-CAR- and 19-BiTE-mediated synapses in human primary T lymphocytes. In the present study, we have performed a detailed analysis on the characteristics and potential outcomes of both types of anti-CD19-mediated target cell-T cell interactions. For this purpose, we have used the Jurkat human T cell line, which has been widely used to study T cell activation, signaling, and IS assembly.[36] Contrary to primary T cells, Jurkat cells can be easily expanded and long-term cultured after transduction without losing CAR expression or BiTE secretion, avoiding transduction-to-transduction differences and loss of transgene expression. In addition, clonal stimulation by superantigens provides a proper control that mimics the canonical IS and, together with the high transduction efficiency achieved in Jurkat cells, allows to perform experiments with a high number of T cell-target cell interactions. Jurkat cell stimulation with SEE and B-cell lines has been previously used for synapse studies, [37] and Jurkat cells have been employed to evaluate the CAR- and BsAb-induced IS and signaling in T cells.[31,38]

Therefore, human Jurkat T cells were conveniently transduced with lentiviral vectors encoding 19-CAR or 19-BiTE, as determined by western blot and flow cytometry. Importantly, in 19-BiTE transduced STAb-T19 cells a VCN-dependent cell surface staining was observed with an anti-His-tag mAb, indicating that secreted 19-BiTEs are loaded onto the TCR/CD3 complexes on the T cell surface, and this process of "cis-/trans-CD3 decoration" results in an effective and specific adhesion of T cells to CD19-coated wells. To the best of our knowledge, this is the first report describing the ability of "BiTE-decorated" T cells to bind to human CD19, which would endow them with the ability to selectively target and kill $CD19^+$ tumor cells *in vivo*.

TCR engagement leads to the formation of the IS, a highly organized structure composed of concentric SMACs, which must be finely tuned to achieve proper T cell activation and effective immune responses.[39,40] The precise spatial and temporal topology of the IS assembled in response to CARs and BITEs is poorly understood, but it has been reported that CAR-mediated synapse exhibited major differences relative to the typical TCR-initiated IS.[26,40] Thus, previous studies have described a disorganized multifocal pattern, differing from the canonical "bull's eye" structure in CAR-mediated IS,[26] and with a poor organization of the actin ring.[41] Unlike CARs, small-sized T cells engaging bsAbs have been previously reported to induce the formation of a canonical IS between T lymphocytes and tumor cells.[29] Different bsAb formats have shown an efficient peripheral and central recruitment of F-actin and CD3 at the synapse, where proper polarization of TCR signaling is occurring.[42] Indeed, BiTE-initiated IS has been found to be identical in structure and molecular composition to TCR-induced IS.[30,31] Accordingly, our previous and current results showed that F-actin is not properly cleared from the central area of interaction in J-CAR-T19 cells compared to conventional TCR-IS. In addition, J-CAR-T19 cells were able to recruit CD3 to the IS but failed to centralize it in the cSMAC. Importantly, a crucial event in synapse formation is the movement of TCR/CD3 microclusters to the inner SMAC (cSMAC).[43] Actin plays an important role in this centripetal movement of TCR microclusters, [44–46] and the actin retrograde flow sustains the PLCγ1 signaling,[47] which is a key step in the T cell activation process triggered by the TCR.[48–50] Opposite to CAR-mediated synapse, 19-BiTE- and BLI-induced synapses are similar to those observed in the well-established RAJI-SEE-Jurkat IS model, which configures a canonical synapse,[51] with actin clearance and CD3 accumulation in the cSMAC. Nevertheless, it should be noted that, although the dSMAC was formed in J-STAb-T19 cells and BLI-stimulated cells, the central area of the IS with low content of actin was smaller. Actin clearance is also important for the secretion of lytic granules or cytokines to the synaptic cleft.[52] We envisage that actin networks organized at the IS induced in J-STAb-T19 cells will be ready for proper secretion of lytic granules in a similar way than the canonical IS organized in CTLs.

To determine the functional impact of such differences, we analyzed the activation of early T cell signaling pathways after coculture with $CD19^+$ target cells. Data showed shorter signaling in J-CAR-T19 cells compared to control Raji-SEE-stimulated J-NT-T cells. This might be related to the observation that the time required for the CAR to assembly a functional IS is shorter than the time required by the TCR.[27] Thus, CAR-stimulated T cells dissociate faster than TCR-stimulated T cells from killed tumor targets, which may enable a more efficient serial killing.[26] However, rather than leading to more efficient tumor clearance, CAR-mediated killing was reduced compared to that mediated by TCR ligation.[53] This could be due to several reasons. First, because T cell exhaustion occurs after repeated T cell activation, we might speculate that the faster kinetics of serial killing would render CAR-T cells more rapidly prone to exhaustion. Second, the reduced killing capacity of CAR-T cells compared with TCR-stimulated T cells has been attributed to strong downregulation of CARs.[53]

An important issue regarding target-T cell interactions is the dynamics of cell surface molecules that enable the TAA-specific recognition and activation of effector cells, since a low density of activation-triggering molecules might reduce the cytotoxic potential of redirected effectors. We had previously observed a fast and drastic 19-CAR downmodulation upon interaction with CD19 that has been confirmed in the present study. Analysis of 19-CAR location after co-culture with $CD19^+$ target cells showed an increase of 19-CAR co-localization with the lysosomal marker LAMP1, which would be in accordance with the previously described lysosomal degradation of internalized 19-CARs.[54] In contrast, 19-BiTE-mediated interactions elicited signaling kinetics similar to those generated by TCR-mediated interactions. In addition, we found a reduction of cell-surface CD3 detection after STAb-T19 cell coculture with $CD19^+$ cells. Such a reduction could be partially explained by epitope competition between 19-BiTE and the anti-CD3 mAb used for detection. On the other hand, CD3 downmodulation could obey the physiological dynamics of the TCR/CD3 during a

canonical antigen stimulation, in which a decrease in the cell surface-TCR/CD3 complex occurs after ligation due to prevention of recycling of internalized complexes.[55] Loss of CD3 might also be associated with trogocytosis, a process of intercellular and bidirectional transfer of plasma membrane fragments along with their associated molecules, frequently observed at the IS between APCs and T cells.[35] The transferred proteins can be internalized by the receiving cells or displayed on their cell surface.[35,56,57] The transfer of CD3 observed in our work is consistent with seminal observations of the presence of TCR components at exosomes delivered to the synaptic cleft.[58,59] In addition, antibody-mediated trogocytosis has been previously described[60] even by bsAbs.[61–63] Moreover, bidirectional trogocytosis between B and T cells mediated by CD19 × CD3 bsAbs has been documented, and it might be a common phenomenon on T cell-redirecting bsAbs.[63] Consequences of trogocytic transfer are diverse, depending on the functions of proteins embedded in the transferred membrane patches, and can both enhance or suppress immune responses.[64] Nevertheless, it is indicative of a more physiological response, and further investigation on the potential relevance of 19-BiTE-mediated CD3 uptake by $CD19^+$ target cells is required.

In summary, we have demonstrated that the topology of the IS induced by the 19-BiTE and the 19-CAR in primary T cells is reproduced in Jurkat T cells, providing us a useful model to perform further studies and precisely define the impact of the IS architecture on the functional capacity, cytotoxic potential, and persistence of CAR-T19 and STAb-T19 cells. In fact, we have shown for the first time that two different antibody-based T cell-redirecting molecules carrying the same anti-CD19 clone have opposite outcomes in terms of IS formation and signaling. Further studies on primary T lymphocytes will be necessary to validate these findings and to determine whether such differences could represent an advantage of STAb-T cells over CAR-T cells in cancer immunotherapy.

Acknowledgments

We thank the technical assistance of the fluorescence microscopy facility staff of the Complutense University of Madrid.

Disclosure statement

BB and LA-V are inventors on a patent related to STAb-T cell therapy, filed by the Fundación de Investigación 12 de Octubre, IDIBAPS/Hospital Clinic, and Fundación CRIS contra el Cáncer. LA-V is cofounder of Leadartis S.L., a spin-off focused on unrelated interest.

Funding

This work was supported by the Spanish Ministry of Science and Innovation (PID2020115444GB-I00 and RTC-2017-5944-1 to PR-N; and SAF2017-89437-P, PID2020-117323RB-I00, and PDC2021-121711-I00 to LA-V), partially supported by the European Regional Development Fund (ERDF); the Carlos III Health Institute (ISCIII, PI20/01030 to BB; and DTS20/00089 to LA-V), partially supported by the ERDF; the Spanish Association Against Cancer (AECC 19084 to LA-V; INNOV211832BLAN toB.B); and the CRIS Cancer Foundation (FCRIS-IFI-2018 and FCRIS-2021-0090 to LA-V). ISCIII-RICORS is supported within the Next Generation EU program (Plan de Recuperacion, Transformacion y Resiliencia). LD-A was supported by a Rio Hortega fellowship from the ISCIII (CM20/00004). OA-S was supported by a PhD fellowship from the Complutense University of Madrid. CD-A was supported by a predoctoral fellowship from the Spanish Ministry of Science and Innovation (PRE2018-083445).

ORCID

Ángel Ramírez-Fernández http://orcid.org/0000-0002-3265-6878
Óscar Aguilar-Sopeña http://orcid.org/0000-0002-2435-8598
Pedro Roda-Navarro http://orcid.org/0000-0003-3799-8823
Luis Álvarez-Vallina http://orcid.org/0000-0003-3053-6757
Belén Blanco http://orcid.org/0000-0001-5085-7756

References

1. Blanco B, Compte M, Lykkemark S, Sanz L, Alvarez-Vallina L. T cell-redirecting strategies to 'STAb' tumors: beyond CARs and bispecific antibodies. Trends Immunol. 2019;40(3):243–257. doi:10.1016/j.it.2019.01.008.
2. Barrett DM, Singh N, Porter DL, Grupp SA, June CH. Chimeric antigen receptor therapy for cancer. Annu Rev Med. 2014;65(1):333–347. doi:10.1146/annurev-med-060512-150254.
3. Maude SL, Laetsch TW, Buechner J, Rives S, Boyer M, Bittencourt H, Bader P, Verneris MR, Stefanski HE, Myers GD. Tisagenlecleucel in children and young adults with B-cell lymphoblastic leukemia. N Engl J Med. 2018;378(5):439–448. doi:10.1056/NEJMoa1709866.
4. Neelapu SS, Locke FL, Bartlett NL, Lekakis LJ, Miklos DB, Jacobson CA, Braunschweig I, Oluwole OO, Siddiqi T, Lin Y. Axicabtagene ciloleucel CAR T-cell therapy in refractory large B-cell lymphoma. N Engl J Med. 2017;377(26):2531–2544. doi:10.1056/NEJMoa1707447.
5. Mullard A. FDA approves first BCMA-targeted CAR-T cell therapy. Nat Rev Drug Discov. 2021;20:332.
6. Xu X, Sun Q, Liang X, Chen Z, Zhang X, Zhou X, Li M, Tu H, Liu Y, Tu S. Mechanisms of relapse after CD19 CAR T-cell therapy for acute lymphoblastic leukemia and its prevention and treatment strategies. Front Immunol. 2019;10:2664. doi:10.3389/fimmu.2019.02664.
7. Alonso-Camino V, Harwood SL, Alvarez-Mendez A, Alvarez-Vallina L. Efficacy and toxicity management of CAR-T-cell immunotherapy: a matter of responsiveness control or tumour-specificity? Biochem Soc Trans. 2016;44(2):40611. doi:10.1042/BST20150286.
8. Kontermann RE, Brinkmann U. Bispecific antibodies. Drug Discov Today. 2015;20(7):838–847. doi:10.1016/j.drudis.2015.02.008.
9. Nunez-Prado N, Compte M, Harwood S, Alvarez-Mendez A, Lykkemark S, Sanz L, Álvarez-Vallina L. The coming of age of engineered multivalent antibodies. Drug Discov Today. 2015;20(5):588–594. doi:10.1016/j.drudis.2015.02.013.
10. Przepiorka D, Ko CW, Deisseroth A, Yancey CL, Candau-Chacon R, Chiu HJ. FDA Approval: blinatumomab. Clin Cancer Res. 2015;21(18):4035–4039. doi:10.1158/1078-0432.CCR-15-0612.
11. Blinatumomab approval expanded based on MRD. Cancer Discov. 2018;8(6):OF3. doi:10.1158/2159-8290.CD-NB2018-059.
12. Lutterbuese R, Raum T, Kischel R, Hoffmann P, Mangold S, Rattel B. T cell-engaging BiTE antibodies specific for EGFR potently eliminate. Proc Natl Acad Sci U S A. 2010;107(28):12605–12610. doi:10.1073/pnas.1000976107.
13. Kantarjian H, Stein A, Gokbuget N, Fielding AK, Schuh AC, Ribera JM. Blinatumomab versus chemotherapy for advanced acute lymphoblastic leukemia. N Engl J Med. 2017;376(9):836–847. doi:10.1056/NEJMoa1609783.
14. Jabbour E, Dull J, Yilmaz M, Khoury JD, Ravandi F, Jain N. Outcome of patients with relapsed/refractory acute lymphoblastic leukemia after blinatumomab failure: no change in the level of CD19 expression. Am J Hematol. 2018;93(3):371–374. doi:10.1002/ajh.24987.

15. Goebeler ME, Knop S, Viardot A, Kufer P, Topp MS, Einsele H. Bispecific T-cell engager (BiTE) antibody construct blinatumomab for the treatment of patients with relapsed/refractory non-Hodgkin lymphoma: final results from a phase I study. J Clin Oncol. 2016;34(10):1104–1111. doi:10.1200/JCO.2014.59.1586.
16. Topp MS, Gokbuget N, Stein AS, Zugmaier G, O'Brien S, Bargou RC, Dombret H, Fielding AK, Heffner L, Larson RA. Safety and activity of blinatumomab for adult patients with relapsed or refractory B-precursor acute lymphoblastic leukaemia: a multicentre, single-arm, phase 2 study. Lancet Oncol. 2015;16(1):57–66. doi:10.1016/S1470-2045(14)71170-2.
17. Davis KL, Mackall CL. Immunotherapy for acute lymphoblastic leukemia: from famine to feast. Blood Adv. 2016;1(3):265–269. doi:10.1182/bloodadvances.2016000034.
18. Molina JC, Shah NN. CAR T cells better than BiTEs. Blood Adv. 2021;5(2):602–606. doi:10.1182/bloodadvances.2020003554.
19. Sanz L, Blanco B, Alvarez-Vallina L. Antibodies and gene therapy: teaching old 'magic bullets' new tricks. Trends Immunol. 2004;25(2):85–91. doi:10.1016/j.it.2003.12.001.
20. Alvarez-Vallina L. Genetic approaches for antigen-selective cell therapy. Curr Gene Ther. 2001;1(4):385–397. doi:10.2174/1566523013348418.
21. Compte M, Blanco B, Serrano F, Cuesta AM, Sanz L, Bernad A, Holliger P, Álvarez-Vallina L. Inhibition of tumor growth in vivo by in situ secretion of bispecific anti-CEA x anti-CD3 diabodies from lentivirally transduced human lymphocytes. Cancer Gene Ther. 2007;14(4):380–388. doi:10.1038/sj.cgt.7701021.
22. Velasquez MP, Torres D, Iwahori K, Kakarla S, Arber C, Rodriguez-Cruz T. T cells expressing CD19-specific engager molecules for the immunotherapy of CD19-positive malignancies. Sci Rep. 2016;6(1):27130. doi:10.1038/srep27130.
23. Liu X, Barrett DM, Jiang S, Fang C, Kalos M, Grupp SA, June CH, Zhao Y. Improved antileukemia activities of adoptively transferred T cells expressing bispecific T-cell engager in mice. Blood Cancer J. 2016;6(6):e430. doi:10.1038/bcj.2016.38.
24. Iwahori K, Kakarla S, Velasquez MP, Yu F, Yi Z, Gerken C, Song X-T, Gottschalk S. Engager T cells: a new class of antigen-specific T cells that redirect bystander T cells. Mol Ther. 2015;23(1):171–178. doi:10.1038/mt.2014.156.
25. Mukherjee M, Mace EM, Carisey AF, Ahmed N, Orange JS. Quantitative imaging approaches to study the CAR immunological synapse. Mol Ther. 2017;25(8):1757–1768. doi:10.1016/j.ymthe.2017.06.003.
26. Davenport AJ, Cross RS, Watson KA, Liao Y, Shi W, Prince HM, Beavis PA, Trapani JA, Kershaw MH, Ritchie DS. Chimeric antigen receptor T cells form nonclassical and potent immune synapses driving rapid cytotoxicity. Proc Natl Acad Sci U S A. 2018;115(9):E2068E2076. doi:10.1073/pnas.1716266115.
27. Watanabe K, Kuramitsu S, Posey AD Jr., June CH. Expanding the therapeutic window for CAR T cell therapy in solid tumors: the knowns and unknowns of CAR T cell biology. Front Immunol. 2018;9:2486. doi:10.3389/fimmu.2018.02486.
28. Blanco B, Ramirez-Fernandez A, Bueno C, Argemí-Muntadas L, Fuentes P, Aguilar-Sopeña O. Overcoming CAR-mediated CD19 downmodulation and leukemia relapse with T lymphocytes secreting anti-CD19 T cell engagers. Cancer Immunol Res. 2022. in press doi:10.1158/2326-6066.CIR-21-0853)
29. Huehls AM, Coupet TA, Sentman CL. Bispecific T-cell engagers for cancer immunotherapy. Immunol Cell Biol. 2015;93(3):290–296. doi:10.1038/icb.2014.93.
30. Offner S, Hofmeister R, Romaniuk A, Kufer P, Baeuerle PA. Induction of regular cytolytic T cell synapses by bispecific single-chain antibody constructs on MHC class I-negative tumor cells. Mol Immunol. 2006;43(6):763–771. doi:10.1016/j.molimm.2005.03.007.
31. Kouhestani D, Geis M, Alsouri S, Bumm TGP, Einsele H, Sauer M, Stuhler G. Variant signaling topology at the cancer cell-T-cell interface induced by a two component T-cell engager. Cell Mol Immunol. 2021;18(6):1568–1570. doi:10.1038/s41423-020-0507-7.
32. Haryadi R, Ho S, Kok YJ, Pu HX, Zheng L, Pereira NA, Li B, Bi X, Goh L-T, Yang Y. Optimization of heavy chain and light chain signal peptides for high level expression of therapeutic antibodies in CHO cells. PLoS One. 2015;10(2):e0116878. doi:10.1371/journal.pone.0116878.
33. Castella M, Boronat A, Martin-Ibanez R, Rodriguez V, Sune G, Caballero M, Marzal B, Pérez-Amill L, Martín-Antonio B, Castaño J. Development of a novel anti-CD19 chimeric antigen receptor: a paradigm for an Affordable CAR T cell production at academic institutions. Mol Ther Methods Clin Dev. 2019;12:134–144. doi:10.1016/j.omtm.2018.11.010.
34. Compte M, Alvarez-Cienfuegos A, Nunez-Prado N, Sainz-Pastor N, BlancoToribio A, Pescador N, Sanz L, Álvarez-Vallina L. Functional comparison of single-chain and two chain anti-CD3-based bispecific antibodies in gene immunotherapy applications. Oncoimmunology. 2014;3(5):e28810. doi:10.4161/onci.28810.
35. Joly E, Hudrisier D. What is trogocytosis and what is its purpose? Nat Immunol. 2003;4(9):815. doi:10.1038/ni0903-815.
36. Cassioli C, Balint S, Compeer EB, Felce JH, Gamberucci A, Della BC, Felce SL, Brunetti J, Valvo S, Pende D. Increasing LFA-1 expression enhances immune synapse architecture and T cell receptor signaling in Jurkat E6.1 cells. Front Cell Dev Biol. 2021;9:673446. doi:10.3389/fcell.2021.673446.
37. Munoz P, Mittelbrunn M, de la Fuente H, Perez-Martinez M, Garcia-Perez A, Ariza-Veguillas A, Malavasi F, Zubiaur M, Sánchez-Madrid F, Sancho J. Antigen-induced clustering of surface CD38 and recruitment of intracellular CD38 to the immunologic synapse. Blood. 2008;111(7):3653–3664. doi:10.1182/blood-2007-07-101600.
38. Dong R, Libby KA, Blaeschke F, Fuchs W, Marson A, Vale RD, Su X. Rewired signaling network in T cells expressing the chimeric antigen receptor (CAR). EMBO J. 2020;39(16):e104730. doi:10.15252/embj.2020104730.
39. Soares H, Lasserre R, Alcover A. Orchestrating cytoskeleton and intracellular vesicle traffic to build functional immunological synapses. Immunol Rev. 2013;256(1):118–132. doi:10.1111/imr.12110.
40. Roda-Navarro P, Alvarez-Vallina L. Understanding the spatial topology ofArtificial immunological synapses assembled in T cell-redirecting strategies: a major issue in cancer immunotherapy. Front Cell Dev Biol. 2019;7:370.
41. Xiong W, Chen Y, Kang X, Chen Z, Zheng P, Hsu YH, Jang JH, Qin L, Liu H, Dotti G. Immunological synapse predicts effectiveness of chimeric antigen receptor cells. Mol Ther. 2018;26(4):963–975. doi:10.1016/j.ymthe.2018.01.020.
42. Harwood SL, Alvarez-Cienfuegos A, Nunez-Prado N, Compte M, HernandezPerez S, Merino N, Bonet J, Navarro R, Van Bergen En Henegouwen PMP, Lykkemark S. ATTACK, a novel bispecific T cell-recruiting antibody with trivalent EGFR binding and monovalent CD3 binding for cancer immunotherapy. Oncoimmunology. 2017;7(1):e1377874. doi:10.1080/2162402X.2017.1377874.
43. Varma R, Campi G, Yokosuka T, Saito T, Dustin ML. T cell receptor-proximal signals are sustained in peripheral microclusters and terminated in the central supramolecular activation cluster. Immunity. 2006;25(1):117–127. doi:10.1016/j.immuni.2006.04.010.
44. Hashimoto-Tane A, Yokosuka T, Sakata-Sogawa K, Sakuma M, Ishihara C, Tokunaga M, Saito T. Dynein-driven transport of T cell receptor microclusters regulates immune synapse formation and T cell activation. Immunity. 2011;34(6):919–931. doi:10.1016/j.immuni.2011.05.012.
45. Yi J, Wu XS, Crites T, Hammer JA III, Pollard TD. Actin retrograde flow and actomyosin II arc contraction drive receptor cluster dynamics at the immunological synapse in Jurkat T cells. Mol Biol Cell. 2012;23(5):834–852. doi:10.1091/mbc.e11-08-0731.
46. Murugesan S, Hong J, Yi J, Li D, Beach JR, Shao L. Formin-generated actomyosin arcs propel T cell receptor microcluster movement at the immune synapse. J Cell Biol. 2016;215(3):383–399. doi:10.1083/jcb.201603080.

47. Babich A, Li S, O'Connor RS, Milone MC, Freedman BD, Burkhardt JK. F-actin polymerization and retrograde flow drive sustained PLCgamma1 signaling during T cell activation. J Cell Biol. 2012;197(6):775–787. doi:10.1083/jcb.201201018.
48. Desai DM, Newton ME, Kadlecek T, Weiss A. Stimulation of the phosphatidylinositol pathway can induce T-cell activation. Nature. 1990;348(6296):669. doi:10.1038/348066a0.
49. Bonvini E, DeBell KE, Veri MC, Graham L, Stoica B, Laborda J, Aman MJ, DiBaldassarre A, Miscia S, Rellahan BL. On the mechanism coupling phospholipase Cgamma1 to the B- and T-cell antigen receptors. Adv Enzyme Regul. 2003;43(1):245–269. doi:10.1016/S0065-2571(02)00033-X.
50. Das V, Nal B, Dujeancourt A, Thoulouze MI, Galli T, Roux P, Dautry-Varsat A, Alcover A. Activation induced polarized recycling targets T cell antigen receptors to the immunological synapse; involvement of SNARE complexes. Immunity. 2004;20(5):577–588. doi:10.1016/S1074-7613(04)00106-2.
51. Montoya MC, Sancho D, Vicente-Manzanares M, Sanchez-Madrid F. Cell adhesion and polarity during immune interactions. Immunol Rev. 2002;186(1):6882. doi:10.1034/j.1600-065X.2002.18607.x.
52. Martin-Cofreces NB, Vicente-Manzanares M, Sanchez-Madrid F. Adhesive interactions delineate the topography of the immune synapse. Front Cell Dev Biol. 2018;6:149. doi:10.3389/fcell.2018.00149.
53. Davenport AJ, Jenkins MR, Cross RS, Yong CS, Prince HM, Ritchie DS, Trapani JA, Kershaw MH, Darcy PK, Neeson PJ. CAR-T cells inflict sequential killing of multiple tumor target cells. Cancer Immunol Res. 2015;3(5):483–494. doi:10.1158/2326-6066.CIR-15-0048.
54. Li W, Qiu S, Chen J, Jiang S, Chen W, Jiang J, Wang F, Si W, Shu Y, Wei P. Chimeric antigen receptor designed to prevent ubiquitination and downregulation showed durable antitumor efficacy. Immunity. 2020;53(2):456–470. doi:10.1016/j.immuni.2020.07.011.
55. Liu H, Rhodes M, Wiest DL, Vignali DA. On the dynamics of TCR:CD3 complex cell surface expression and downmodulation. Immunity. 2000;13(5):66575. doi:10.1016/S1074-7613(00)00066-2.
56. Zeng Q, Schwarz H. The role of trogocytosis in immune surveillance of Hodgkin lymphoma. Oncoimmunology. 2020;9(1):1781334. doi:10.1080/2162402X.2020.1781334.
57. Li G, Bethune MT, Wong S, Joglekar AV, Leonard MT, Wang JK, Kim JT, Cheng D, Peng S, Zaretsky JM. T cell antigen discovery via trogocytosis. Nat Methods. 2019;16(2):183–190. doi:10.1038/s41592-018-0305-7.
58. Peters PJ, Geuze HJ, Van der Donk HA, Slot JW, Griffith JM, Stam NJ, Clevers HC, Borst J. Molecules relevant for T cell-target cell interaction are present in cytolytic granules of human T lymphocytes. Eur J Immunol. 1989;19(8):1469–1475. doi:10.1002/eji.1830190819.
59. Peters PJ, Geuze HJ, Van der Donk HA, Borst J. A new model for lethal hit delivery by cytotoxic T lymphocytes. Immunol Today. 1990;11:28–32. doi:10.1016/0167-5699(90)90008-W.
60. Iwasaki S, Masuda S, Baba T, Tomaru U, Katsumata K, Kasahara M, Ishizu A. Plasma-dependent, antibody- and Fcgamma receptor-mediated translocation of CD8 molecules from T cells to monocytes. Cytometry A. 2011;79(1):46–56. doi:10.1002/cyto.a.20984.
61. Rossi EA, Chang CH, Goldenberg DM, Bachmann MP. Anti-CD22/CD20 bispecific antibody with enhanced trogocytosis for treatment of Lupus. PLoS One. 2014;9(5):e98315. doi:10.1371/journal.pone.0098315.
62. Vijayaraghavan S, Lipfert L, Chevalier K, Bushey BS, Henley B, Lenhart R, Sendecki J, Beqiri M, Millar HJ, Packman K. Amivantamab (JNJ-61186372), an Fc enhanced EGFR/cMet bispecific antibody, induces receptor downmodulation and antitumor activity by monocyte/macrophage trogocytosis. Mol Cancer Ther. 2020;19(10):2044–2056. doi:10.1158/1535-7163.MCT-20-0071.
63. Rossi EA, Rossi DL, Cardillo TM, Chang CH, Goldenberg DM. Redirected T cell killing of solid cancers targeted with an anti-CD3/Trop-2-bispecific antibody is enhanced in combination with interferon-alpha. Mol Cancer Ther. 2014;13(10):2341–2351. doi:10.1158/1535-7163.MCT-14-0345.
64. Ahmed KA, Munegowda MA, Xie Y, Xiang J. Intercellular trogocytosis plays an important role in modulation of immune responses. Cell Mol Immunol. 2008;5(4):261–9, 718. doi:10.1038/cmi.2008.32.

Supplemental material

Supplemental Tables

pPLC	J-CAR-T19 vs JSTAb-T19	J-STAb-T19 vs BLI	J-STAb-T19 vs SEE	J-CAR-T19 vs SEE	J-CAR-T19 vs BLI	BLI vs SEE
5 min	0.0025	0.3226	0.1992	0.0322	0.0773	0.1955
15 min	<0.0001	0.6709	0.3504	0.0194	0.111	0.4883
pERK	J-CAR-T19 vs JSTAb-T19	J-STAb-T19 vs BLI	J-STAb-T19 vs SEE	J-CAR-T19 vs SEE	J-CAR-T19 vs BLI	BLI vs SEE
5 min	0.7004	0.9578	0.9515	0.6164	0.6081	0.9853
15 min	0.1243	0.8964	0.7296	0.1091	0.0734	0.7726

Table S1. Statistical analysis of PLCγ and ERK phosphorylation in J-NT-T, J-CART19 and J-STAb-T19 cells 5 and 15 minutes after co-culture with $CD19^{+}$ Raji cells.

Supplemental Figures

Figure supplementary 1

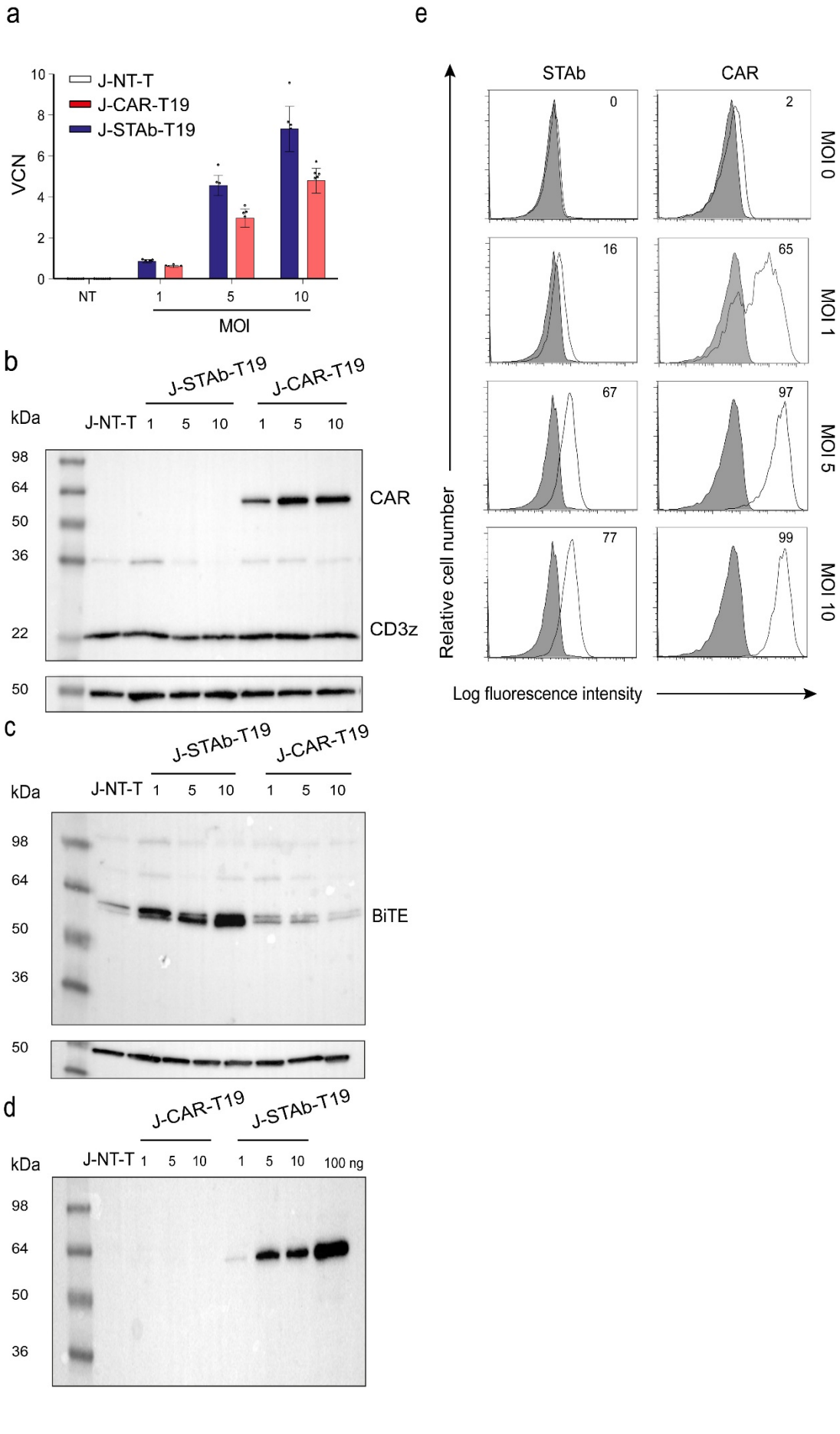
a
J-NT-T
J-CAR-T19
J-STAb-T19
VCN
MOI
NT
b
J-STAb-T19
J-CAR-T19
kDa
J-NT-T
CAR
CD3z
c
BiTE
d
100 ng
e
STAb
CAR
MOI 0
MOI 1
MOI 5
MOI 10
Relative cell number
Log fluorescence intensity

Figure S1. **Generation and characterization of J-STAb-T19 and J-CAR-T19 cells.** (a) Determination of the vector copy number (VCN) of integrated lentiviruses in Jurkat T cells transduced at different MOIs with 19-CAR-(J-CAR-T19, red bars) or 19-BiTE-(J-STAb-T19, blue bars) encoding lentiviruses. (b) Analysis of the intracellular levels of endogenous CD3ζ and 19-CAR in non-transduced (J-NT-T), J-STAb-T19 and J-CART19 cells. (c) Determination of the intracellular levels of 19-BiTE in J-NT-T, J-STAbT19 and J-CAR-T19 cells. (d) Detection of secreted 19-BiTE in the conditioned media from J-NT-T, J-STAb-T19 and J-CAR-T19 cells. (e) Jurkat T cells were stained to detect cell surface-expressed 19-CAR or cell surface-bound 19-BiTE; one representative experiment out of three is shown.

Figure supplementary 2

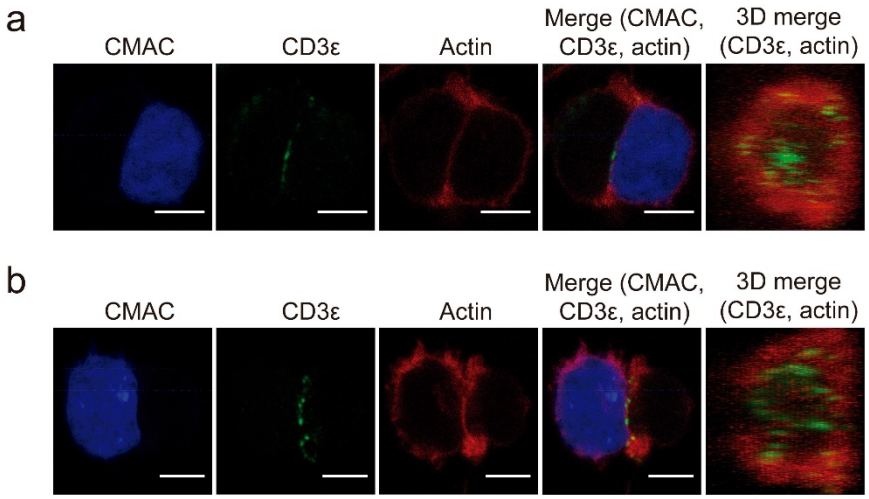

Figure S2. Representative images of (a) a properly assembled IS, with actin localized in the distal ring (dSMAC) of the synapse and CD3 coalesced in the inner circle (cSMAC) and (b) disorganized synapse with incomplete actin clearance from the center and CD3 scattered throughout the synapse. Non-transduced Jurkat (J-NT-T) cells were incubated for 15 minutes with SEE-loaded, CMAC (blue) labelled Raji cells. Distribution of CD3ε (green channel) and actin (red channel) is shown, as well as the merged images. Scale
bar corresponds to 5 μm. The IS topology obtained from the 3D reconstructions of region of interest placed at the IS in confocal stacks containing the red and the green channels is shown.

Figure supplementary 3

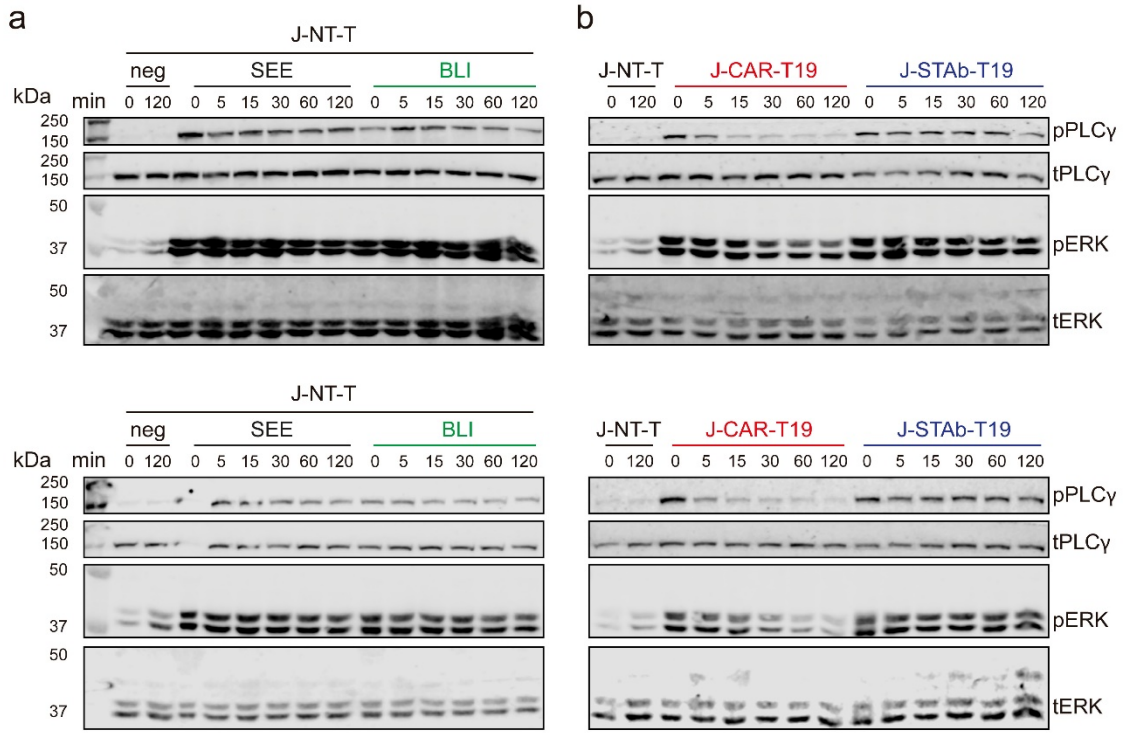

Figure S3. Western blot for quantification of PLCγ1 and ERK1/2 activation. J-CART19 and J-STAb-T19 cells were stimulated for the indicated minutes (min) with Raji cells. As activation controls, J-NT-T cells were incubated with Raji cells loaded with SEE or 5nM BLI. Negative (-) control samples correspond J-NT-T cells incubated with unloaded Raji cells.

DISCUSIÓN

En este trabajo hemos desarrollado una estrategia de inmunoterapia, denominada STAb-T19, para el tratamiento de neoplasias hematológicas $CD19^+$, basada en la secreción de TCEs anti-CD19 x anti-CD3 en formato BiTE por linfocitos T modificados genéticamente. Las células STAb-T19 han demostrado ser más efectivas que células T que expresan un CAR anti-CD19 de segunda generación (CAR-T19), induciendo una mayor citotoxicidad específica, evitando el escape tumoral *in vitro* y la recaída de la leucemia *in vivo.*

Una de las principales ventajas de la estrategia STAb-T respecto a la terapia CAR-T es que permite un reclutamiento policlonal de las células T. En nuestro estudio hemos demostrado que las células STAb-T19 ejercen una acción citotóxica más rápida y eficaz que las células CAR-T19 incluso a ratios E:T muy bajas. Esto demuestra que el BiTE-19 secretado *in situ* tiene la capacidad de unirse de manera eficiente al CD3 de todas las células T circundantes, modificadas o no genéticamente, convirtiéndolas en efectoras capaces de reconocer células tumorales y destruirlas. Las células STAb-T19 se distinguen por alcanzar una elevada actividad citotóxica a ratios E:T en los que los niveles de secreción de INFγ son bajos, lo que sugiere un perfil de toxicidad favorable. Esto podría implicar que un tratamiento efectivo con células STAb-T19 requeriría dosis más bajas que las empleadas en las terapias CAR-T19, aspecto que sería de particular relevancia en aquellos casos en los que no es posible obtener una cantidad adecuada de células T debido al estado linfopénico de muchos pacientes multitratados, o por posibles problemas de fabricación (115). Por lo tanto, una reducción en el número de células terapéuticamente efectivas resultaría en un aumento del número de pacientes que se podrían beneficiar de la terapia STAb-T19 y reducir significativamente el coste del tratamiento. Además, la progresión de la enfermedad durante el proceso de fabricación podría impedir la administración de la terapia CAR-T a tiempo (115), en cuyo caso el requisito de un menor número de células y, por tanto, un tiempo de fabricación más corto, supondrían importantes ventajas.

Las células STAb-T19 previenen el escape tumoral *in vitro* incluso a ratios E:T extremadamente bajas (1:32). Por el contrario, las células CAR-T19 no evitan el escape de la leucemia, asociado con una reducción rápida y drástica de la expresión de CD19 en la membrana de las células leucémicas y del CAR en la superficie de la célula T. Nuestros

resultados demuestran que el CD19 es internalizado y degradado en los lisosomas. Este fenómeno conduce a la aparición de una subpoblación de células leucémicas que reducen de manera transitoria la expresión de CD19 en su superficie, evadiendo la respuesta de las células CAR-T19. Cuando la presión selectiva mediada por el CAR disminuye o desaparece, las células leucémicas recuperan la expresión del marcador en superficie y progresan. Se ha demostrado que la densidad del antígeno diana desempeña un importante papel en la modulación de la activación de las células CAR-T, que solo ocurre si se alcanza un determinado umbral de densidad (116). Por lo tanto, una reducción parcial o completa del CD19 podría explicar la menor actividad citotóxica de las células CAR-T19. Es importante destacar que la disminución de los niveles de expresión de CD19 también se ha observado con células CAR-T que expresan un CAR anti-CD19 de segunda generación, cuyo scFv deriva del clon FMC63, utilizado para la fabricación de los cuatro productos CAR-T anti-CD19 comerciales actualmente aprobados por la FDA (117). La tasa de internalización de CD19 tras unir diferentes anticuerpos anti-CD19 solubles varía considerablemente (118, 119) y se ha demostrado que sólo una pequeña fracción de scFv anti-CD19 monovalente soluble derivado del clon FMC63 internaliza tras su interacción con CD19 (120). Esto sugiere que el anclaje a la membrana del scFv anti-CD19 en la molécula de CAR es fundamental para inducir la internalización de CD19, y podría explicar por qué no observamos internalización tras la interacción mediada por el BiTE-19.

Este fenómeno, no descrito previamente, de disminución de CD19 tras la interacción con el CAR-T19 podría tener un gran impacto *in vivo*. Aunque ambas estrategias muestran una eficacia similar *in vivo* en modelos a corto plazo (40-60 días), observamos importantes diferencias cuando comparamos ambas terapias en un modelo PDX a largo plazo (más de 100 días). En este modelo, las células STAb-T19 erradicaron eficazmente las células leucémicas mientras que en el grupo tratado con células CAR-T19 se detectó recidiva leucémica. Hasta la fecha, en la mayoría de los estudios *in vivo* llevados a cabo para estudiar la eficacia de las terapias CAR-T19, en los que se alcanzan remisiones completas, se han realizado períodos de observación de duración corta o intermedia, lo que podría conducir a una subestimación del riesgo de recaída.

Además de CD19, el CAR-19 expresado en membrana también experimenta una rápida disminución tras la interacción con el Ag. De hecho, la modulación negativa inducida por la unión al ligando es una característica común de los receptores de Ag, como el TCR (121). Se ha reportado previamente que la disminución del CAR es debida a su ubiquitinación y posterior degradación lisosomal (122), y conduce a la atenuación de la capacidad de las células CAR-T para destruir células tumorales (122-124). Por el contrario, no se ha observado una reducción tan drástica de la expresión de CD3 tras la interacción mediada por el BiTE-19.

De este modo, aunque las estrategias de redirección mediadas por CAR-19 y BiTE-19 son conceptualmente similares, presentan importantes diferencias en su interacción con el Ag. El CAR-19 es una proteína transmembrana artificial tipo I, con una arquitectura modular variable, que interactúa directamente con CD19, mientras que el BiTE-19 es una proteína soluble, que actúa como puente entre dos proteínas transmembrana tipo I, CD19 y la subunidad CD3ε del complejo TCR/CD3 (125). Estas diferencias son potencialmente importantes y pueden incidir de forma directa sobre la formación de la sinapsis. La SI canónica, mediada por la interacción a través del TCR, es una estructura altamente organizada en la que intervienen diferentes moléculas, que se disponen en anillos concéntricos denominados SMACs. Esta estructura debe organizarse de forma precisa para lograr una activación adecuada de la célula T (109, 110). Estudios previos han descrito que la SI mediada por el CAR exhibe un patrón multifocal desorganizado, diferente a la estructura canónica en "ojo de buey" (29, 113). A diferencia del CAR, los TCEs inducen la formación de una SI más fisiológica entre la célula T y la célula tumoral (44). De hecho, se ha demostrado que diferentes formatos de AcBis tienen la capacidad de movilizar eficientemente la F-actina hacia la periferia y los cúmulos de CD3 hacia el interior de la SI, produciendo una polarización adecuada de la señalización del TCR (108). Por ello las sinapsis promovidas por los BiTEs se consideran idénticas en estructura y composición molecular a la sinapsis inducida por el TCR (45, 126). Nuestros datos confirman los obtenidos en estudios previos, y muestran diferencias significativas en la topología de las SIs promovidas por el CAR-19 y el BiTE-19 en células T primarias. Mientras que las células CAR-T19 forman sinapsis desorganizadas, no fisiológicas (28-30), el BiTE-19 induce la formación de sinapsis

canónicas (45, 126), que promueven una degranulación eficiente, y previenen la internalización y degradación de CD19 mediadas por el CAR-19.

Para profundizar en las características y posibles consecuencias funcionales de ambos tipos de sinapsis se realizó un análisis más detallado de las interacciones linfocito T:célula tumoral mediadas por el CAR-19 y el BiTE-19. Este análisis se realizó con el modelo celular T Jurkat, ampliamente utilizado para estudiar la activación, señalización y ensamblaje de la sinapsis en linfocitos T (127-129). Para ello, se transdujeron células Jurkat con los vectores lentivirales que codifican el CAR-19 y el BiTE-19 y se realizaron la caracterización de las SIs y estudios funcionales. En las células Jurkat STAb-T19 se observó un marcaje de membrana con un AcMo anti-His, cuya intensidad era dependiente del número de copias del virus integradas (VCN, del inglés, *Virus copy number*), sugiriendo que el BiTE-19 secretado se une a los complejos TCR/CD3 en la superficie de las células T. Este proceso de cis-/trans "decoración" del CD3 permite a la célula T adherirse de forma específica y eficiente a CD19 humano y dota a las células T "decoradas" con el BiTE de la capacidad de reconocer específicamente células $CD19^+$.

Los estudios de sinapsis realizados con células Jurkat confirman los resultados obtenidos con células T primarias, observando que el CAR-19 induce la formación de una SI desorganizada, con grupos dispersos de CD3 y una organización difusa de la F-actina en comparación con la SI inducida vía TCR. La F-actina desempeña un papel fundamental en este movimiento centrípeto de los microclústeres de TCR (130-132), y el flujo retrógrado de la misma mantiene la señalización de PLCγ1 (133), evento clave en el proceso de activación celular desencadenado por el TCR (111, 134, 135). A diferencia de la sinapsis mediada por el CAR-19, los TCEs anti-CD19, BiTE-19 y *blinatumomab,* indujeron SIs similares a las observadas en un modelo bien establecido que utiliza la enterotoxina estafilocócica E (SEE, del inglés, *Staphylococcal Enterotoxin E*) para activar células T Jurkat a través del TCR en presencia de células diana Raji $CD19^+$, dando lugar a la formación de una sinapsis con una configuración canónica (136). El aclaramiento de F-actina también es importante para la secreción de citoquinas y de los gránulos líticos en la hendidura sináptica (112). Previsiblemente, la organización de la F-actina inducida en la SI de las células Jurkat STAb-T19 permitirá una secreción adecuada de los gránulos líticos, de modo similar a la producida durante la SI de los linfocitos T citotóxicos. Sin

embargo, debemos señalar que, aunque el SMAC distal se formó tanto en las células Jurkat STAb-T19 como en las células estimuladas con *blinatumomab*, el área central de la sinapsis fue de menor tamaño que en los controles realizados con el modelo Raji-SEE-Jurkat.

Para determinar el impacto de las diferencias observadas en las SIs promovidas por el BiTE-19 y el CAR-19, se analizó la activación de vías de señalización tempranas de la célula T tras el co-cultivo con células $CD19^{+}$. Los datos obtenidos mostraron una cinética de señalización más corta en las células Jurkat CAR-T19 en comparación con el grupo control, Jurkat no transducidas estimuladas con Raji-SEE. Esto podría estar relacionado con un estudio previo que indica que el tiempo requerido por el CAR para ensamblar SI funcionales es más corto que el requerido por el TCR, por lo que las células CAR-T se disocian de las células tumorales más rápidamente que las estimuladas vía TCR (29). *A priori* esta característica debería proporcionar a las células CAR-T una capacidad de *serial killing* más eficiente. Paradójicamente, esta característica no se asocia con una eliminación tumoral más efectiva y, en el citado estudio, la citotoxicidad mediada por el CAR fue inferior a la inducida por el TCR (123). Esto podría deberse a varias razones. En primer lugar, podríamos especular que una cinética de *serial killing* más rápida podría hacer a las células CAR-T más propensas al agotamiento celular debido a la activación reiterada. En segundo lugar, la menor capacidad citotóxica de las células CAR-T en comparación con las células T estimuladas a través del TCR se ha asociado a la acusada disminución del CAR en membrana tras la interacción con el AAT diana (123). Esta disminución del CAR, que habíamos observado en células CAR-T primarias, ha sido confirmada en el modelo Jurkat CAR-T19, en el que además hemos analizado la ubicación del CAR tras la interacción con CD19, mostrando una co-localización con la proteína 1 de membrana asociada a lisosomas (LAMP1). Esta observación concuerda con un trabajo previo que describe la degradación lisosomal de los CARs internalizados (122). En contraste con los datos observados con las células Jurkat CAR-T, las interacciones mediadas por el BiTE-19 inducen una cinética de señalización similar a la generada vía TCR.

En cuanto al efecto negativo que puede tener la disminución en membrana de la molécula activadora de la célula T, se detectó una reducción de la expresión del CD3 en

la superficie de las células Jurkat STAb-T19 tras la interacción con las células $CD19^+$. Sin embargo, este descenso fue mucho menos acusado que la reducción del CAR-19, lo que permite a las células Jurkat STAb-T disponer de una densidad adecuada de moléculas para interaccionar con el CD19 expresado en la célula diana. Además, esta disminución de CD3 podría explicarse parcialmente por la competencia de epítopos entre el AcMo anti-CD3 utilizado para su detección y el BiTE-19. Por otra parte, la disminución de CD3 podría obedecer a la propia dinámica fisiológica del complejo TCR/CD3 durante la estimulación antigénica, en la que se produce una disminución del TCR/CD3 debido a la inhibición del reciclaje de los complejos internalizados (121). La pérdida del CD3 también podría asociarse con fenómenos de trogocitosis, proceso de transferencia intercelular y bidireccional de fragmentos de membrana plasmática junto con sus moléculas asociadas, observado con frecuencia en la sinapsis entre células presentadoras de antígeno y células T (101). Las proteínas transferidas pueden ser internalizadas por las células receptoras o exhibidas en su propia superficie (101, 137, 138). La transferencia de CD3 desde las células Jurkat STAb-T19 hacia las células $CD19^+$ observada en nuestro estudio es consistente con la presencia de componentes del complejo TCR en exosomas transferidos al espacio sináptico (139, 140). Igualmente, han sido descritos fenómenos de trogocitosis mediados por Acs (141), incluso por AcBis (142-144). Es más, la trogocitosis bidireccional entre células B y T mediada por TCEs anti-CD19 x anti-CD3 ha sido observada previamente, sugiriendo que este proceso podría ser un fenómeno común en la redirección de células T mediada por TCEs (144). Las consecuencias del proceso de trogocitosis son diversas, dependiendo de la función de las proteínas embebidas en los fragmentos de membrana transferidos, y puede tanto suprimir como potenciar la respuesta inmune (145). No obstante, es indicativo de una respuesta fisiológica, y será necesario investigar en profundidad la potencial relevancia de la captación de CD3 por las células diana $CD19^+$ mediada por el BiTE-19.

En definitiva, hemos comprobado que la topología de las SIs inducidas en células T primarias por el BiTE-19 y el CAR-19 son diferentes y estos resultados se reproducen en la línea celular T Jurkat, lo que nos proporciona un modelo muy útil para realizar futuros estudios que permitan definir con precisión el impacto de la arquitectura de la SI en la capacidad funcional, el potencial citotóxico y la persistencia de células CAR-T19

y STAb-T19. Cabe destacar que hemos demostrado por primera vez que dos moléculas diferentes, con capacidad de redirigir células T frente al mismo Ag utilizando el mismo clon anti-CD19, desencadenan resultados diferentes en términos de señalización y formación de sinapsis.

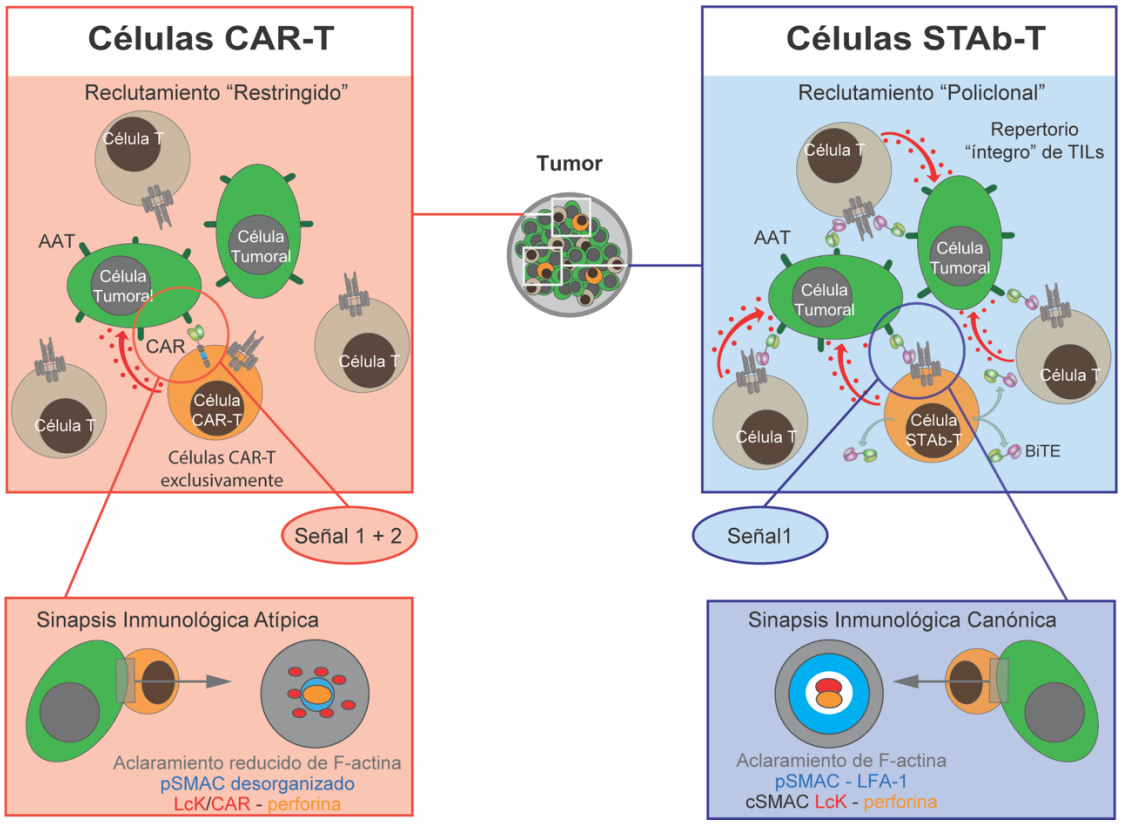

Figura 7. Representación esquemática de las estrategias de redirección de células T. En la figura se representan células CAR-T que expresan un receptor de antígeno quimérico de segunda generación, y células STAb-T que secretan un TCE en formato BiTE. Las flechas y los puntos rojos indican el reconocimiento y ataque a las células tumorales (células verdes) por parte de las células T activadas mediante el CAR o el BiTE: linfocitos T infiltrantes del tumor (TILs, del inglés, *Tumor Infiltrating Lymphocytes*; células grises) modificados o no genéticamente. El CAR de segunda generación proporciona las señales 1 y 2 al interaccionar con el AAT, mientras que los BiTEs no proporcionan la señal de co-estimulación. Asimismo, se representa la estructura de las SIs promovidas por el CAR y el BiTE: la SI mediada por el CAR muestra una estructura desorganizada, mientras que la SI mediada por el BiTE muestra una estructura canónica, bien organizada. Figura modificada de (125).

Así pues, podemos concluir que, en la terapia STAb-T19, la secreción continua de BiTE-19 y la persistencia del Ag diana en la superficie de las células tumorales, unidas la generación de sinapsis canónicas, permite el reclutamiento del repertorio de linfocitos T endógenos, dando lugar a una eliminación rápida y eficaz de las células tumorales, que podría prevenir la recaída de la leucemia frecuentemente asociada con las terapias CAR-T19. Estos resultados avalan el interés por evaluar la capacidad terapéutica y el perfil de toxicidad de las células STAb-T19 en un contexto clínico.

CONCLUSIONES

1. Las células STAb-T19 secretan BiTE-19 funcional que se une al complejo TCR/CD3 de la célula T, "decorando" su superficie, lo que permite el reconocimiento específico de células $CD19^+$.
2. El BiTE-19 secretado induce la formación de SIs canónicas, similares a las inducidas a través del TCR, en las que se produce una acumulación de la F-actina en el anillo distal (dSMAC) y un acúmulo de CD3 en el anillo central (cSMAC) de la sinapsis. Sin embargo, el CAR-19 forma una SI desorganizada con acúmulos dispersos de CD3 y una distribución difusa de la F-actina.
3. Las cinéticas de activación de PLCγ1 y ERK1/2 en las células Jurkat STAb-T19 son similares a las obtenidas en las células Jurkat estimuladas a través del TCR, mientras que las células Jurkat CAR-T19 generan una señalización más transitoria.
4. La interacción CAR-19:CD19 origina una disminución en los niveles de expresión de CD19 en las células leucémicas y de CAR-19 en las células CAR-T19. Ambas moléculas son internalizadas y se localizan en el compartimento lisosomal.
5. En las células Jurkat STAb-T19 se produce una reducción moderada en los niveles de expresión del CD3 en superficie, debido en parte, a su captación por las células $CD19^+$ tras la interacción mediada por el BiTE-19.
6. Las células STAb-T19 reclutan células T no modificadas (efecto *bystander*) y ejercen una respuesta citotóxica más rápida y potente que las células CAR-T19, previniendo el escape tumoral *in vitro* a ratios célula efectora:célula diana muy bajas.
7. Ambas terapias controlan la progresión de la enfermedad en modelos *in vivo* a corto plazo, pero solo las células STAb-T19 previenen la recaída leucémica en modelos *in vivo* a largo plazo.
8. Estos resultados demuestran el potencial de la terapia STAb-T19 como alternativa a las estrategias de redirección de células T actualmente utilizadas en clínica y avalan la realización de ensayos clínicos para evaluar su eficacia y seguridad.

BIBLIOGRAFÍA

1. Burnet FM. Immunological aspects of malignant disease. Lancet. 1967;1(7501):1171-4.
2. Dunn GP, Bruce AT, Ikeda H, Old LJ, Schreiber RD. Cancer immunoediting: from immunosurveillance to tumor escape. Nat Immunol. 2002;3(11):991-8.
3. O'Donnell JS, Teng MWL, Smyth MJ. Cancer immunoediting and resistance to T cell-based immunotherapy. Nat Rev Clin Oncol. 2019;16(3):151-67.
4. Schreiber RD, Old LJ, Smyth MJ. Cancer immunoediting: integrating immunity's roles in cancer suppression and promotion. Science. 2011;331(6024):1565-70.
5. Blattman JN, Greenberg PD. Cancer immunotherapy: a treatment for the masses. Science. 2004;305(5681):200-5.
6. Mellman I, Coukos G, Dranoff G. Cancer immunotherapy comes of age. Nature. 2011;480(7378):480-9.
7. Ribas A, Wolchok JD. Cancer immunotherapy using checkpoint blockade. Science. 2018;359(6382):1350-5.
8. June CH, O'Connor RS, Kawalekar OU, Ghassemi S, Milone MC. CAR T cell immunotherapy for human cancer. Science. 2018;359(6382):1361-5.
9. Alvarez-Vallina L. Genetic approaches for antigen-selective cell therapy. Curr Gene Ther. 2001;1(4):385-97.
10. Sanz L, Blanco B, Alvarez-Vallina L. Antibodies and gene therapy: teaching old 'magic bullets' new tricks. Trends Immunol. 2004;25(2):85-91.
11. Chen DS, Mellman I. Oncology meets immunology: the cancer-immunity cycle. Immunity. 2013;39(1):1-10.
12. Swartz MA, Hirosue S, Hubbell JA. Engineering approaches to immunotherapy. Sci Transl Med. 2012;4(148):148rv9.
13. Blanco B, Compte M, Lykkemark S, Sanz L, Alvarez-Vallina L. T Cell-Redirecting Strategies to 'STAb' Tumors: Beyond CARs and Bispecific Antibodies. Trends Immunol. 2019;40(3):243-57.
14. Garrido F, Perea F, Bernal M, Sanchez-Palencia A, Aptsiauri N, Ruiz-Cabello F. The Escape of Cancer from T Cell-Mediated Immune Surveillance: HLA Class I Loss and Tumor Tissue Architecture. Vaccines (Basel). 2017;5(1).
15. Barrett DM, Singh N, Porter DL, Grupp SA, June CH. Chimeric antigen receptor therapy for cancer. Annu Rev Med. 2014;65:333-47.

16. Junghans RP. The challenges of solid tumor for designer CAR-T therapies: a 25-year perspective. Cancer Gene Ther. 2017;24(3):89-99.
17. Zhao L, Cao YJ. Engineered T Cell Therapy for Cancer in the Clinic. Front Immunol. 2019;10:2250.
18. Maude SL, Laetsch TW, Buechner J, Rives S, Boyer M, Bittencourt H, et al. Tisagenlecleucel in Children and Young Adults with B-Cell Lymphoblastic Leukemia. N Engl J Med. 2018;378(5):439-48.
19. Neelapu SS, Locke FL, Bartlett NL, Lekakis LJ, Miklos DB, Jacobson CA, et al. Axicabtagene Ciloleucel CAR T-Cell Therapy in Refractory Large B-Cell Lymphoma. N Engl J Med. 2017;377(26):2531-44.
20. Salmikangas P, Kinsella N, Chamberlain P. Chimeric Antigen Receptor T-Cells (CAR T-Cells) for Cancer Immunotherapy - Moving Target for Industry? Pharm Res. 2018;35(8):152.
21. Milone MC, Fish JD, Carpenito C, Carroll RG, Binder GK, Teachey D, et al. Chimeric receptors containing CD137 signal transduction domains mediate enhanced survival of T cells and increased antileukemic efficacy in vivo. Mol Ther. 2009;17(8):1453-64.
22. Kochenderfer JN, Feldman SA, Zhao Y, Xu H, Black MA, Morgan RA, et al. Construction and preclinical evaluation of an anti-CD19 chimeric antigen receptor. J Immunother. 2009;32(7):689-702.
23. Alonso-Camino V, Harwood SL, Alvarez-Mendez A, Alvarez-Vallina L. Efficacy and toxicity management of CAR-T-cell immunotherapy: a matter of responsiveness control or tumour-specificity? Biochem Soc Trans. 2016;44(2):406-11.
24. Hartmann J, Schussler-Lenz M, Bondanza A, Buchholz CJ. Clinical development of CAR T cells-challenges and opportunities in translating innovative treatment concepts. EMBO Mol Med. 2017;9(9):1183-97.
25. Brudno JN, Kochenderfer JN. Toxicities of chimeric antigen receptor T cells: recognition and management. Blood. 2016;127(26):3321-30.
26. Xu X, Sun Q, Liang X, Chen Z, Zhang X, Zhou X, et al. Mechanisms of Relapse After CD19 CAR T-Cell Therapy for Acute Lymphoblastic Leukemia and Its Prevention and Treatment Strategies. Front Immunol. 2019;10:2664.

27. Shah NN, Fry TJ. Mechanisms of resistance to CAR T cell therapy. Nat Rev Clin Oncol. 2019;16(6):372-85.
28. Mukherjee M, Mace EM, Carisey AF, Ahmed N, Orange JS. Quantitative Imaging Approaches to Study the CAR Immunological Synapse. Mol Ther. 2017;25(8):1757-68.
29. Davenport AJ, Cross RS, Watson KA, Liao Y, Shi W, Prince HM, et al. Chimeric antigen receptor T cells form nonclassical and potent immune synapses driving rapid cytotoxicity. Proc Natl Acad Sci U S A. 2018;115(9):E2068-E76.
30. Watanabe K, Kuramitsu S, Posey AD, Jr., June CH. Expanding the Therapeutic Window for CAR T Cell Therapy in Solid Tumors: The Knowns and Unknowns of CAR T Cell Biology. Front Immunol. 2018;9:2486.
31. Xiong W, Chen Y, Kang X, Chen Z, Zheng P, Hsu YH, et al. Immunological Synapse Predicts Effectiveness of Chimeric Antigen Receptor Cells. Mol Ther. 2018;26(4):963-75.
32. van der Neut Kolfschoten M, Schuurman J, Losen M, Bleeker WK, Martinez-Martinez P, Vermeulen E, et al. Anti-inflammatory activity of human IgG4 antibodies by dynamic Fab arm exchange. Science. 2007;317(5844):1554-7.
33. Labrijn AF, Buijsse AO, van den Bremer ET, Verwilligen AY, Bleeker WK, Thorpe SJ, et al. Therapeutic IgG4 antibodies engage in Fab-arm exchange with endogenous human IgG4 in vivo. Nat Biotechnol. 2009;27(8):767-71.
34. Yang X, Ambrogelly A. Enlarging the repertoire of therapeutic monoclonal antibodies platforms: domesticating half molecule exchange to produce stable IgG4 and IgG1 bispecific antibodies. Curr Opin Biotechnol. 2014;30:225-9.
35. Nisonoff A, Rivers MM. Recombination of a mixture of univalent antibody fragments of different specificity. Arch Biochem Biophys. 1961;93:460-2.
36. Nunez-Prado N, Compte M, Harwood S, Alvarez-Mendez A, Lykkemark S, Sanz L, et al. The coming of age of engineered multivalent antibodies. Drug Discov Today. 2015;20(5):588-94.
37. Brinkmann U, Kontermann RE. The making of bispecific antibodies. MAbs. 2017;9(2):182-212.
38. Blanco B, Dominguez-Alonso C, Alvarez-Vallina L. Bispecific Immunomodulatory Antibodies for Cancer Immunotherapy. Clin Cancer Res. 2021;27(20):5457-64.

39. Borlak J, Langer F, Spanel R, Schondorfer G, Dittrich C. Immune-mediated liver injury of the cancer therapeutic antibody catumaxomab targeting EpCAM, CD3 and Fcgamma receptors. Oncotarget. 2016;7(19):28059-74.
40. Holliger P, Prospero T, Winter G. "Diabodies": small bivalent and bispecific antibody fragments. Proc Natl Acad Sci U S A. 1993;90(14):6444-8.
41. Mack M, Riethmuller G, Kufer P. A small bispecific antibody construct expressed as a functional single-chain molecule with high tumor cell cytotoxicity. Proc Natl Acad Sci U S A. 1995;92(15):7021-5.
42. Brischwein K, Parr L, Pflanz S, Volkland J, Lumsden J, Klinger M, et al. Strictly target cell-dependent activation of T cells by bispecific single-chain antibody constructs of the BiTE class. J Immunother. 2007;30(8):798-807.
43. Loffler A, Kufer P, Lutterbuse R, Zettl F, Daniel PT, Schwenkenbecher JM, et al. A recombinant bispecific single-chain antibody, CD19 x CD3, induces rapid and high lymphoma-directed cytotoxicity by unstimulated T lymphocytes. Blood. 2000;95(6):2098-103.
44. Huehls AM, Coupet TA, Sentman CL. Bispecific T-cell engagers for cancer immunotherapy. Immunol Cell Biol. 2015;93(3):290-6.
45. Offner S, Hofmeister R, Romaniuk A, Kufer P, Baeuerle PA. Induction of regular cytolytic T cell synapses by bispecific single-chain antibody constructs on MHC class I-negative tumor cells. Mol Immunol. 2006;43(6):763-71.
46. Ma J, Mo Y, Tang M, Shen J, Qi Y, Zhao W, et al. Bispecific Antibodies: From Research to Clinical Application. Front Immunol. 2021;12:626616.
47. Przepiorka D, Ko CW, Deisseroth A, Yancey CL, Candau-Chacon R, Chiu HJ, et al. FDA Approval: Blinatumomab. Clin Cancer Res. 2015;21(18):4035-9.
48. Blinatumomab Approval Expanded Based on MRD. Cancer Discov. 2018;8(6):OF3.
49. Kantarjian H, Stein A, Gokbuget N, Fielding AK, Schuh AC, Ribera JM, et al. Blinatumomab versus Chemotherapy for Advanced Acute Lymphoblastic Leukemia. N Engl J Med. 2017;376(9):836-47.
50. Goebeler ME, Knop S, Viardot A, Kufer P, Topp MS, Einsele H, et al. Bispecific T-Cell Engager (BiTE) Antibody Construct Blinatumomab for the Treatment of Patients With Relapsed/Refractory Non-Hodgkin Lymphoma: Final Results From a Phase I Study. J Clin Oncol. 2016;34(10):1104-11.

51. Topp MS, Gokbuget N, Stein AS, Zugmaier G, O'Brien S, Bargou RC, et al. Safety and activity of blinatumomab for adult patients with relapsed or refractory B-precursor acute lymphoblastic leukaemia: a multicentre, single-arm, phase 2 study. Lancet Oncol. 2015;16(1):57-66.
52. Garber K. Bispecific antibodies rise again. Nat Rev Drug Discov. 2014;13(11):799-801.
53. Sanchez-Martin D, Sanz L, Alvarez-Vallina L. Engineering human cells for in vivo secretion of antibody and non-antibody therapeutic proteins. Curr Opin Biotechnol. 2011;22(6):924-30.
54. Blanco B, Holliger P, Vile RG, Alvarez-Vallina L. Induction of human T lymphocyte cytotoxicity and inhibition of tumor growth by tumor-specific diabody-based molecules secreted from gene-modified bystander cells. J Immunol. 2003;171(2):1070-7.
55. Compte M, Blanco B, Serrano F, Cuesta AM, Sanz L, Bernad A, et al. Inhibition of tumor growth in vivo by in situ secretion of bispecific anti-CEA x anti-CD3 diabodies from lentivirally transduced human lymphocytes. Cancer Gene Ther. 2007;14(4):380-8.
56. Iwahori K, Kakarla S, Velasquez MP, Yu F, Yi Z, Gerken C, et al. Engager T cells: a new class of antigen-specific T cells that redirect bystander T cells. Mol Ther. 2015;23(1):171-8.
57. Liu X, Barrett DM, Jiang S, Fang C, Kalos M, Grupp SA, et al. Improved anti-leukemia activities of adoptively transferred T cells expressing bispecific T-cell engager in mice. Blood Cancer J. 2016;6(6):e430.
58. Velasquez MP, Torres D, Iwahori K, Kakarla S, Arber C, Rodriguez-Cruz T, et al. T cells expressing CD19-specific Engager Molecules for the Immunotherapy of CD19-positive Malignancies. Sci Rep. 2016;6:27130.
59. Bonifant CL, Szoor A, Torres D, Joseph N, Velasquez MP, Iwahori K, et al. CD123-Engager T Cells as a Novel Immunotherapeutic for Acute Myeloid Leukemia. Mol Ther. 2016;24(9):1615-26.
60. Gattinoni L, Speiser DE, Lichterfeld M, Bonini C. T memory stem cells in health and disease. Nat Med. 2017;23(1):18-27.

61. Crompton JG, Sukumar M, Restifo NP. Uncoupling T-cell expansion from effector differentiation in cell-based immunotherapy. Immunol Rev. 2014;257(1):264-76.
62. Silva VL, Al-Jamal WT. Exploiting the cancer niche: Tumor-associated macrophages and hypoxia as promising synergistic targets for nano-based therapy. J Control Release. 2017;253:82-96.
63. Shaffer BC, Le Luduec JB, Forlenza C, Jakubowski AA, Perales MA, Young JW, et al. Phase II Study of Haploidentical Natural Killer Cell Infusion for Treatment of Relapsed or Persistent Myeloid Malignancies Following Allogeneic Hematopoietic Cell Transplantation. Biol Blood Marrow Transplant. 2016;22(4):705-9.
64. Liu D, Tian S, Zhang K, Xiong W, Lubaki NM, Chen Z, et al. Chimeric antigen receptor (CAR)-modified natural killer cell-based immunotherapy and immunological synapse formation in cancer and HIV. Protein Cell. 2017;8(12):861-77.
65. Sage EK, Thakrar RM, Janes SM. Genetically modified mesenchymal stromal cells in cancer therapy. Cytotherapy. 2016;18(11):1435-45.
66. Sheridan C. First off-the-shelf mesenchymal stem cell therapy nears European approval. Nat Biotechnol. 2018;36(3):212-4.
67. Sanz L, Santos-Valle P, Alonso-Camino V, Salas C, Serrano A, Vicario JL, et al. Long-term in vivo imaging of human angiogenesis: critical role of bone marrow-derived mesenchymal stem cells for the generation of durable blood vessels. Microvasc Res. 2008;75(3):308-14.
68. Karnoub AE, Dash AB, Vo AP, Sullivan A, Brooks MW, Bell GW, et al. Mesenchymal stem cells within tumour stroma promote breast cancer metastasis. Nature. 2007;449(7162):557-63.
69. Compte M, Nunez-Prado N, Sanz L, Alvarez-Vallina L. Immunotherapeutic organoids: a new approach to cancer treatment. Biomatter. 2013;3(1).
70. Compte M, Cuesta AM, Sanchez-Martin D, Alonso-Camino V, Vicario JL, Sanz L, et al. Tumor immunotherapy using gene-modified human mesenchymal stem cells loaded into synthetic extracellular matrix scaffolds. Stem Cells. 2009;27(3):753-60.
71. Ankrum JA, Ong JF, Karp JM. Mesenchymal stem cells: immune evasive, not immune privileged. Nat Biotechnol. 2014;32(3):252-60.
72. Saenz del Burgo L, Compte M, Aceves M, Hernandez RM, Sanz L, Alvarez-Vallina L, et al. Microencapsulation of therapeutic bispecific antibodies producing cells:

immunotherapeutic organoids for cancer management. J Drug Target. 2015;23(2):170-9.

73. Koike N, Fukumura D, Gralla O, Au P, Schechner JS, Jain RK. Tissue engineering: creation of long-lasting blood vessels. Nature. 2004;428(6979):138-9.
74. Stadler CR, Bahr-Mahmud H, Celik L, Hebich B, Roth AS, Roth RP, et al. Elimination of large tumors in mice by mRNA-encoded bispecific antibodies. Nat Med. 2017;23(7):815-7.
75. Pang X, Ma F, Zhang P, Zhong Y, Zhang J, Wang T, et al. Treatment of Human B-Cell Lymphomas Using Minicircle DNA Vector Expressing Anti-CD3/CD20 in a Mouse Model. Hum Gene Ther. 2017;28(2):216-25.
76. Gotwals P, Cameron S, Cipolletta D, Cremasco V, Crystal A, Hewes B, et al. Prospects for combining targeted and conventional cancer therapy with immunotherapy. Nat Rev Cancer. 2017;17(5):286-301.
77. Ruella M, Barrett DM, Kenderian SS, Shestova O, Hofmann TJ, Perazzelli J, et al. Dual CD19 and CD123 targeting prevents antigen-loss relapses after CD19-directed immunotherapies. J Clin Invest. 2016;126(10):3814-26.
78. Oelkrug C, Ramage JM. Enhancement of T cell recruitment and infiltration into tumours. Clin Exp Immunol. 2014;178(1):1-8.
79. Forget MA, Tavera RJ, Haymaker C, Ramachandran R, Malu S, Zhang M, et al. A Novel Method to Generate and Expand Clinical-Grade, Genetically Modified, Tumor-Infiltrating Lymphocytes. Front Immunol. 2017;8:908.
80. Garetto S, Sardi C, Martini E, Roselli G, Morone D, Angioni R, et al. Tailored chemokine receptor modification improves homing of adoptive therapy T cells in a spontaneous tumor model. Oncotarget. 2016;7(28):43010-26.
81. Schmidts A, Maus MV. Making CAR T Cells a Solid Option for Solid Tumors. Front Immunol. 2018;9:2593.
82. Alvarez-Vallina L, Hawkins RE. Antigen-specific targeting of CD28-mediated T cell co-stimulation using chimeric single-chain antibody variable fragment-CD28 receptors. Eur J Immunol. 1996;26(10):2304-9.
83. Guedan S, Posey AD, Jr., Shaw C, Wing A, Da T, Patel PR, et al. Enhancing CAR T cell persistence through ICOS and 4-1BB costimulation. JCI Insight. 2018;3(1).

84. Choi BD, Yu X, Castano AP, Bouffard AA, Schmidts A, Larson RC, et al. CAR-T cells secreting BiTEs circumvent antigen escape without detectable toxicity. Nat Biotechnol. 2019;37(9):1049-58.
85. Blanco B, Holliger P, Alvarez-Vallina L. Autocrine costimulation: tumor-specific CD28-mediated costimulation of T cells by in situ production of a bifunctional B7-anti-CEA diabody fusion protein. Cancer Gene Ther. 2002;9(3):275-81.
86. Velasquez MP, Szoor A, Vaidya A, Thakkar A, Nguyen P, Wu MF, et al. CD28 and 41BB Costimulation Enhances the Effector Function of CD19-Specific Engager T Cells. Cancer Immunol Res. 2017;5(10):860-70.
87. Koneru M, O'Cearbhaill R, Pendharkar S, Spriggs DR, Brentjens RJ. A phase I clinical trial of adoptive T cell therapy using IL-12 secreting MUC-16(ecto) directed chimeric antigen receptors for recurrent ovarian cancer. J Transl Med. 2015;13:102.
88. Pegram HJ, Purdon TJ, van Leeuwen DG, Curran KJ, Giralt SA, Barker JN, et al. IL-12-secreting CD19-targeted cord blood-derived T cells for the immunotherapy of B-cell acute lymphoblastic leukemia. Leukemia. 2015;29(2):415-22.
89. Perna SK, Pagliara D, Mahendravada A, Liu H, Brenner MK, Savoldo B, et al. Interleukin-7 mediates selective expansion of tumor-redirected cytotoxic T lymphocytes (CTLs) without enhancement of regulatory T-cell inhibition. Clin Cancer Res. 2014;20(1):131-9.
90. Chmielewski M, Hombach AA, Abken H. Of CARs and TRUCKs: chimeric antigen receptor (CAR) T cells engineered with an inducible cytokine to modulate the tumor stroma. Immunol Rev. 2014;257(1):83-90.
91. Kunert A, Chmielewski M, Wijers R, Berrevoets C, Abken H, Debets R. Intra-tumoral production of IL18, but not IL12, by TCR-engineered T cells is non-toxic and counteracts immune evasion of solid tumors. Oncoimmunology. 2017;7(1):e1378842.
92. Wei SC, Duffy CR, Allison JP. Fundamental Mechanisms of Immune Checkpoint Blockade Therapy. Cancer Discov. 2018;8(9):1069-86.
93. Armand P. Immune checkpoint blockade in hematologic malignancies. Blood. 2015;125(22):3393-400.

94. Cherkassky L, Morello A, Villena-Vargas J, Feng Y, Dimitrov DS, Jones DR, et al. Human CAR T cells with cell-intrinsic PD-1 checkpoint blockade resist tumor-mediated inhibition. J Clin Invest. 2016;126(8):3130-44.
95. Rafiq S, Yeku OO, Jackson HJ, Purdon TJ, van Leeuwen DG, Drakes DJ, et al. Targeted delivery of a PD-1-blocking scFv by CAR-T cells enhances anti-tumor efficacy in vivo. Nat Biotechnol. 2018;36(9):847-56.
96. Chang CH, Wang Y, Li R, Rossi DL, Liu D, Rossi EA, et al. Combination Therapy with Bispecific Antibodies and PD-1 Blockade Enhances the Antitumor Potency of T Cells. Cancer Res. 2017;77(19):5384-94.
97. Yoon DH, Osborn MJ, Tolar J, Kim CJ. Incorporation of Immune Checkpoint Blockade into Chimeric Antigen Receptor T Cells (CAR-Ts): Combination or Built-In CAR-T. Int J Mol Sci. 2018;19(2).
98. Eyquem J, Mansilla-Soto J, Giavridis T, van der Stegen SJ, Hamieh M, Cunanan KM, et al. Targeting a CAR to the TRAC locus with CRISPR/Cas9 enhances tumour rejection. Nature. 2017;543(7643):113-7.
99. Sotillo E, Barrett DM, Black KL, Bagashev A, Oldridge D, Wu G, et al. Convergence of Acquired Mutations and Alternative Splicing of CD19 Enables Resistance to CART-19 Immunotherapy. Cancer Discov. 2015;5(12):1282-95.
100. Viardot A, Bargou R. Bispecific antibodies in haematological malignancies. Cancer Treat Rev. 2018;65:87-95.
101. Joly E, Hudrisier D. What is trogocytosis and what is its purpose? Nat Immunol. 2003;4(9):815.
102. Hamieh M, Dobrin A, Cabriolu A, van der Stegen SJC, Giavridis T, Mansilla-Soto J, et al. CAR T cell trogocytosis and cooperative killing regulate tumour antigen escape. Nature. 2019;568(7750):112-6.
103. Hegde M, Corder A, Chow KK, Mukherjee M, Ashoori A, Kew Y, et al. Combinational targeting offsets antigen escape and enhances effector functions of adoptively transferred T cells in glioblastoma. Mol Ther. 2013;21(11):2087-101.
104. Roskopf CC, Braciak TA, Fenn NC, Kobold S, Fey GH, Hopfner KP, et al. Dual-targeting triplebody 33-3-19 mediates selective lysis of biphenotypic CD19+ CD33+ leukemia cells. Oncotarget. 2016;7(16):22579-89.

105. Kugler M, Stein C, Kellner C, Mentz K, Saul D, Schwenkert M, et al. A recombinant trispecific single-chain Fv derivative directed against CD123 and CD33 mediates effective elimination of acute myeloid leukaemia cells by dual targeting. Br J Haematol. 2010;150(5):574-86.
106. Compte M, Alvarez-Cienfuegos A, Nunez-Prado N, Sainz-Pastor N, Blanco-Toribio A, Pescador N, et al. Functional comparison of single-chain and two-chain anti-CD3-based bispecific antibodies in gene immunotherapy applications. Oncoimmunology. 2014;3:e28810.
107. Molgaard K, Harwood SL, Compte M, Merino N, Bonet J, Alvarez-Cienfuegos A, et al. Bispecific light T-cell engagers for gene-based immunotherapy of epidermal growth factor receptor (EGFR)-positive malignancies. Cancer Immunol Immunother. 2018;67(8):1251-60.
108. Harwood SL, Alvarez-Cienfuegos A, Nunez-Prado N, Compte M, Hernandez-Perez S, Merino N, et al. ATTACK, a novel bispecific T cell-recruiting antibody with trivalent EGFR binding and monovalent CD3 binding for cancer immunotherapy. Oncoimmunology. 2017;7(1):e1377874.
109. Roda-Navarro P, Alvarez-Vallina L. Understanding the Spatial Topology of Artificial Immunological Synapses Assembled in T Cell-Redirecting Strategies: A Major Issue in Cancer Immunotherapy. Front Cell Dev Biol. 2019;7:370.
110. Soares H, Lasserre R, Alcover A. Orchestrating cytoskeleton and intracellular vesicle traffic to build functional immunological synapses. Immunol Rev. 2013;256(1):118-32.
111. Das V, Nal B, Dujeancourt A, Thoulouze MI, Galli T, Roux P, et al. Activation-induced polarized recycling targets T cell antigen receptors to the immunological synapse; involvement of SNARE complexes. Immunity. 2004;20(5):577-88.
112. Martin-Cofreces NB, Vicente-Manzanares M, Sanchez-Madrid F. Adhesive Interactions Delineate the Topography of the Immune Synapse. Front Cell Dev Biol. 2018;6:149.
113. Xiong W, Chen Y, Kang X, Chen Z, Zheng P, Hsu YH, et al. Immunological Synapse Predicts Effectiveness of Chimeric Antigen Receptor Cells. Mol Ther. 2021;29(3):1349-51.

114. Li J, Stagg NJ, Johnston J, Harris MJ, Menzies SA, DiCara D, et al. Membrane-Proximal Epitope Facilitates Efficient T Cell Synapse Formation by Anti-FcRH5/CD3 and Is a Requirement for Myeloma Cell Killing. Cancer Cell. 2017;31(3):383-95.
115. Graham C, Jozwik A, Pepper A, Benjamin R. Allogeneic CAR-T Cells: More than Ease of Access? Cells. 2018;7(10).
116. Majzner RG, Mackall CL. Tumor Antigen Escape from CAR T-cell Therapy. Cancer Discov. 2018;8(10):1219-26.
117. Frigault MJ, Maus MV. State of the art in CAR T cell therapy for CD19+ B cell malignancies. J Clin Invest. 2020;130(4):1586-94.
118. Sapra P, Allen TM. Internalizing antibodies are necessary for improved therapeutic efficacy of antibody-targeted liposomal drugs. Cancer Res. 2002;62(24):7190-4.
119. Horton HM, Bernett MJ, Pong E, Peipp M, Karki S, Chu SY, et al. Potent in vitro and in vivo activity of an Fc-engineered anti-CD19 monoclonal antibody against lymphoma and leukemia. Cancer Res. 2008;68(19):8049-57.
120. Du X, Beers R, Fitzgerald DJ, Pastan I. Differential cellular internalization of anti-CD19 and -CD22 immunotoxins results in different cytotoxic activity. Cancer Res. 2008;68(15):6300-5.
121. Liu H, Rhodes M, Wiest DL, Vignali DA. On the dynamics of TCR:CD3 complex cell surface expression and downmodulation. Immunity. 2000;13(5):665-75.
122. Li W, Qiu S, Chen J, Jiang S, Chen W, Jiang J, et al. Chimeric Antigen Receptor Designed to Prevent Ubiquitination and Downregulation Showed Durable Antitumor Efficacy. Immunity. 2020;53(2):456-70 e6.
123. Davenport AJ, Jenkins MR, Cross RS, Yong CS, Prince HM, Ritchie DS, et al. CAR-T Cells Inflict Sequential Killing of Multiple Tumor Target Cells. Cancer Immunol Res. 2015;3(5):483-94.
124. Walker AJ, Majzner RG, Zhang L, Wanhainen K, Long AH, Nguyen SM, et al. Tumor Antigen and Receptor Densities Regulate Efficacy of a Chimeric Antigen Receptor Targeting Anaplastic Lymphoma Kinase. Mol Ther. 2017;25(9):2189-201.
125. Blanco B, Ramirez-Fernandez A, Alvarez-Vallina L. Engineering Immune Cells for in vivo Secretion of Tumor-Specific T Cell-Redirecting Bispecific Antibodies. Front Immunol. 2020;11:1792.

126. Kouhestani D, Geis M, Alsouri S, Bumm TGP, Einsele H, Sauer M, et al. Variant signaling topology at the cancer cell-T-cell interface induced by a two-component T-cell engager. Cell Mol Immunol. 2021;18(6):1568-70.
127. Balagopalan L, Yi J, Nguyen T, McIntire KM, Harned AS, Narayan K, et al. Plasma membrane LAT activation precedes vesicular recruitment defining two phases of early T-cell activation. Nat Commun. 2018;9(1):2013.
128. Hartzell CA, Jankowska KI, Burkhardt JK, Lewis RS. Calcium influx through CRAC channels controls actin organization and dynamics at the immune synapse. Elife. 2016;5.
129. Phee H, Abraham RT, Weiss A. Dynamic recruitment of PAK1 to the immunological synapse is mediated by PIX independently of SLP-76 and Vav1. Nat Immunol. 2005;6(6):608-17.
130. Hashimoto-Tane A, Yokosuka T, Sakata-Sogawa K, Sakuma M, Ishihara C, Tokunaga M, et al. Dynein-driven transport of T cell receptor microclusters regulates immune synapse formation and T cell activation. Immunity. 2011;34(6):919-31.
131. Yi J, Wu XS, Crites T, Hammer JA, 3rd. Actin retrograde flow and actomyosin II arc contraction drive receptor cluster dynamics at the immunological synapse in Jurkat T cells. Mol Biol Cell. 2012;23(5):834-52.
132. Murugesan S, Hong J, Yi J, Li D, Beach JR, Shao L, et al. Formin-generated actomyosin arcs propel T cell receptor microcluster movement at the immune synapse. J Cell Biol. 2016;215(3):383-99.
133. Babich A, Li S, O'Connor RS, Milone MC, Freedman BD, Burkhardt JK. F-actin polymerization and retrograde flow drive sustained PLCgamma1 signaling during T cell activation. J Cell Biol. 2012;197(6):775-87.
134. Desai DM, Newton ME, Kadlecek T, Weiss A. Stimulation of the phosphatidylinositol pathway can induce T-cell activation. Nature. 1990;348(6296):66-9.
135. Bonvini E, DeBell KE, Veri MC, Graham L, Stoica B, Laborda J, et al. On the mechanism coupling phospholipase Cgamma1 to the B- and T-cell antigen receptors. Adv Enzyme Regul. 2003;43:245-69.
136. Montoya MC, Sancho D, Vicente-Manzanares M, Sanchez-Madrid F. Cell adhesion and polarity during immune interactions. Immunol Rev. 2002;186:68-82.

137. Zeng Q, Schwarz H. The role of trogocytosis in immune surveillance of Hodgkin lymphoma. Oncoimmunology. 2020;9(1):1781334.
138. Li G, Bethune MT, Wong S, Joglekar AV, Leonard MT, Wang JK, et al. T cell antigen discovery via trogocytosis. Nat Methods. 2019;16(2):183-90.
139. Peters PJ, Geuze HJ, Van der Donk HA, Slot JW, Griffith JM, Stam NJ, et al. Molecules relevant for T cell-target cell interaction are present in cytolytic granules of human T lymphocytes. Eur J Immunol. 1989;19(8):1469-75.
140. Peters PJ, Geuze HJ, van der Donk HA, Borst J. A new model for lethal hit delivery by cytotoxic T lymphocytes. Immunol Today. 1990;11(1):28-32.
141. Iwasaki S, Masuda S, Baba T, Tomaru U, Katsumata K, Kasahara M, et al. Plasma-dependent, antibody- and Fcgamma receptor-mediated translocation of CD8 molecules from T cells to monocytes. Cytometry A. 2011;79(1):46-56.
142. Rossi EA, Chang CH, Goldenberg DM. Anti-CD22/CD20 Bispecific antibody with enhanced trogocytosis for treatment of Lupus. PLoS One. 2014;9(5):e98315.
143. Vijayaraghavan S, Lipfert L, Chevalier K, Bushey BS, Henley B, Lenhart R, et al. Amivantamab (JNJ-61186372), an Fc Enhanced EGFR/cMet Bispecific Antibody, Induces Receptor Downmodulation and Antitumor Activity by Monocyte/Macrophage Trogocytosis. Mol Cancer Ther. 2020;19(10):2044-56.
144. Rossi EA, Rossi DL, Cardillo TM, Chang CH, Goldenberg DM. Redirected T-cell killing of solid cancers targeted with an anti-CD3/Trop-2-bispecific antibody is enhanced in combination with interferon-alpha. Mol Cancer Ther. 2014;13(10):2341-51.
145. Ahmed KA, Munegowda MA, Xie Y, Xiang J. Intercellular trogocytosis plays an important role in modulation of immune responses. Cell Mol Immunol. 2008;5(4):261-9.

ANEXOS

Tabla 2: AcBis aprobados y en fase de estudio clínico.

Mecanismos de acción de los AcBis	Nombre	Diana 1	Diana 2	Formato	Instituciones I & D	Indicación	Fase de Estudio (Identificador)
Reclutamiento y activación de las células inmunes	MGD011	CD3	CD19	DART	MacroGenics	Linfoma de célula B	Fase II (NCT03635593)
	AFM11		CD19	TandAbs	Affimed	LNH	Fase I (NCT02848911)
	Blinatumomab		CD19	BiTE	Amgen	LLA	**Aprobado**
	AMG562		CD19	HLE-BiTE	Amgen	Linfoma	Fase I (NCT03571828)
	A-319		CD19	ITab	Generon	LLA	Fase I (NCT04056975)
	RG7828		CD20	KIH	Roche	Neoplasias Hematológicas	Fase I/II (NCT03677141)
	REGN1979		CD20	No disponible	Regeneron	Neoplasias Hematológicas	Fase II (NCT03888105)
	RG6026		CD20	CrossMab/ KIH/TCB	Roche	LNH	Fase I (NCT03075696)
	GEN3013		CD20	DuoBody	Genmab	Neoplasias Hematológicas	Fase I/II (NCT03625037)
	FBTA05		CD20	Triomab	Trion	Linfoma de célula B	Fase I/II (NCT01138579)
	Plamotamab		CD20	Xmab	Xencor	Neoplasias Hematológicas	Fase I (NCT02924402)
	AMG330		CD33	BiTE	Amgen	LMA	Fase I (NCT04478695)
	AMG673		CD33	HLE-BiTE	Amgen	LMA	Fase I (NCT03224819)
	AMV-564		CD33	TandAb	Amphivena Therapeutics	LMA	Fase I (NCT04128423)
	GEM333		CD33	scDb	GEMoaB Monoclonals	LMA	Fase I (NCT03516760)
	GBR 1342		CD38	BEAT	Glenmark Pharmaceuticals	MM	Fase I/II (NCT03309111)
	AMG424		CD38	Xmab	Amgen	MM	Fase I (NCT03445663)
	AMG420		BCMA	BiTE	Amgen	MM	Fase I (NCT03836053)
	AMG701		BCMA	HLE-BiTE	Amgen	MM	Fase I (NCT03287908)
	JNJ-64007957		BCMA	DuoBody	Janssen	MM	Fase I (NCT03145181)
	EM801		BCMA	CrossMab/ KIH	Celgene	MM	Fase I (NCT03486067)
	PF-06863135		BCMA	No disponible	Pfizer	MM	Fase I (NCT03269136)
	REGN5458		BCMA	No disponible	Regeneron	MM	Fase I/II (NCT03761108)
	TNB-383B		BCMA	No disponible	AbbVie	MM	Fase I (NCT03933735)
	APVO436		CD123	(scFv-Fc)2	Aptevo Therapeutics	LMA	Fase I (NCT03647800)
	MGD006		CD123	DART	MacroGenics	LMA	Fase II (NCT03739606)
	Xmab14045		CD123	Xmab	Xencor	LMA/LMC	Fase I (NCT02730312)
	JNJ-63709178		CD123	DuoBody	Janssen	LMA	Fase I (NCT02715011)
	MCLA-117		CLEC12A	Biclonics	Merus	LMA	Fase I (NCT03038230)
	RG6160		FcRH5	BiTE	Genentech	MM	Fase I (NCT03275103)

Reclutamiento y activación de las células inmunes	AMG427	CD3	FLT3	HLE-BiTE	Amgen	LMA	Fase I (NCT03541369)
	JNJ-64407564		GPRC5D	DuoBody	Janssen	MM	Fase I (NCT03399799)
	AMG111		CEA	BiTE	Amgen	GIST	Fase I (NCT01284231)
	RG7802		CEA	CrossMAb	Roche	Tumores Sólidos	Fase I (NCT02650713)
	Solitomab		EpCAM	BiTE	Amgen	Ascitis malignas	Fase I (NCT00635596)
	Catumaxomab		EpCAM	Triomab	Trion	Ascitis malignas	**Aprobado**
	Pasotuxizumab		PSMA	BiTE	Bayer	CaP	Fase I (NCT02806973)
	HPN-424		PSMA	DART	Harpoon	CaP	Fase I/II (NCT03577028)
	AMG160		PSMA	HLE-BiTE	Amgen	CaP	Fase I (NCT03792841)
	MOR209		PSMA	ADAPTIR	Aptevo Therapeutics	CaP	Fase I (NCT02262910)
	BAY2010112		PSMA	BiTE	Bayer	CaP	Fase I (NCT01723475)
	Ertumaxomab		HER2	Triomab	Trion	Cáncer de mama	Fase II (NCT00351858)
	GBR1302		HER2	BEAT	Glenmark Pharmaceuticals	Tumores Sólidos	Fase I (NCT02829372)
	M802		HER2	YBODY	YZYBio	Tumores Sólidos	Fase I (NCT04501770)
	RG6194		HER2	No disponible	Genentech	Tumores Sólidos	Fase I (NCT03448042)
	PF06671008		P-cadherin	DART/KIH	MacroGenics	Tumores Sólidos	Fase I (NCT02659631)
	MGD007		gpA33	DART	MacroGenics	CCR	Fase I/II (NCT03531632)
	MGD009		B7H3	DART/KIH	MacroGenics	Tumores Sólidos	Fase I (NCT02628535)
	AMG757		DLL3	HLE-BiTE	Amgen	CPCP	Fase I (NCT03319940)
	REGN4018		MUC16	No disponible	Regeneron	Tumores Sólidos	Fase I (NCT03564340)
	AMG596		EGFRvIII	BiTE	Amgen	Glioblastoma	Fase I (NCT03296696)
	ERY974		GPC3	ART-Ig	Chugai	CG/CEE	Fase I (NCT02748837)
	Tidutamab		SSTR2	Xmab	Xencor	Tumores Sólidos	Fase I (NCT03411915)
	huGD2-BsAb		GD2	No disponible	Y-mAbs	Neuroblastoma	Fase I/II (NCT03860207)
	MGD014		HIV-1 Env	DART/KIH	Macrogenics	VIH-1	Fase I (NCT03570918)
	AFM13	CD16	CD30	TandAbs	Affimed	LH	Fase II (NCT04101331)
	GTB-3550		CD33	TriKE	GT Biopharma	Neoplasias Hematológicas	Fase I/II (NCT03214666)
	TG-1801	CD47	CD19	κλ body	TG Therapeutics	Linfoma de célula B	Fase I (NCT03804996)
Bloqueo de puntos de control del sistema inmune	XmAb23104	PD1	ICOS	Xmab	Xencor	Tumores Sólidos	Fase I (NCT03752398)
	AK104		CTLA4	ITab	Akesobio AU	CG	Fase II (NCT04380805)
	MGD019		CTLA4	DART	Macrogenics	Tumores Sólidos	Fase I (NCT03761017)
	XmAb20717		CTLA4	Xmab	Xencor	Tumores Sólidos	Fase I (NCT03517488)
	MEDI5752		CTLA4	DuetMab/ KIH	AstraZeneca	Tumores Sólidos	Fase I (NCT04522323)

Bloqueo de puntos de control del sistema inmune	MGD013		LAG3	DART	Macrogenics	Tumores Sólidos	Fase II/III (NCT04082364)
	RG7769		TIM3	CrossMab/ KIH	Roche	Tumores Sólidos	Fase I (NCT03708328)
	LY3434172		PDL1	KIH	Eli Lilly	Tumores Sólidos	Fase I (NCT03936959)
	FS118	PD-L1	LAG3	No disponible	F-Star	Tumores Sólidos	Fase I (NCT03440437)
	KN046		CTLA4	CRIB	Alphamab	Tumores Sólidos	Fase II (NCT04469725)
	LY3415244		TIM3	No disponible	Eli Lilly	Tumores Sólidos	Fase I (NCT03752177)
Bloqueo de factores inflamatorios	ATN103	HSA	TNF	Nanobody	Ablynx	AR	Fase II (NCT01063803)
	ALX0061		IL6R	Nanobody	Ablynx	AR	Fase II (NCT02518620)
	ALX0761		IL17A/F	Nanobody	Ablynx	Psoriasis	No disponible
	ALX0141		RANKL	Nanobody	Ablynx	Osteoporosis	No disponible
	SAR156597	IL-13	IL4	DVD-Ig	Sanofi	FPI	Fase II (NCT02921971)
	GSK2434735		IL4	DVD-Ig	GlaxoSmithKline	Asma	Fase II (NCT01563042)
	RG7990		IL17	No disponible	Genentech	Asma	Fase I (NCT02748642)
	AMG570	BAFF	ICOSL	No disponible	Amgen	AR	Fase II (NCT04058028)
	LY3090106		IL-17A	IgG4-(scFv)2	Eli Lilly		Fase I (NCT03736772)
	MEDI7352	NGF	TNF	scFv-Fc-Fab	Medimmune	OA	Fase II (NCT03755934)
Bloqueo de vías de señalización	ABT165	EGFR	DLL4	DVD-Ig	AbbVie	Tumores Sólidos	Fase II (NCT03368859)
	ABL-001		DLL4	IgG-scFv	ABL Bio	Tumores Sólidos	Fase I (NCT03292783)
	Navicixizumab		DLL4	No disponible	Celgene/Oncomed	Tumores Sólidos	Fase I (NCT03030287)
	RG7221		Ang-2	CrossMAb	Roche	CCR	Fase I (NCT01688206)
	BI 836880		ANG2	nanobody	Ablynx	CPNM	Fase I (NCT02689505)
	RO5520985		ANG2	CrossMab/ KIH	Roche	Tumores Sólidos	Fase I (NCT02715531)
	Amivantamab		c-MET	DuoBody	Janssen R&D	CPNM	**Aprobado**
	EMB01		c-MET	FIT-Ig	Epimab Biotherapeutics	Tumores Sólidos	Fase I (NCT03797391)
	MCLA-158		LGR5	Biclonics	Merus	CCR	Fase I (NCT03526835)
	MCLA-128	HER2	HER3	No disponible	Merus	Cáncer de mama	Fase II (NCT03321981)
	KN026		HER2	CRIB	Alphamab	Tumores Sólidos	Fase II (NCT04521179)
	MBS301		HER2	KIH	Beijing Mabworks Biotech	Tumores Sólidos	Fase I (NCT03842085)
	ZW25		HER2	Azymetric	Zymeworks	Tumores Sólidos	Fase II (NCT04513665)
	MP0274		HER2	No disponible	Molecular Partners AG	Tumores Sólidos	Fase I (NCT03084926)
	RG7386	FAP	DR5	CrossMAb	Roche	Tumores Sólidos	Fase I (NCT02558140)
	MGD010	CD32B	CD79B	DART	MacroGenics	Enfermedades autoinmunes	Fase I (NCT02376036)

Bloqueo de vías de señalización	RG7992	FGFR1	KLB	KIH	Genentech	Diabetes tipo II	Fase II (NCT04171765)
	MEDI3902	PsI	Pcrv	scFv-Fc-Fab	Medimmune	Neumonía	Fase II (NCT02696902)
	BI1034020	Aβ40	Aβ42	nanobody	Boehringer ingelheim	Alzheimer	Fase I (NCT01958060)
	Emicizumab	FIXa	FX	ART-Ig	Roche	Hemofilia A	**Aprobado**

Abreviaturas: AR, *Artritis Reumatoide;* CEE*, Carcinoma Escamoso del Esófago;* CaP, *Cáncer de Próstata;* CCR*, Cáncer Colorrectal;* CG, *Cáncer Gástrico;* CPCP*, Cáncer de Pulmón de Célula Pequeña;* CPNM, *Carcinoma Pulmonar no Microcítico;* FPI, *Fibrosis Pulmonar Idiopática;* GIST, *Tumores del Estroma Gastrointestinal;* LH*, Linfoma Hodgkin;* LLA, *Leucemia Linfoblástica Aguda;* LMA*, Leucemia Mieloide Aguda;* LMC*, Leucemia Mieloide Crónica;* LNH, *Linfoma No Hodgkin;* MM*, Mieloma Múltiple;* OA, *Osteoartritis;* VIH-1, *Virus de la Inmunodeficiencia Humana-1.* Abreviaturas del inglés: ART-Ig, *Bispecific Antibody manufacturing technology;* BEAT, *Bispecific Engagement by Antibodies based on T cell receptor;* CRIB*, Charge Repulsion Induced Bispecific;* DVD-Ig, CrossMab, *IgG-like bispecific antibody;* DART, *Dual Affinity Retargeting*; *Dual Variable Domain Immunoglobulin;* FIT-Ig, *Fabs-In-Tandem Immunoglobulin;* HLE-BiTE, *Half-Life Extended BiTE*; ITab, *Immune-Therapy antibody;* κλ body, *Non-engineered, Ig-like bispecific antibodies;* KIH, *Knobs-In-Holes bispecific antibody*; TandAb, *Tandem Diabody*; TriKE, *Trispecific Killer Engager;* TrioMab, *family of Trifunctional Bispecific Antibodies;* scDb, *bispecific single chain Diabody;* SCLC*, Small-Cell Lung Cancer*. Figura modificada de (46).

El trabajo desarrollado durante esta Tesis Doctoral ha generado una serie de resultados que han sido recogidos en dos artículos científicos y una revisión. Además, como resultado de colaboraciones con otros grupos de investigación, también se han publicado varios artículos no relacionados directamente con esta Tesis Doctoral.

ARTÍCULOS DIRECTAMENTE RELACIONADOS CON LA TESIS DOCTORAL

1. Blanco B[#], **Ramírez-Fernández Á[#]**, Bueno C, Argemí-Muntadas L, Fuentes P, Aguilar-Sopeña Ó, Gutierrez-Agüera F, Zanetti SR, Tapia-Galisteo A, Díez-Alonso L, Segura-Tudela A, Castellà M, Marzal B, Betriu S, Harwood SL, Compte M, Lykkemark S, Erce-Llamazares A, Rubio-Pérez L, Jiménez-Reinoso A, Domínguez-Alonso C, Neves M, Morales P, Paz-Artal E, Guedan S, Sanz L, Toribio ML, Roda-Navarro P, Juan M, Menéndez P, Álvarez-Vallina L. Overcoming CAR-mediated CD19 downmodulation and leukemia relapse with T lymphocytes secreting anti-CD19 T cell engagers. *Cancer Immunology Research*. 10(4):498-511. DOI: 10.1158/2326-6066.CIR-21-0853.
2. **Ramírez-Fernández Á[#]**, Aguilar-Sopeña Ó[#], Díez-Alonso L, Segura-Tudela A, Domínguez-Alonso C, Roda-Navarro P, Álvarez-Vallina L, Blanco B. (2022). Synapse topology and downmodulation events determine the functional outcome of anti-CD19 T cell-redirecting strategies. *Oncoimmunology*. 11(1):2054106. DOI: 10.1080/2162402X.2022.2054106.
3. Blanco B, **Ramírez-Fernández Á**, Álvarez-Vallina L. (2020). Engineering Immune Cells for in vivo Secretion of Tumor-Specific T Cell-Redirecting Bispecific Antibodies. *Frontiers in Immunology*. 11:1792. DOI: 10.3389/fimmu.2020.01792.

ARTÍCULOS NO RELACIONADOS DIRECTAMENTE CON LA TESIS DOCTORAL

1. Compte M, Harwood SL, Erce-Llamazares A, Tapia-Galisteo A, Romero E, Ferrer I, Garrido-Martin EM, Enguita AB, Ochoa MC, Blanco B, Oteo M, Merino N, Nehme-Álvarez D, Hangiu O, Domínguez-Alonso C, Zonca M, **Ramírez-Fernández A**, Blanco FJ, Morcillo MA, Muñoz IG, Melero I, Rodriguez-Peralto JL, Paz-Ares L, Sanz L, Alvarez-Vallina L. (2021). An Fc-free EGFR-specific 4-1BB-agonistic Trimerbody Displays Broad Antitumor Activity in Humanized Murine Cancer Models without

Toxicity. *Clinical Cancer Research*. 27(11):3167-3177. DOI: 10.1158/1078-0432.CCR-20-4625.

2. Laguna-Goya R, Utrero-Rico A, Talayero P, Lasa-Lazaro M, **Ramírez-Fernández A**, Naranjo L, Segura-Tudela A, Cabrera-Marante O, Rodriguez de Frias E, Garcia-Garcia R, Fernández-Ruiz M, Aguado JM, Martinez-Lopez J, Lopez EA, Catalan M, Serrano A, Paz-Artal E. (2020). IL-6-based mortality risk model for hospitalized patients with COVID-19. *Journal of Allergy and Clinical Immunology*. 146(4):799-807.e9. DOI: 10.1016/j.jaci.2020.07.009.

frontiers in Immunology

REVIEW
published: 13 August 2020
doi: 10.3389/fimmu.2020.01792

Engineering Immune Cells for *in vivo* Secretion of Tumor-Specific T Cell-Redirecting Bispecific Antibodies

Belén Blanco[1,2], *Ángel Ramírez-Fernández*[1,2] *and Luis Alvarez-Vallina*[1,2]*

[1] Cancer Immunotherapy Unit (UNICA), Department of Immunology, Hospital Universitario 12 de Octubre, Madrid, Spain,
[2] Immuno-Oncology and Immunotherapy Group, Instituto de Investigación Sanitaria 12 de Octubre (imas12), Madrid, Spain

Immunotherapeutic approaches based on the redirection of T cell activity toward tumor cells are actively being investigated. The impressive clinical success of the continuously intravenously infused T cell-redirecting bispecific antibody (T-bsAb) blinatumomab (anti-CD19 x anti-CD3), and of engineered T cells expressing anti-CD19 chimeric antigen receptors (CAR-T cells) in hematological malignancies, has led to renewed interest in a novel cancer immunotherapy strategy that combines features of antibody- and cell-based therapies. This emerging approach is based on the endogenous secretion of T-bsAbs by engineered T cells (STAb-T cells). Adoptive transfer of genetically modified STAb-T cells has demonstrated potent anti-tumor activity in both solid tumor and hematologic preclinical xenograft models. We review here the potential benefits of the STAb-T strategy over similar approaches currently being used in clinic, and we discuss the potential combination of this promising strategy with the well-established CAR-T cell approach.

Keywords: cancer immunotherapy, T cell-redirection, bispecific antibodies, chimeric antigen receptors, *in situ* secretion

OPEN ACCESS

Edited by:
Axel Schambach,
Hannover Medical School, Germany

Reviewed by:
Christoph Rader,
The Scripps Research Institute, United States
Michael Heuser,
Hannover Medical School, Germany
Elizabeth A. Griffiths,
University at Buffalo, United States

***Correspondence:**
Luis Alvarez-Vallina
lav.imas12@h12o.es

Specialty section:
This article was submitted to Cancer Immunity and Immunotherapy, a section of the journal Frontiers in Immunology

Received: *17 May 2020*
Accepted: *06 July 2020*
Published: *13 August 2020*

Citation:
Blanco B, Ramírez-Fernández Á and Alvarez-Vallina L (2020) Engineering Immune Cells for in vivo Secretion of Tumor-Specific T Cell-Redirecting Bispecific Antibodies. Front. Immunol. 11:1792. doi: 10.3389/fimmu.2020.01792

INTRODUCTION

The immune system plays an important role in shaping the immunogenicity of tumors (1). The T cell receptor (TCR)-mediated recognition of processed tumor-associated antigens (TAAs) drives the elimination or sculpting of developing cancer cells, which can generate immune-resistant cell variants (1, 2). Due to this selective immune pressure, these variant cells display a multitude of evasion mechanisms from immune recognition and destruction, such as abnormalities in the antigen presentation machinery (2), and the generation of an immunosuppressive environment that promotes tumor growth (3). In the past few decades extensive research has been made to develop cancer immunotherapy approaches aimed at stimulating anti-tumor T cell responses (4, 5). Most notably the emergence of immune checkpoint inhibitors blocking negative regulators of T cell immunity (6), the systemic administration of bispecific antibodies (bsAbs) (7), and the adoptive transfer of genetically engineered T cells expressing chimeric antigen receptors (CARs) (8). However, only a limited proportion of patients benefit from these strategies. Therefore, intense efforts are being made to improve the currently available immunotherapies and to design new strategies to strengthen anti-tumor immune responses.

CURRENT T CELL-REDIRECTING STRATEGIES

T cell-redirecting immunotherapies are intended to specifically eliminate tumor cells by physically joining lymphocytes and cancer cells using tumor-targeted cell-cell bridging (CCB) molecules (9). CCBs can be generated using engineering approaches to manipulate the membrane of immune cells (cell surface engineering), to create artificial soluble molecules (antibody engineering) or a combination thereof (4, 5). In fact, some of these CCB-based strategies, such as membrane-anchored CARs or soluble T cell-redirecting bsAbs (T-bsAbs), are revolutionizing the treatment of B cell malignancies (10).

CAR-Engineered T (CAR-T) Cells

CARs are synthetic receptors consisting of three domains: an antigen-binding ectodomain, the transmembrane domain, and the signaling endodomain (5). The ectodomain is usually a single-chain fragment variable (scFv) antibody, that allows the synthetic receptor to specifically recognize a user-defined cell surface TAA in an major histocompatibility complex (MHC)-independent manner, and is tethered to the transmembrane domain through the spacer or hinge region (8) (**Figure 1**). The third component is the endodomain, most often the CD3ζ intracellular signaling domain linked to one or more co-stimulatory domains (5, 11). First-generation CARs contain solely the intracellular signaling region of CD3ζ (12). Second-generation CARs generated by adding a co-stimulatory domain (from CD28 or CD137) in tandem with the CD3ζ chain (13) have been a major advance in CAR-T cell therapy because co-stimulation is a necessary component of physiological T cell activation, thereby improving proliferation, survival, cytokine secretion and cytotoxicity. Third-generation CARs further expanded on the second-generation by adding an additional co-stimulatory domain (14, 15).

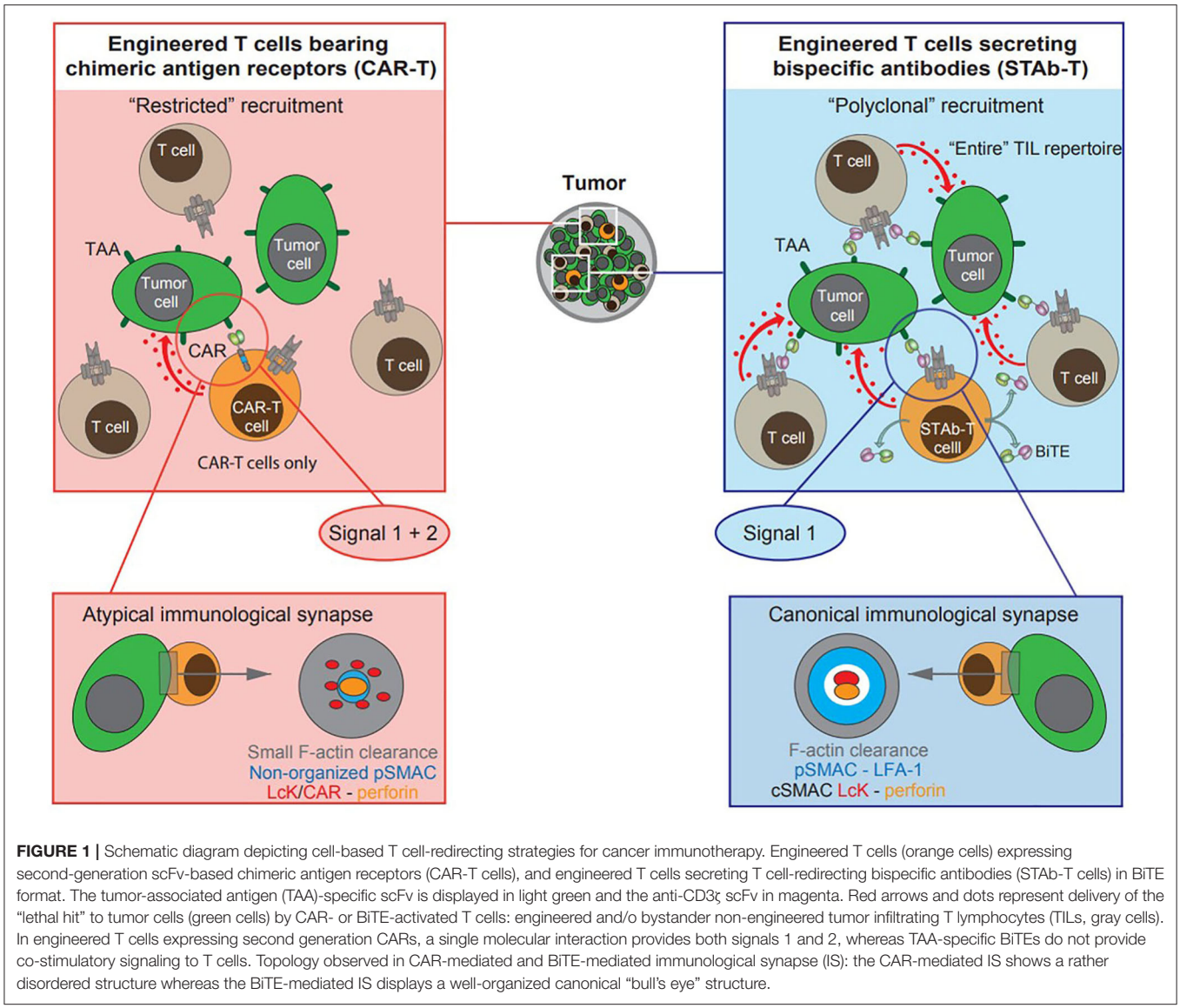

FIGURE 1 | Schematic diagram depicting cell-based T cell-redirecting strategies for cancer immunotherapy. Engineered T cells (orange cells) expressing second-generation scFv-based chimeric antigen receptors (CAR-T cells), and engineered T cells secreting T cell-redirecting bispecific antibodies (STAb-T cells) in BiTE format. The tumor-associated antigen (TAA)-specific scFv is displayed in light green and the anti-CD3ζ scFv in magenta. Red arrows and dots represent delivery of the "lethal hit" to tumor cells (green cells) by CAR- or BiTE-activated T cells: engineered and/o bystander non-engineered tumor infiltrating T lymphocytes (TILs, gray cells). In engineered T cells expressing second generation CARs, a single molecular interaction provides both signals 1 and 2, whereas TAA-specific BiTEs do not provide co-stimulatory signaling to T cells. Topology observed in CAR-mediated and BiTE-mediated immunological synapse (IS): the CAR-mediated IS shows a rather disordered structure whereas the BiTE-mediated IS displays a well-organized canonical "bull's eye" structure.

TABLE 1 | Pros and cons of current T cell-redirecting strategies.

	Adoptive cell therapies		Protein-based therapies
	CAR-T cells	STAb-T cells	Systemic administration T-bsAbs
Active trafficking to tumor sites	✓	✓	×
Co-stimulatory signal/s	✓	×[a]/✓[b]	×
Long lifespan	✓	✓	×[c]/✓[d]
"Off-the-shelf" therapy	×[e]/✓[f]	×[g]/✓[h]	✓
Polyclonal recruitment of T cells	×	✓	✓
Canonical immunological synapse	×	✓	✓

[a]*Monocystronic approach.*
[b]*Bicystronic approach.*
[c]*Bolus therapy with small Fc-less T-bsAbs (e.g., BiTE).*
[d]*Continuous intravenous infusion (CIV)/Half-extension technologies or Fc-engineered Ig "silent" T-bsAbs.*
[e]*Autologous CAR-T cells.*
[f]*"Universal" CAR-T cells.*
[g]*On-tumor strategy.*
[h]*Off-tumor strategy/"Universal" STAb-T cells.*

This structure endows CAR-T cells with several valuable attributes for a T cell-redirecting strategy. As CARs are not MHC-restricted, they can be used to treat patients without regard to MHC haplotypes, and circumvent MHC down-regulation, one of the most important mechanisms of immune evasion (11). In addition, CARs provide both activating and co-stimulatory signals which are required to achieve full T cell activation (**Figure 1** and **Table 1**) (16). The success of anti-CD19 CAR-T cells in clinical trials prompted the approval of two second generation CAR-T cells products, tisagenlecleucel (2017) and axicabtagene ciloleucel (2018), by the US FDA for the treatment of pediatric and young adult patients with relapsed or refractory B cell acute lymphoblastic leukemia (B-ALL) (17) and adult patients with relapsed or refractory large B cell lymphomas (18), respectively.

Nevertheless, the use of CAR-T cells presents some limitations (19), mainly severe toxicities related to a massive release of pro-inflammatory cytokines (cytokine release syndrome, CRS) and neurotoxicity (20). In addition, the majority of TAAs are also expressed on normal tissues, leading to on-target/off-tumor toxicity (19, 21). Solid tumors present additional challenges, due to the highly immunosuppressive tumor environment. Additionally, 30–60% of patients that achieve complete response, relapse after anti-CD19 CAR-T cell therapy (22).

Bispecific Antibodies

BsAbs are artificial molecules recognizing two different epitopes either on the same or on different antigens, and by simultaneously recognizing a cell surface TAA and an activating receptor on the T cell surface (CD3e), are able to activate and redirect T effector cells to kill cancer cells in a MHC-independent manner (5, 23). In recent years a considerable number of new bsAb formats have been designed, many of which are small-sized Fc-less molecules, built by connecting scFv and/or single-variable domain/heavy chain-only (V_{HH}) antibodies (23, 24). These antibodies are specifically designed to promote an efficient T cell/tumor cell synapse formation, and avoiding Fc-induced off-target toxicities (24). Among them, diabodies consist of two polypeptidic chains containing counterpaired V_H and V_L domains, connected by a short linker that prevents intramolecular pairings, resulting in the formation of dimeric molecules (55 kDa) (25). Tandem scFvs (ta-scFvs), consist of two scFvs connected by a flexible linker on a single polypeptide chain (57 kDa) (26). Those bispecific ta-scFv antibodies recognizing a tumor cell surface TAA and CD3e on T cells are so-called **bi**specific **T** cell-**e**ngagers (BiTEs) (26). The bispecific **li**ght **T**-cell **e**ngager (LiTE), consisting of a TAA-specific V_{HH} antibody fused to an anti-CD3scFv, is a recent evolution of this concept (27). The smaller size (43 kDa) and quicker diffusion of LiTE antibodies could allow them to reach tumor areas, which are inaccessible for larger bsAbs (27).

More than 30 T cell-redirecting bsAbs (T-bsAbs) have entered clinical development (28), but only one is presently in clinical use: blinatumomab, an anti-CD19 BiTE, for the treatment of relapsed/refractory B-ALL (29) and minimal residual disease-positive B-ALL (30). Despite the impressive responses observed with blinatumomab (31, 32), significant challenges still hamper the clinical application of BiTEs and similar bsAb formats. Off-target toxicities (mainly CRS and neurotoxicity), due to the expression of the targeted TAA on non-tumor cells, is a major concern for patients treated with systemically administered BiTEs (33). In addition, the short serum half-life of small-sized T-bsAbs requires continuous intravenous administration at a constant flow rate using infusion pumps (34). Another concern regarding the use of T-bsAbs is the lack of co-stimulatory signaling capacity. However, the ability of BiTEs to induce potent T cell cytotoxicity in the absence of co-stimulation has been well-documented (35). Although the reasons for this "co-stimulation independence" are not clear, it may result from the ability of Fc-less T-bsAbs to induce the formation of conventional mature immunological synapses (ISs) between T cells and tumor cells (36, 37).

NEXT-GENERATION T CELL-REDIRECTING STRATEGIES

As previously described, both CAR-T cells and systemically infused T-bsAbs have shown encouraging clinical responses but still must overcome important hurdles. In an attempt to combine the strengths of both therapies a novel strategy based on the endogenous **s**ecretion of **T**-bs**Ab**s (STAb) is being developed. We have previously classified STAb strategies as "*on-tumor*" and "*off-tumor*" depending on whether the T-bsAbs are secreted in the tumoral or peritumoral environment or from tumor-distant locations, respectively (10). The *in vivo* production of small-sized T-bsAbs by genetically modified T cells could result in effective and persistent concentrations of antibodies, compensating for their short-serum half-life (10). Moreover, this approach might

circumvent problems of tumor penetration and systemic toxicity, due to tumor trafficking of adoptively transferred T cells and subsequent intratumoral secretion of T-bsAbs (**Table 1**) (10). In addition, *in vivo* secretion avoids potential concerns regarding the formulation and long-term storage of bsAb therapeutics, preventing aggregation and deterioration (10, 38). Finally, in the STAb-T strategy, and in contrast with CAR-T therapy, T cell recruitment is not restricted to engineered T cells, as T-bsAbs secreted in the tumor may redirect bystander non-engineered infiltrating T cells to tumor cells, leading to a significant boost in anti-tumor T cell responses (**Figure 1** and **Table 1**) (4).

The STAb concept is now attracting attention but is not new. In 2003, a study demonstrated that human cells could be engineered to secrete a functionally active anti-CEA x anti-CD3 diabody, with ability to redirect T cell-mediated cytotoxicity against CEA-expressing tumor cells *in vitro*, and recruit bystander T cells *in vivo* to delay tumor growth (39). Moreover, anti-CEA x anti-CD3 diabody-secreting primary T cells were generated by lentiviral transduction and such STAb-T cells significantly reduced *in vivo* tumor growth in human colon cancer xenografts (40). More recently, the ability of an anti-EphA2 BiTE secreted by retrovirally transduced primary T cells demonstrated the ability of STAb-T cells to redirect the cytotoxic activity of non-transduced T cells specifically to $EphA2^+$ cancer cells *in vitro* and showed potent anti-tumor activity *in vivo* (41). Likewise, systemic infusion of retrovirally transduced T cells secreting an anti-CD19 BiTE induced tumor regression of leukemia and lymphoma in preclinical models (42). Another study reported that STAb-T cells secreting an anti-CD123 BiTE redirected bystander T cell cytotoxicity against $CD123^+$ acute myelod leukemia (AML) cells and induced regression of AML in xenograft models (43). Interestingly, efficient STAb-T cells have been generated not only using viral vectors, but also by RNA-transfection. In this regard, anti-CD19 STAb-T cells generated by electroporation of a messenger RNA encoding an anti-CD19 BiTE showed superior anti-tumor activities compared with RNA anti-CD19 CAR-T cells, achieving complete remission in a leukemia mouse model (44). It has been demonstrated that *in situ* secreted anti-CD19 BiTEs are loaded onto the T cell surface (42, 44). Therefore, it is tempting to speculate that the "arming of the CD3 complex" by *in vivo* secreted BiTEs in the peritumoral environment, could provide a significant therapeutic advantage over systemically administered BiTEs (e.g., blinatumomab).

Other cell types, such as mesenchymal stem cells (MSCs), and endothelial cells are suitable candidates to be engineered for "off-tumor" STAb strategies, based on the endogenous secretion of T-bsAbs from tumor-distant sites (45–47). The feasibility of *in vivo* secretion of T-bsAbs after systemic or local delivery of several types of nucleic acids or viruses has also been demonstrated (10, 48). Systemic administration of engineered mRNA (49) or minicircle DNA encoding T-bsAbs (50) induced sustained antibody secretion in mice and elimination of established human carcinoma xenografts. In another study, a single intramuscular injection of plasmid DNA induced secretion of functional T-bsAbs for 4 months and delayed cancer progression in mice (51). In addition, several types of oncolytic viruses have been armed with expression cassettes encoding T-bsAbs, to combine both direct oncolysis and T cell-mediated killing (52–55).

Nevertheless, T cells represent ideal vehicles for STAb therapy due to their capacity to migrate to tumor sites and their ability to act simultaneously as antibody factories and effectors (10). In addition, T-bsAb-mediated activation has been shown to induce an increase in transgene expression (41), which may favor the secretion of the T-bsAbs primarily at the tumor site and, consequently, reducing systemic toxicity.

OPEN QUESTIONS AND FUTURE PROSPECTS

Co-stimulatory and Co-inhibitory Receptors

Although only extensive research and clinical trials will determine the ultimate therapeutic potential of next-generation T cell-redirecting strategies, the STAb strategy may have important conceptual advantages over the CAR strategy (10), such as the polyclonal recruitment of the entire pool of tumor infiltrating T cells, and the reduction of systemic on-target/off-tumor toxicity due to the local secretion of the T-bsAbs (**Figure 1** and **Table 1**) (4, 5). In fact, Liu et al. have shown greater anti-leukemia activities of anti-CD19 BiTE-RNA electroporated T cells, compared to anti-CD19 CAR RNA-electroporated T cells in a Nalm6 tumor model (44). The authors highlighted the potential of anti-CD19 STAb-T cells to cure $CD19^+$ neoplasia with controlled toxicities (44). By contrast, Choi et al. have reported differences between CAR-T and STAb-T cells in terms of persistence and exhaustion, supporting the notion that CAR-T cells might be superior (56). In the experimental system used, T cell activation mediated by a locally secreted anti-EGFR BiTE resulted in a progeny of phenotypically exhausted cells, with reduced proliferative capacity and persistence, compared to anti-EGFRvIII CAR-activated T cells (56). The authors suggest that these differences may be attributable to the 4-1BB co-stimulatory domain used in the CAR construct (56), although the influence of other factors, such as the different TAA targeted, their cell density, as well as the location of the epitope recognized by both anti-EGFR and anti-EGFRvIII scFvs has not been considered. The positive effects of 4-1BB-mediated co-stimulation on reducing T cell exhaustion have also been demonstrated on engineered T cells expressing a second-generation anti-CD19 CAR (BBζ) (57).

STAb-T cells have demonstrated significant anti-tumor activity in different preclinical models, without additional co-stimulation (40–42, 44, 58). However, the provision of co-stimulatory signals may be instrumental to enhance anti-tumor efficacy especially in the context of solid tumors. In fact, we have demonstrated that simultaneous secretion of an anti-CEA x anti-CD3 diabody and a tumor-specific co-stimulatory ligand comprising the extracellular portion of CD80 fused to an anti-CEA antibody (59) increased anti-tumor activity in human colon carcinoma xenografts (4). Recent studies have shown that the expression of 4-1BB and CD80 ligands on the surface of engineered T cells secreting and anti-CD19 BiTE significantly increased the antileukemia activity *in vivo* (60). Collectively, these studies showed that STAb-T cells could be easily equipped

with physiological or tumor-specific co-stimulation systems using cell surface or antibody engineering strategies.

On the other hand, blockade of the PD-1/PD-L1 interaction can induce durable anti-tumor responses in a wide range of solid and hematological tumors (61). Several blocking antibodies against PD-1/PD-L1 have been approved for clinical use in humans (6), and preclinical studies have demonstrated that combining PD-1/PD-L1 axis blockade with CAR-T cells or systemically administered T-bsAb can improve anti-tumor activity (62–64). Importantly, several studies have demonstrated the therapeutic potential of engineered CAR-T cells secreting either anti-PD-1 or anti-PD-L1 blocking antibodies, and are currently being evaluated in clinical trials (65). In addition, CAR-T cells that express PD-1 dominant-negative receptors (66) or chimeric PD-1:CD28 switch-receptors (67) have been reported to increase anti-tumor effects and reduce susceptibility to tumor-induced T cell dysfunction. Finally, the rapid advancements in precision genome editing techniques, such as CRISPR-Cas9 system, has enabled to disrupt PD-1 function in CAR-T cells/T cells for cancer therapy (68, 69). All these "protective strategies" could also be easily implemented in a STAb-T cell context to improve their therapeutic potential.

Tumor Antigen Escape

Another relevant issue in a tumor-specific T cell-redirecting context is the loss of the targeted TAA. Here, it is important to highlight that among relapsing patients treated with anti-CD19 CAR-T cells, 10–20% are CD19-negative (22), while CD19 loss is infrequent following blinatumomab therapy (7). Several mechanisms have been proposed to explain antigen loss, such as accumulation of genetic and epigenetic mutations during tumor progression and selection of antigen-negative variants due to immune pressure (22). Interestingly, trogocytosis, a process whereby lymphocytes capture fragments of the plasma membrane from antigen-presenting cells and express them on their own surface (70), has been reported to occur following CAR-T cell interaction with CD19 (71). Trogocytosis leads to reversible antigen loss that reduces both TAA density on tumor cells and CAR expression on the T cell surface, presumably as a consequence of CAR internalization. Moreover, the transfer of CD19 protein from leukemia cells to T cells promotes fratricidal T cell killing and T cell exhaustion (71). Trogocytic target acquisition seems to be a general feature of CAR-T cells, as this phenomenon has been observed with CARs targeting different antigens (71). Regarding BiTE-stimulated T cells, trogocytic mechanisms have not been reported so far, although additional studies are needed to further clarify this issue.

Immunological Synapse

An important unresolved issue refers to structure of the IS formed by the CCB molecules in T cell redirecting strategies (**Figure 1**) (36). Although CAR-T cell stimulation induces an efficient microtubule organizing center and lytic granule secretion, even faster than in the canonical TCR-initiated IS, the actin cytoskeleton is not completely depleted from the center of the synapse, that exhibited a disorganized multifocal signaling cluster structure, with major differences relative to the typical TCR-initiated IS (36, 72–74). Unlike CARs, small-sized T-bsAbs are able to induce the formation of a canonical "bull's eye" IS between T lymphocytes and tumor cells (35). Indeed, BiTE-initiated IS has been found to be identical in structure and molecular composition to TCR-induced IS (37). Further studies are needed to more precisely define the impact of the topology of the IS on the functional capacity and cytotoxic potential of CAR-T and STAb-T cells (36).

Development of Off-the-Shelf Universal Adoptive Cell Therapies

The use of allogeneic cells from healthy donors has significant advantages over autologous approaches, such as the immediate availability of cryopreserved batches and reduced cost. We have demonstrated that engineered MSCs might be incorporated into biocompatible scaffolds to secrete T-bsAbs that can act distantly at the tumor site, and can be retrieved a after a given period of time when the intended therapeutic effect has been achieved (45). Therefore, off-the-shelf stocks of gene-modified human allogeneic STAb MSCs might be easily generated and microencapsulated and implanted subcutaneously according to clinical need (75). The development of universal allogeneic CAR-T cells is an active area of research, and different strategies are being investigated to reduce the risk of graft-vs.-host disease and make cells less visible to the host immune system (76). Similar approaches could easily be implemented to the generation of universal STAb-T cells.

FINAL CONSIDERATIONS

STAb-T cell-based strategies have demonstrated encouraging anti-tumor effects in preclinical models, but their safety needs to be further explored in controlled clinical trials. Nevertheless, the administration of CAR-T or STAb-T therapies may not necessarily be mutually exclusive and both approaches might be used sequentially or simultaneously (56). Moreover, the use of CAR-T cells and STAb-T cells targeting different TAA could be relevant to overcome antigen loss, in a fashion similar to dual-antigen CAR-T cell targeting strategies (77–80). Such a strategy might consist of the simultaneous administration of CAR and STAb-T cells or the generation of a single cell product expressing both CCBs.

AUTHOR CONTRIBUTIONS

BB and LA-V contributed to the conception and design of this review. BB and ÁR-F wrote the first draft of the manuscript. All authors contributed to manuscript revision, read and approved the submitted version.

FUNDING

LA-V was supported by grants from the Spanish Ministry of Economy and Competitiveness (SAF2017-89437-P and RTC-2017-5944-1), the CRIS Cancer Foundation (FCRIS-IFI-2018), and the Spanish Association Against Cancer (AECC, 19084).

REFERENCES

1. Schreiber RD, Old LJ, Smyth MJ. Cancer immunoediting: integrating immunity's roles in cancer suppression and promotion. *Science.* (2011) 331:1565–70. doi: 10.1126/science.1203486
2. Khong HT, Restifo NP. Natural selection of tumor variants in the generation of "tumor escape" phenotypes. *Nat Immunol.* (2002) 3:999–1005. doi: 10.1038/ni1102-999
3. Rabinovich GA, Gabrilovich D, Sotomayor EM. Immunosuppressive strategies that are mediated by tumor cells. *Annu Rev Immunol.* (2007) 25:267–96. doi: 10.1146/annurev.immunol.25.022106.141609
4. Alvarez-Vallina L. Genetic approaches for antigen-selective cell therapy. *Curr Gene Ther.* (2001) 1:385–97. doi: 10.2174/1566523013348418
5. Sanz L, Blanco B, Alvarez-Vallina L. Antibodies and gene therapy: teaching old 'magic bullets' new tricks. *Trends Immunol.* (2004) 25:85–91. doi: 10.1016/j.it.2003.12.001
6. Ribas A, Wolchok JD. Cancer immunotherapy using checkpoint blockade. *Science.* (2018) 359:1350–5. doi: 10.1126/science.aar4060
7. Viardot A, Bargou R. Bispecific antibodies in haematological malignancies. *Cancer Treat Rev.* (2018) 65:87–95. doi: 10.1016/j.ctrv.2018.04.002
8. June CH, O'Connor RS, Kawalekar OU, Ghassemi S, Milone MC. CAR T cell immunotherapy for human cancer. *Science.* (2018) 359:1361–5. doi: 10.1126/science.aar6711
9. Swartz MA, Hirosue S, Hubbell JA. Engineering approaches to immunotherapy. *Sci Transl Med.* (2012) 4:148rv9. doi: 10.1126/scitranslmed.3003763
10. Blanco B, Compte M, Lykkemark S, Sanz L, Alvarez-Vallina L. T cell-redirecting strategies to 'STAb' tumors: beyond CARs and bispecific antibodies. *Trends Immunol.* (2019) 40:243–57. doi: 10.1016/j.it.2019.01.008
11. Barrett DM, Singh N, Porter DL, Grupp SA, June CH. Chimeric antigen receptor therapy for cancer. *Annu Rev Med.* (2014) 65:333–47. doi: 10.1146/annurev-med-060512-150254
12. Gross G, Waks T, Eshhar Z. Expression of immunoglobulin-T-cell receptor chimeric molecules as functional receptors with antibody-type specificity. *Proc Natl Acad Sci U S A.* (1989) 86:10024–8. doi: 10.1073/pnas.86.24.10024
13. Finney HM, Lawson AD, Bebbington CR, Weir AN. Chimeric receptors providing both primary and costimulatory signaling in T cells from a single gene product. *J Immunol.* (1998) 161:2791–7.
14. Carpenito C, Milone MC, Hassan R, Simonet JC, Lakhal M, Suhoski MM, et al. Control of large, established tumor xenografts with genetically retargeted human T cells containing CD28 and CD137 domains. *Proc Natl Acad Sci U S A.* (2009) 106:3360–5. doi: 10.1073/pnas.0813101106
15. Milone MC, Fish JD, Carpenito C, Carroll RG, Binder GK, Teachey D, et al. Chimeric receptors containing CD137 signal transduction domains mediate enhanced survival of T cells and increased antileukemic efficacy *in vivo*. *Mol Ther.* (2009) 17:1453–64. doi: 10.1038/mt.2009.83
16. Weinkove R, George P, Dasyam N, McLellan AD. Selecting costimulatory domains for chimeric antigen receptors: functional and clinical considerations. *Clin Transl Immunology.* (2019) 8:e1049. doi: 10.1002/cti2.1049
17. Maude SL, Laetsch TW, Buechner J, Rives S, Boyer M, Bittencourt H, et al. Tisagenlecleucel in children and young adults with B-cell lymphoblastic leukemia. *N Engl J Med.* (2018) 378:439–48. doi: 10.1056/NEJMoa1709866
18. Neelapu SS, Locke FL, Bartlett NL, Lekakis LJ, Miklos DB, Jacobson CA, et al. Axicabtagene ciloleucel CAR T-cell therapy in refractory large B-cell lymphoma. *N Engl J Med.* (2017) 377:2531–44. doi: 10.1056/NEJMoa1707447
19. Alonso-Camino V, Harwood SL, Alvarez-Mendez A, Alvarez-Vallina L. Efficacy and toxicity management of CAR-T-cell immunotherapy: a matter of responsiveness control or tumour-specificity? *Biochem Soc Trans.* (2016) 44:406–11. doi: 10.1042/BST20150286
20. Brudno JN, Kochenderfer JN. Recent advances in CAR T-cell toxicity: mechanisms, manifestations and management. *Blood Rev.* (2019) 34:45–55. doi: 10.1016/j.blre.2018.11.002
21. Morgan RA, Yang JC, Kitano M, Dudley ME, Laurencot CM, Rosenberg SA. Case report of a serious adverse event following the administration of T cells transduced with a chimeric antigen receptor recognizing ERBB2. *Mol Ther.* (2010) 18:843–51. doi: 10.1038/mt.2010.24
22. Xu X, Sun Q, Liang X, Chen Z, Zhang X, Zhou X, et al. Mechanisms of relapse after CD19 CAR T-cell therapy for acute lymphoblastic leukemia and its prevention and treatment strategies. *Front Immunol.* (2019) 10:2664. doi: 10.3389/fimmu.2019.02664
23. Brinkmann U, Kontermann RE. The making of bispecific antibodies. *MAbs.* (2017) 9:182–212. doi: 10.1080/19420862.2016.1268307
24. Nunez-Prado N, Compte M, Harwood S, Alvarez-Mendez A, Lykkemark S, Sanz L, et al. The coming of age of engineered multivalent antibodies. *Drug Discov Today.* (2015) 20:588–94. doi: 10.1016/j.drudis.2015.02.013
25. Holliger P, Prospero T, Winter G. "Diabodies": small bivalent and bispecific antibody fragments. *Proc Natl Acad Sci U S A.* (1993) 90:6444–8. doi: 10.1073/pnas.90.14.6444
26. Mack M, Riethmuller G, Kufer P. A small bispecific antibody construct expressed as a functional single-chain molecule with high tumor cell cytotoxicity. *Proc Natl Acad Sci U S A.* (1995) 92:7021–5. doi: 10.1073/pnas.92.15.7021
27. Harwood SL, Alvarez-Cienfuegos A, Nunez-Prado N, Compte M, Hernandez-Perez S, Merino N, et al. ATTACK, a novel bispecific T cell-recruiting antibody with trivalent EGFR binding and monovalent CD3 binding for cancer immunotherapy. *Oncoimmunology.* (2017) 7:e1377874. doi: 10.1080/2162402X.2017.1377874
28. Labrijn AF, Janmaat ML, Reichert JM, Parren PWHI. Bispecific antibodies: a mechanistic review of the pipeline. *Nat Rev Drug Discov.* (2019) 18:585–608. doi: 10.1038/s41573-019-0028-1
29. Przepiorka D, Ko CW, Deisseroth A, Yancey CL, Candau-Chacon R, Chiu HJ, et al. FDA approval: blinatumomab. *Clin Cancer Res.* (2015) 21:4035–9. doi: 10.1158/1078-0432.CCR-15-0612
30. Blinatumomab Approval Expanded Based on MRD. *Cancer Discov.* (2018) 8:OF3. doi: 10.1158/2159-8290.CD-NB2018-059
31. Kantarjian H, Stein A, Gokbuget N, Fielding AK, Schuh AC, Ribera JM, et al. Blinatumomab versus chemotherapy for advanced acute lymphoblastic leukemia. *N Engl J Med.* (2017) 376:836–47. doi: 10.1056/NEJMoa1609783
32. Topp MS, Gokbuget N, Stein AS, Zugmaier G, O'Brien S, Bargou RC, et al. Safety and activity of blinatumomab for adult patients with relapsed or refractory B-precursor acute lymphoblastic leukaemia: a multicentre, single-arm, phase 2 study. *Lancet Oncol.* (2015) 16:57–66. doi: 10.1016/S1470-2045(14)71170-2
33. Jain T, Litzow MR. No free rides: management of toxicities of novel immunotherapies in ALL, including financial. *Blood Adv.* (2018) 2:3393–403. doi: 10.1182/bloodadvances.2018020198
34. Garber K. Bispecific antibodies rise again. *Nat Rev Drug Discov.* (2014) 13:799–801. doi: 10.1038/nrd4478
35. Huehls AM, Coupet TA, Sentman CL. Bispecific T-cell engagers for cancer immunotherapy. *Immunol Cell Biol.* (2015) 93:290–6. doi: 10.1038/icb.2014.93
36. Roda-Navarro P, Alvarez-Vallina L. Understanding the spatial topology of artificial immunological synapses assembled in T cell-redirecting strategies: a major issue in cancer immunotherapy. *Front Cell Dev Biol.* (2019) 7:370. doi: 10.3389/fcell.2019.00370
37. Offner S, Hofmeister R, Romaniuk A, Kufer P, Baeuerle PA. Induction of regular cytolytic T cell synapses by bispecific single-chain antibody constructs on MHC class I-negative tumor cells. *Mol Immunol.* (2006) 43:763–71. doi: 10.1016/j.molimm.2005.03.007
38. Sanchez-Martin D, Sanz L, Alvarez-Vallina L. Engineering human cells for *in vivo* secretion of antibody and non-antibody therapeutic proteins. *Curr Opin Biotechnol.* (2011) 22:924–30. doi: 10.1016/j.copbio.2011.03.001
39. Blanco B, Holliger P, Vile RG, Alvarez-Vallina L. Induction of human T lymphocyte cytotoxicity and inhibition of tumor growth by tumor-specific diabody-based molecules secreted from gene-modified bystander cells. *J Immunol.* (2003) 171:1070–7. doi: 10.4049/jimmunol.171.2.1070
40. Compte M, Blanco B, Serrano F, Cuesta AM, Sanz L, Bernad A, et al. Inhibition of tumor growth *in vivo* by *in situ* secretion of bispecific anti-CEA x anti-CD3 diabodies from lentivirally transduced human lymphocytes. *Cancer Gene Ther.* (2007) 14:380–8. doi: 10.1038/sj.cgt.7701021
41. Iwahori K, Kakarla S, Velasquez MP, Yu F, Yi Z, Gerken C, et al. Engager T cells: a new class of antigen-specific T cells that redirect bystander T cells. *Mol Ther.* (2015) 23:171–8. doi: 10.1038/mt.2014.156

42. Velasquez MP, Torres D, Iwahori K, Kakarla S, Arber C, Rodriguez-Cruz T, et al. T cells expressing CD19-specific engager molecules for the immunotherapy of CD19-positive malignancies. *Sci Rep.* (2016) 6:27130. doi: 10.1038/srep27130
43. Bonifant CL, Szoor A, Torres D, Joseph N, Velasquez MP, Iwahori K, et al. CD123-engager T cells as a novel immunotherapeutic for acute myeloid leukemia. *Mol Ther.* (2016) 24:1615–26. doi: 10.1038/mt.2016.116
44. Liu X, Barrett DM, Jiang S, Fang C, Kalos M, Grupp SA, et al. Improved anti-leukemia activities of adoptively transferred T cells expressing bispecific T-cell engager in mice. *Blood Cancer J.* (2016) 6:e430. doi: 10.1038/bcj.2016.38
45. Compte M, Cuesta AM, Sanchez-Martin D, Alonso-Camino V, Vicario JL, Sanz L, et al. Tumor immunotherapy using gene-modified human mesenchymal stem cells loaded into synthetic extracellular matrix scaffolds. *Stem Cells.* (2009) 27:753–60. doi: 10.1634/stemcells.2008-0831
46. Compte M, Alonso-Camino V, Santos-Valle P, Cuesta AM, Sanchez-Martin D, Lopez MR, et al. Factory neovessels: engineered human blood vessels secreting therapeutic proteins as a new drug delivery system. *Gene Ther.* (2010) 17:745–51. doi: 10.1038/gt.2010.33
47. Sanz L, Compte M, Guijarro-Munoz I, Alvarez-Vallina L. Non-hematopoietic stem cells as factories for *in vivo* therapeutic protein production. *Gene Ther.* (2012) 19:1–7. doi: 10.1038/gt.2011.68
48. Rader C. Bispecific antibodies in cancer immunotherapy. *Curr Opin Biotechnol.* (2019) 65:9–16. doi: 10.1016/j.copbio.2019.11.020
49. Stadler CR, Bahr-Mahmud H, Celik L, Hebich B, Roth AS, Roth RP, et al. Elimination of large tumors in mice by mRNA-encoded bispecific antibodies. *Nat Med.* (2017) 23:815–7. doi: 10.1038/nm.4356
50. Pang X, Ma F, Zhang P, Zhong Y, Zhang J, Wang T, et al. Treatment of human B-cell lymphomas using minicircle DNA vector expressing anti-CD3/CD20 in a mouse model. *Hum Gene Ther.* (2017) 28:216–25. doi: 10.1089/hum.2016.122
51. Perales-Puchalt A, Duperret EK, Yang X, Hernandez P, Wojtak K, Zhu X, et al. DNA-encoded bispecific T cell engagers and antibodies present long-term antitumor activity. *JCI Insight.* (2019) 4:e126086. doi: 10.1172/jci.insight.126086
52. Fajardo CA, Guedan S, Rojas LA, Moreno R, Arias-Badia M, de SJ, et al. Oncolytic adenoviral delivery of an EGFR-targeting T-cell engager improves antitumor efficacy. *Cancer Res.* (2017) 77:2052–63. doi: 10.1158/0008-5472.CAN-16-1708
53. Speck T, Heidbuechel JPW, Veinalde R, Jaeger D, von KC, Ball CR, et al. Targeted BiTE expression by an oncolytic vector augments therapeutic efficacy against solid tumors. *Clin Cancer Res.* (2018) 24:2128–37. doi: 10.1158/1078-0432.CCR-17-2651
54. Freedman JD, Duffy MR, Lei-Rossmann J, Muntzer A, Scott EM, Hagel J, et al. An oncolytic virus expressing a T-cell engager simultaneously targets cancer and immunosuppressive stromal cells. *Cancer Res.* (2018) 78:6852–65. doi: 10.1158/0008-5472.CAN-18-1750
55. de SJ, Fajardo CA, Moreno R, Ramos MD, Farrera-Sal M, Alemany R. Targeting the tumor stroma with an oncolytic adenovirus secreting a fibroblast activation protein-targeted bispecific T-cell engager. *J Immunother Cancer.* (2019) 7:19. doi: 10.1186/s40425-019-0505-4
56. Choi BD, Yu X, Castano AP, Bouffard AA, Schmidts A, Larson RC, et al. CAR-T cells secreting BiTEs circumvent antigen escape without detectable toxicity. *Nat Biotechnol.* (2019) 37:1049–58. doi: 10.1038/s41587-019-0192-1
57. Long AH, Haso WM, Shern JF, Wanhainen KM, Murgai M, Ingaramo M, et al. 4-1BB costimulation ameliorates T cell exhaustion induced by tonic signaling of chimeric antigen receptors. *Nat Med.* (2015) 21:581–90. doi: 10.1038/nm.3838
58. Molgaard K, Compte M, Nunez-Prado N, Harwood SL, Sanz L, Alvarez-Vallina L. Balanced secretion of anti-CEA x anti-CD3 diabody chains using the 2A self-cleaving peptide maximizes diabody assembly and tumor-specific cytotoxicity. *Gene Ther.* (2017) 24:208–14. doi: 10.1038/gt.2017.3
59. Blanco B, Holliger P, Alvarez-Vallina L. Autocrine costimulation: tumor-specific CD28-mediated costimulation of T cells by *in situ* production of a bifunctional B7-anti-CEA diabody fusion protein. *Cancer Gene Ther.* (2002) 9:275–81. doi: 10.1038/sj.cgt.7700438
60. Velasquez MP, Szoor A, Vaidya A, Thakkar A, Nguyen P, Wu MF, et al. CD28 and 41BB costimulation enhances the effector function of CD19-specific engager T cells. *Cancer Immunol Res.* (2017) 5:860–70. doi: 10.1158/2326-6066.CIR-17-0171
61. Armand P. Immune checkpoint blockade in hematologic malignancies. *Blood.* (2015) 125:3393–400. doi: 10.1182/blood-2015-02-567453
62. Cherkassky L, Morello A, Villena-Vargas J, Feng Y, Dimitrov DS, Jones DR, et al. Human CAR T cells with cell-intrinsic PD-1 checkpoint blockade resist tumor-mediated inhibition. *J Clin Invest.* (2016) 126:3130–44. doi: 10.1172/JCI83092
63. Rafiq S, Yeku OO, Jackson HJ, Purdon TJ, van Leeuwen DG, Drakes DJ, et al. Targeted delivery of a PD-1-blocking scFv by CAR-T cells enhances anti-tumor efficacy *in vivo*. *Nat Biotechnol.* (2018) 36:847–56. doi: 10.1038/nbt.4195
64. Chang CH, Wang Y, Li R, Rossi DL, Liu D, Rossi EA, et al. Combination therapy with bispecific antibodies and PD-1 blockade enhances the antitumor potency of T cells. *Cancer Res.* (2017) 77:5384–94. doi: 10.1158/0008-5472.CAN-16-3431
65. Yoon DH, Osborn MJ, Tolar J, Kim CJ. Incorporation of immune checkpoint blockade into chimeric antigen receptor T cells (CAR-Ts): combination or built-in CAR-T. *Int J Mol Sci.* (2018) 19:340. doi: 10.3390/ijms19020340
66. Chen N, Morello A, Tano Z, Adusumilli PS. CAR T-cell intrinsic PD-1 checkpoint blockade: A two-in-one approach for solid tumor immunotherapy. *Oncoimmunology.* (2017) 6:e1273302. doi: 10.1080/2162402X.2016.1273302
67. Liu X, Ranganathan R, Jiang S, Fang C, Sun J, Kim S, et al. A chimeric switch-receptor targeting PD1 augments the efficacy of second-generation CAR T cells in advanced solid tumors. *Cancer Res.* (2016) 76:1578–90. doi: 10.1158/0008-5472.CAN-15-2524
68. McGowan E, Lin Q, Ma G, Yin H, Chen S, Lin Y. PD-1 disrupted CAR-T cells in the treatment of solid tumors: promises and challenges. *Biomed Pharmacother.* (2020) 121:109625. doi: 10.1016/j.biopha.2019.109625
69. Stadtmauer EA, Fraietta JA, Davis MM, Cohen AD, Weber KL, Lancaster E, et al. CRISPR-engineered T cells in patients with refractory cancer. *Science.* (2020) 367:eaba7365. doi: 10.1126/science.aba7365
70. Joly E, Hudrisier D. What is trogocytosis and what is its purpose? *Nat Immunol.* (2003) 4:815. doi: 10.1038/ni0903-815
71. Hamieh M, Dobrin A, Cabriolu A, van der Stegen SJC, Giavridis T, Mansilla-Soto J, et al. CAR T cell trogocytosis and cooperative killing regulate tumour antigen escape. *Nature.* (2019) 568:112–6. doi: 10.1038/s41586-019-1054-1
72. Davenport AJ, Cross RS, Watson KA, Liao Y, Shi W, Prince HM, et al. Chimeric antigen receptor T cells form nonclassical and potent immune synapses driving rapid cytotoxicity. *Proc Natl Acad Sci U S A.* (2018) 115:E2068–76. doi: 10.1073/pnas.1716266115
73. Mukherjee M, Mace EM, Carisey AF, Ahmed N, Orange JS. Quantitative imaging approaches to study the CAR immunological synapse. *Mol Ther.* (2017) 25:1757–68. doi: 10.1016/j.ymthe.2017.06.003
74. Watanabe K, Kuramitsu S, Posey AD Jr, June CH. Expanding the therapeutic window for CAR T cell therapy in solid tumors: the knowns and unknowns of CAR T cell biology. *Front Immunol.* (2018) 9:2486. doi: 10.3389/fimmu.2018.02486
75. Saenz del BL, Compte M, Aceves M, Hernandez RM, Sanz L, Alvarez-Vallina L, et al. Microencapsulation of therapeutic bispecific antibodies producing cells: immunotherapeutic organoids for cancer management. *J Drug Target.* (2015) 23:170–9. doi: 10.3109/1061186X.2014.971327
76. Depil S, Duchateau P, Grupp SA, Mufti G, Poirot L. 'Off-the-shelf' allogeneic CAR T cells: development and challenges. *Nat Rev Drug Discov.* (2020) 19:185–99. doi: 10.1038/s41573-019-0051-2
77. Ruella M, Barrett DM, Kenderian SS, Shestova O, Hofmann TJ, Perazzelli J, et al. Dual CD19 and CD123 targeting prevents antigen-loss relapses after CD19-directed immunotherapies. *J Clin Invest.* (2016) 126:3814–26. doi: 10.1172/JCI87366

78. Hegde M, Corder A, Chow KK, Mukherjee M, Ashoori A, Kew Y, et al. Combinational targeting offsets antigen escape and enhances effector functions of adoptively transferred T cells in glioblastoma. *Mol Ther.* (2013) 21:2087–101. doi: 10.1038/mt.2013.185
79. Hegde M, Mukherjee M, Grada Z, Pignata A, Landi D, Navai SA, et al. Tandem CAR T cells targeting HER2 and IL13Ralpha2 mitigate tumor antigen escape. *J Clin Invest.* (2016) 126:3036–52. doi: 10.1172/JCI83416
80. Zah E, Lin MY, Silva-Benedict A, Jensen MC, Chen YY. T cells expressing CD19/CD20 bispecific chimeric antigen receptors prevent antigen escape by malignant B cells. *Cancer Immunol Res.* (2016) 4:498–508. doi: 10.1158/2326-6066.CIR-15-0231

Conflict of Interest: The authors declare that the research was conducted in the absence of any commercial or financial relationships that could be construed as a potential conflict of interest.